CHAPTER 1

Valence Bond Theory, Its History, Fundamentals, and Applications: A Primer[a]

Sason Shaik* and Philippe C. Hiberty†

**Department of Organic Chemistry and Lise Meitner-Minerva Center for Computational Chemistry, Hebrew University 91904 Jerusalem, Israel*
†Laboratoire de Chimie Physique, Groupe de Chimie Théorique, Université de Paris-Sud, 91405 Orsay Cedex, France

INTRODUCTION

The new quantum mechanics of Heisenberg and Schrödinger have provided chemistry with two general theories of bonding: valence bond (VB) theory and molecular orbital (MO) theory. The two were developed at about the same time, but quickly diverged into rival schools that have competed, sometimes fervently, in charting the mental map and epistemology of chemistry. Until the mid-1950s, VB theory dominated chemistry; then, MO theory took over while VB theory fell into disrepute and was soon almost completely abandoned. From the 1980s onward, VB theory made a strong comeback and has ever since been enjoying a renaissance both in qualitative applications of

[a]This review is dedicated to Roald Hoffmann—A great teacher and a friend.

Reviews in Computational Chemistry, Volume 20
edited by Kenny B. Lipkowitz, Raima Larter, and Thomas R. Cundari
ISBN 0-471-44525-8

the theory and the development of new methods for computational implementation.[1]

One of the great merits of VB theory is its visually intuitive wave function, expressed as a linear combination of chemically meaningful structures. It is this feature that made VB theory so popular in the 1930s–1950s, and, ironically, it is the same feature that accounts for its temporary demise (and ultimate resurgence). The comeback of this theory is, therefore, an important development. A review of VB theory that highlights its insight into chemical problems and discusses some of its state-of-the-art methodologies is timely.

This chapter is aimed at the nonexpert and designed as a tutorial for faculty and students who would like to teach and use VB theory, but possess only a basic knowledge of quantum chemistry. As such, an important focus of the chapter will be the qualitative wisdom of the theory and the way it applies to problems of bonding and reactivity. This part will draw on material discussed in previous works by the authors. Another focus of the chapter will be on the main methods available today for ab initio VB calculations. However, much important work of a technical nature will, by necessity, be left out. Some of this work (but certainly not all) is covered in a recent monograph on VB theory.[1]

A STORY OF VALENCE BOND THEORY, ITS RIVALRY WITH MOLECULAR ORBITAL THEORY, ITS DEMISE, AND EVENTUAL RESURGENCE

Since VB has achieved a reputation in some circles as an obsolete theory, it is important to give a short historical account of its development including the rivalry of VB and MO theory, the fall from favor of VB theory, and the reasons for the dominance of MO theory and the eventual resurgence of VB theory. Part of the historical review is based on material from the fascinating historical accounts of Servos[2] and Brush.[3,4] Other parts are not published historical accounts, but rational analyses of historical events, reflecting our own opinions and comments made by colleagues.

Roots of VB Theory

The roots of VB theory in chemistry can be traced to the famous paper of Lewis "*The Atom and The Molecule*",[5] which introduces the notions of electron-pair bonding and the octet rule.[2] Lewis was seeking an understanding of weak and strong electrolytes in solution, and this interest led him to formulate the concept of the chemical bond as an intrinsic property of the molecule that varies between the covalent (shared-pair) and ionic situations. Lewis' paper predated the introduction of quantum mechanics by 11 years, and constitutes

the first formulation of bonding in terms of the covalent–ionic classification. It is still taught today and provides the foundation for the subsequent construction and generalization of VB theory. Lewis' work eventually had its greatest impact through the work of Langmuir who articulated Lewis' model and applied it across the periodic table.[6]

The overwhelming support of the chemistry community for Lewis' idea that electron pairs play a fundamental role in bonding provided an exciting agenda for research directed at understanding the mechanism by which an electron pair could constitute a bond. The nature of this mechanism remained, however, a mystery until 1927 when Heitler and London traveled to Zurich to work with Schrödinger. In the summer of the same year they published their seminal paper, *Interaction between Neutral Atoms and Homopolar Binding*,[7,8] in which they showed that the bonding in H_2 can be accounted for by the wave function drawn in **1**, in Scheme 1. This wave function is a super-

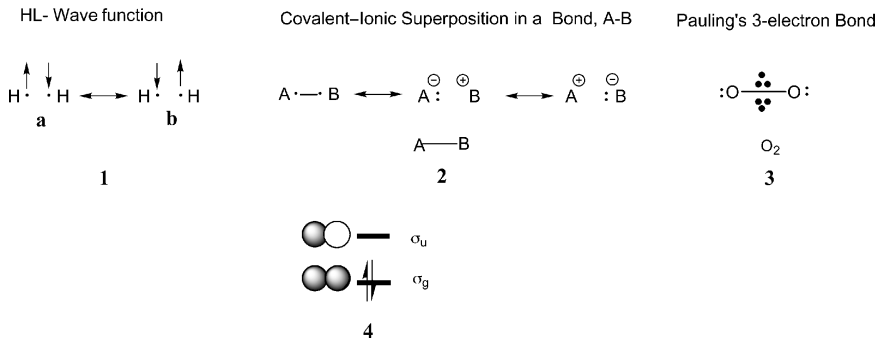

Scheme 1

position of two covalent situations in which one electron is in the spin up configuration (α spin), while the other is spin down (β spin) [form (**a**)], and vice versa in the second form (**b**). Thus, the bonding in H_2 was found to originate in the quantum mechanical "resonance" between the two situations of spin arrangement required to form a singlet electron pair. This "resonance energy" accounted for ~75% of the total bonding of the molecule, and thereby suggested that the wave function in **1**, which is referred to henceforth as the HL (Heitler–London) wave function, can describe the chemical bonding in a satisfactory manner. This "resonance origin" of bonding was a remarkable insight of the new quantum theory, since prior to that time it was not obvious how two neutral species could bond.

The notion of resonance was based on the work of Heisenberg,[9] who showed that, since electrons are indistinguishable particles then, for a two-electron system, with two quantum numbers n and m, there exist two wave

functions that are linear combinations of the two possibilities of arranging these electrons, as shown in Eq. [1].

$$\Psi_A = (1/\sqrt{2})[\phi_n(1)\phi_m(2) + \phi_n(2)\phi_m(1)] \quad [1a]$$

$$\Psi_B = (1/\sqrt{2})[\phi_n(1)\phi_m(2) - \phi_n(2)\phi_m(1)] \quad [1b]$$

As demonstrated by Heisenberg, the mixing of $[\phi_n(1)\phi_m(2)]$ and $[\phi_n(2)\phi_m(1)]$ led to a new energy term that caused splitting between the two wave functions Ψ_A and Ψ_B. He called this term "resonance" using a classical analogy of two oscillators that by virtue of possessing the same frequency resonate with a characteristic exchange energy. In the winter of 1928, London extended the HL wave function and formulated the general principles of covalent or homopolar bonding.[8,10] In both this and the earlier paper[7,10] the authors considered ionic structures for homopolar bonds, but discarded their mixing as being too small. In London's paper,[10] the ionic (so-called polar) bond is also considered. In essence, HL theory was a quantum mechanical version of Lewis' shared-pair theory. Even though Heitler and London did their work independently and perhaps did not know of the Lewis model, the HL wave function described precisely the shared pair of Lewis. In fact, in his landmark paper, Pauling points out that the HL[8] and London's later treatments are "entirely equivalent to G.N. Lewis's successful theory of shared electron pair...".[11]

The HL wave function formed the basis for the version of VB theory that became very popular later, but was also the source of some of the failings that were to later plague VB theory. In 1929, Slater presented his determinant method.[12] In 1931, he generalized the HL model to *n*-electrons by expressing the total wave function as a product of *n*/2 bond wave functions of the HL type.[13] In 1932, Rumer[14] showed how to write down all the possible bond pairing schemes for *n*-electrons and avoid linear dependencies between the forms, which are called canonical structures. We shall hereafter refer to the kind of VB theory that considers only covalent structures as VBHL. Further refinement of the new bonding theory between 1928 and 1933 were mostly quantitative,[15] focusing on improvement of the exponents of the atomic orbitals by Wang, and on the inclusion of polarization functions and ionic terms by Rosen and Weinbaum.

The success of the HL model and its relation to Lewis' model, posed a wonderful opportunity for the young Pauling and Slater to construct a general quantum chemical theory for polyatomic molecules. They both published, in the same year, 1931, several seminal papers in which they each developed the notion of hybridization, the covalent–ionic superposition, and the resonating benzene picture.[13,16–19] Especially effective were Pauling's papers that linked the new theory to the chemical theory of Lewis, and that rested on an encyclopedic command of chemical facts. In the first paper,[18] Pauling presented the electron-pair bond as a superposition of the covalent HL form and the two

possible ionic forms of the bond, as shown in **2** in Scheme 1, and discussed the transition from covalent to ionic bonding. He then developed the notion of hybridization and discussed molecular geometries and bond angles in a variety of molecules, ranging from organic to transition metal compounds. For the latter compounds, he also discussed the magnetic moments in terms of the unpaired spins. In the second paper,[19] Pauling addressed bonding in molecules like diborane, and odd-electron bonds as in the ion molecule H_2^+ and dioxygen, O_2, which Pauling represented as having two three-electron bonds, as shown in **3** in Scheme 1. These two papers were followed by more papers, all published during 1931–1933 in the *Journal of the American Chemical Society*, and collectively entitled "*The Nature of the Chemical Bond*". This series of papers allowed one to describe any bond in any molecule, and culminated in Pauling's famous monograph[20] in which all structural chemistry of the time was treated in terms of the covalent–ionic superposition theory, resonance theory, and hybridization theory. The book, published in 1939, was dedicated to G.N. Lewis, and, in fact, the 1916 paper of Lewis is the only reference cited in the preface to the first edition. Valence bond theory is, in Pauling's view, a quantum chemical version of Lewis' theory of valence. In Pauling's work, the long sought for Allgemeine Chemie (Generalized Chemistry) of Ostwald was, thus, finally found.[2]

Origins of MO Theory and the Roots of VB–MO Rivalry

At the same time that Slater and Pauling were developing their VB theory,[17] Mulliken[21–24] and Hund[25,26] were working on an alternative approach, which would eventually be called molecular orbital (MO) theory. The actual term (MO theory) does not appear until 1932, but the roots of the method can be traced to earlier papers from 1928,[21] in which both Hund and Mulliken made spectral and quantum number assignments of electrons in molecules, based on correlation diagrams of separated to united atoms. According to Brush,[3] the first person to write a wave function for a molecular orbital was Lennard-Jones in 1929, in his treatment of diatomic molecules. In this paper, Lennard-Jones shows with facility that the O_2 molecule is paramagnetic, and mentions that the VBHL method runs into difficulties with this molecule.[27] In MO theory, the electrons in a molecule occupy delocalized orbitals made from linear combinations of atomic orbitals (LCAO). Drawing **4**, Scheme 1, shows the molecular orbitals of the H_2 molecule; the delocalized σ_g MO should be contrasted with the localized HL description in **1**.

The work of Hückel in the early 1930s initially received a chilly reception,[28] but eventually Hückel's work gave MO theory an impetus and developed into a successful and widely applicable tool. In 1930, Hückel used Lennard-Jones' MO ideas on O_2, applied it to C=X (X = C, N, O) double bonds and suggested the concept of σ–π separation.[29] With this novel treatment, Hückel ascribed the restricted rotation in ethylene to the π-type orbital.

Equipped with this facility of σ–π separability, Hückel solved the electronic structure of benzene using both VBHL theory and his new Hückel MO (HMO) approach, the latter giving better "quantitative" results, and hence being preferred.[30] The π-MO picture, **5** in Scheme 2, was quite unique in the sense that it viewed the molecule as a whole, with a σ-frame dressed by π-electrons that occupy three completely delocalized π-orbitals. The HMO picture also allowed Hückel to understand the special stability of benzene.

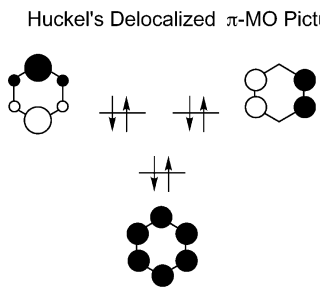

5

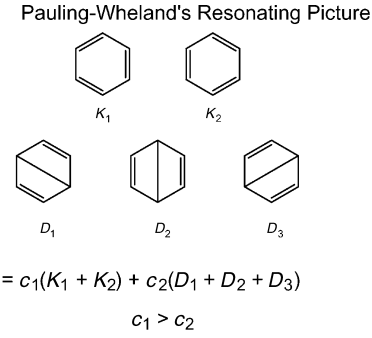

6

Scheme 2

Thus, the molecule was found to have a closed-shell π-component and its energy was calculated to be lower relative to three isolated π bonds in ethylene. In the same paper, Hückel treated the ion molecules of C_5H_5 and C_7H_7 as well as the molecules C_4H_4 (CBD) and C_8H_8 (COT). This allowed him to understand why molecules with six π-electrons have special stability, and why molecules like COT or CBD either do not possess this stability (COT) or had not yet been synthesized (CBD). Already in this paper and in a subsequent one,[31] Hückel begins to lay the foundations for what will become later known as the "Hückel Rule", regarding the special stability of "aromatic" molecules with $4n + 2$ π-electrons.[3] This rule, its extension to "antiaromaticity", and its articulation by organic chemists in the 1950–1970s would become a major cause of the acceptance of MO theory and rejection of VB theory.[4]

The description of benzene in terms of a superposition (resonance) of two Kekulé structures appeared for the first time in the work of Slater, as a case belonging to a class of species in which each atom possesses more neighbors than electrons it can share.[16] Two years later, Pauling and Wheland[32] applied the VBHL theory to benzene. They developed a less cumbersome computational approach, compared with Hückel's previous VBHL treatment,

using the five canonical structures, in **6** in Scheme 2, and approximated the matrix elements between the structures by retaining only close neighbor resonance interactions. Their approach allowed them to extend the treatment to naphthalene and to a great variety of other species. Thus, in the VBHL approach, benzene is described as a "resonance hybrid" of the two Kekulé structures and the three Dewar structures; the latter had already appeared before in Ingold's idea of mesomerism. In his book, published for the first time in 1944, Wheland explains the resonance hybrid with the biological analogy of mule = donkey + horse.[33] The pictorial representation of the wave function, the link to Kekulé's oscillation hypothesis, and the connection to Ingold's mesomerism, all of which were known to chemists, made the VBHL representation very popular among practicing chemists.

With these two seemingly different treatments of benzene, the chemical community was faced with two alternative descriptions of one of its molecular icons. Thus began the VB–MO rivalry that continues to the twenty-first century. The VB–MO rivalry involved many prominent chemists (to mention but a few names, Mulliken, Hückel, J. Mayer, Robinson, Lapworth, Ingold, Sidgwick, Lucas, Bartlett, Dewar, Longuet-Higgins, Coulson, Roberts, Winstein, Brown, etc.). A detailed and interesting account of the nature of this rivalry and the major players can be found in the treatment of Brush.[3,4] Interestingly, as early as the 1930s, Slater[17] and van Vleck and Sherman[34] stated that since the two methods ultimately converge, it is senseless to quibble about the issue of which one is better. Unfortunately, however, this rational attitude does not seem to have made much of an impression.

The "Dance" of Two Theories: One Is Up, the Other Is Down

By the end of World War II, Pauling's resonance theory had become widely accepted while most practicing chemists ignored HMO and MO theories. The reasons for this are analyzed by Brush.[3] Mulliken suggested that the success of VB theory was due to Pauling's skill as a propagandist. According to Hager (a Pauling biographer) VB theory won out in the 1930s because of Pauling's communication skills. However, the most important reason for its dominance is the direct lineage of VB-resonance theory to the structural concepts of chemistry dating from the days of Kekulé. Pauling himself emphasized that his VB theory is a natural evolution of chemical experience, and that it emerges directly from the concept of the chemical bond. This has made VB-resonance theory appear intuitive and "chemically correct". Another great promoter of VB-resonance theory was Ingold who saw in it a quantum chemical version of his own "mesomerism" concept (according to Brush, the terms resonance and mesomerism entered chemical vocabulary at the same time, due to Ingold's assimilation of VB-resonance theory; see Brush,[3] p. 57). Another very important reason for the early acceptance of VB theory is the facile

qualitative application of this theory to all known structural chemistry of the time (in Pauling's book[20]) and to a variety of problems in organic chemistry (in Wheland's book[33]). The combination of an easily applicable general theory and its good fit to experiment, created a rare credibility nexus. By contrast, MO theory seemed diametrically opposed to everything chemists had thought was true about the nature of the chemical bond. Even Mulliken admitted that MO theory departs from "chemical ideology" (see Brush,[3] p. 51). And to complete this sad state of affairs, in this early period MO theory offered no visual representation to compete with the resonance hybrid representation of VB-resonance theory. For all these reasons, by the end of World War II, VB-resonance theory dominated the epistemology of chemists.

By the mid-1950s, the tide had started a slow turn in favor of MO theory, a shift that gained momentum through the mid-1960s. What caused the shift is a combination of factors, of which the following two may be decisive. First, there were the many successes of MO theory: the experimental verification of Hückel's rules;[28] the construction of intuitive MO theories and their wide applicability for rationalization of structures (e.g., Walsh diagrams) and spectra [electronic and electron spin resonance (ESR)]; the highly successful predictive application of MO theory in chemical reactivity; the instant rationalization of the bonding in newly discovered exotic molecules like ferrocene,[35] for which the VB theory description was cumbersome; and the development of widely applicable MO-based computational techniques (e.g., extended Hückel and semiempirical programs). The second reason, on the other side, is that VB theory, in chemistry, suffered a detrimental conceptual arrest that crippled the predictive ability of the theory and started to lead to an accumulation of "failures". Unlike its fresh exciting beginning, in its frozen form of the 1950–1960s, VB theory ceased to guide experimental chemists to new experiments. This lack of utility ultimately led to the complete victory of MO theory. However, the MO victory over VB theory was restricted to resonance theory and other simplified versions of VB theory, not VB theory itself. In fact, by this time, the true VB theory was hardly being practiced anymore in the mainstream chemical community.

One of the major registered "failures" of VB theory is associated with the dioxygen molecule, O_2. Application of the Pauling–Lewis recipe of hybridization and bond pairing to rationalize and predict the electronic structure of molecules fails to predict the paramagneticity of O_2. By contrast, MO theory reveals this paramagneticity instantaneously.[27] Even though VB theory does not really fail with O_2, and Pauling himself preferred, without reasoning why, to describe it in terms of three-electron bonds (**3** in Scheme 1) in his early papers[19] (see also Wheland's description on p. 39 of his book[33]), this "failure" of Pauling's recipe has tainted VB theory and become a fixture of the common chemical wisdom (see Brush[3] p. 49, footnote 112).

A second example concerns the VB treatments of CBD and COT. The use of VBHL theory leads to an incorrect prediction that the resonance energy

of CBD should be as large as or even larger than that of benzene. The facts (that CBD had not yet been made and that COT exhibited no special stability) favored HMO theory. Another impressive success of HMO theory was the prediction that due to the degenerate set of singly occupied MOs, square CBD should distort to a rectangular structure, which provided a theoretical explanation for the ubiquitous phenomena of Jahn-Teller and pseudo-Jahn-Teller effects, amply observed by the community of spectroscopists. Wheland analyzed the CBD problem early on, and his analysis pointed out that inclusion of ionic structures would probably change the VB predictions and make them identical to MO.[33,36,37] Craig showed that VBHL theory in fact correctly assigns the ground state of CBD, by contrast to HMO theory.[38,39] Despite this mixed bag of predictions on properties of CBD, by VBHL or HMO, and despite the fact that modern VB theory has subsequently demonstrated unique and novel insight into the problems of benzene, CBD and their isoelectronic species, the early stamp of the CBD story as a failure of VB theory still persists.

The increasing interest of chemists in large molecules as of the late 1940s started making VB theory impractical, compared with the emerging semiempirical MO methods that allowed the treatment of larger and larger molecules. A great advantage of semiempirical MO calculations was the ability to calculate bond lengths and angles rather than assume them as in VB theory.[4] Skillful communicators like Longuet–Higgins, Coulson, and Dewar were among the leading MO proponents, and they handled MO theory in a visualizable manner, which had been sorely missing before. In 1951, Coulson addressed the Royal Society Meeting and expressed his opinion that despite the great success of VB theory, it had no good theoretical basis; it was just a semiempirical method, he said, of little use for more accurate calculations.[40] In 1949, Dewar's monograph, *Electronic Theory of Organic Chemistry*,[41] summarized the faults of resonance theory, as being cumbersome, inaccurate, and too loose: "it can be played happily by almost anyone without any knowledge of the underlying principles involved". In 1952, Coulson published his book *Valence*,[42] which did for MO theory, at least in part, what Pauling's book[20] had done much earlier for VB theory. In 1960, Mulliken won the Nobel Prize and Platt wrote, "MO is now used far more widely, and simplified versions of it are being taught to college freshmen and even to high school students".[43] Indeed, many communities took to MO theory due to its proven portability and successful predictions.

A decisive defeat was dealt to VB theory when organic chemists were finally able to synthesize transient molecules and establish the stability patterns of $C_8H_8^{2-}$, $C_5H_5^{-,+}$, $C_3H_3^{+,-}$ and $C_7H_7^{+,-}$ during the 1950–1960s.[3,4,28] The results, which followed Hückel's rules, convinced most of the organic chemists that MO theory was right, while VBHL and resonance theories were wrong. From 1960–1978, C_4H_4 was made, and its structure and properties as determined by MO theory challenged initial experimental determination of a square structure.[3,4] The syntheses of nonbenzenoid aromatic compounds

like azulene, tropone, and so on, further established Hückel's rules, and highlighted the failure of resonance theory.[28] This era in organic chemistry marked a decisive down-fall of VB theory.

In 1960, the 3rd edition of Pauling's book was published,[20] and although it was still spellbinding for chemists, it contained errors and omissions. For example, in the discussion of electron deficient boranes, Pauling describes the molecule $B_{12}H_{12}$ instead of $B_{12}H_{12}^{2-}$ (Pauling,[20] p. 378); another example is a very cumbersome description of ferrocene and analogous compounds (on pp. 385–392), for which MO theory presented simple and appealing descriptions. These and other problems in the book, as well as the neglect of then-known species like $C_5H_5^{-,+}$, $C_3H_3^{+,-}$, and $C_7H_7^{+,-}$, reflected the situation that, unlike MO theory, VB theory did not have a useful Aufbau principle that could predict reliably the dependence of molecular stability on the number of electrons. As we have already pointed out, the conceptual development of VB theory had been arrested since the 1950s, in part due to the insistence of Pauling himself that resonance theory was sufficient to deal with most problems (see, e.g., p. 283 in Brush[4]). Sadly, the creator himself contributed to the downfall of his own brainchild.

In 1952, Fukui published his Frontier MO theory,[44] which went initially unnoticed. In 1965, Woodward and Hoffmann published their principle of conservation of orbital symmetry, and applied it to all pericyclic chemical reactions. The immense success of these rules[45] renewed interest in Fukui's approach and together formed a new MO-based framework of thought for chemical reactivity (called, e.g., "giant steps forward in chemical theory" in Morrison and Boyd, pp. 934, 939, 1201, and 1203). This success of MO theory dealt a severe blow to VB theory. In this area too, despite the early calculations of the Diels–Alder and 2 + 2 cycloaddition reactions by Evans,[46] VB theory missed making an impact, in part at least because of its blind adherence to simple resonance theory.[28] All the subsequent VB derivations of the rules (e.g., by Oosterhoff in Ref. 90) were "after the fact" and failed to reestablish the status of VB theory.

The development of photoelectron spectroscopy (PES) and its application to molecules in the 1970s, in the hands of Heilbronner, showed that spectra could be easily interpreted if one assumes that electrons occupy delocalized molecular orbitals.[47,48] This further strengthened the case for MO theory. Moreover, this served to lessen the case for VB theory, because it describes electron pairs that occupy localized bond orbitals. A frequent example of this "failure" of VB theory is the PES of methane, which shows two different ionization peaks. These peaks correspond to the a_1 and t_2 MOs, but not to the four C–H bond orbitals in Pauling's hybridization theory (see a recent paper on a similar issue[49]). With these and similar types of arguments VB theory has eventually fallen into a state of disrepute and become known, at least when the authors were students, either as a "wrong theory" or even a "dead theory".

The late 1960s and early 1970s mark the era of mainframe computing. By contrast to VB theory, which is difficult to implement computationally (due to the non-orthogonality of orbitals), MO theory could be easily implemented (even GVB was implemented through an MO-based formalism—see later). In the early 1970s, Pople and co-workers developed the GAUSSIAN70 package that uses "ab initio MO theory" with no approximations other than the choice of basis set. Sometime later density functional theory made a spectacular entry into chemistry. Suddenly, it became possible to calculate real molecules, and to probe their properties with increasing accuracy. This new and user-friendly tool created a subdiscipline of "computational chemists" who explore the molecular world with the GAUSSIAN series and many other packages that sprouted alongside the dominant one. Calculations continuously reveal "more failures" of Pauling's VB theory, for example, the unimportance of 3*d* orbitals in bonding of main group elements, namely, the "verification" of three-center bonding. Leading textbooks hardly include VB theory anymore, and when they do, they misrepresent the theory.[50,51] Advanced quantum chemistry courses teach MO theory regularly, but books that teach VB theory are virtually nonexistent. The development of user friendly ab initio MO-based software and the lack of similar VB software seem to have put the last nail in the coffin of VB theory and substantiated MO theory as the only legitimate chemical theory of bonding.

Nevertheless, despite this seemingly final judgment and the obituaries showered on VB theory in textbooks and in public opinion, the theory has never really died. Due to its close affinity to chemistry and utmost clarity, it has remained an integral part of the thought process of many chemists, even among proponents of MO theory (see comment by Hoffmann on p. 284 in Brush[4]). Within the chemical dynamics community, moreover, the usage of the theory has never been eliminated, and it exists in several computational methods such as LEPS (London–Eyring–Polanyi–Sato), BEBO (bond energy bond order), DIM (diatomics in molecules), and so on, which were (and still are) used for the generation of potential energy surfaces. Moreover, around the 1970s, but especially from the 1980s and onward, VB theory began to rise from its ashes, to dispel many myths about its "failures" and to offer a sound and attractive alternative to MO theory. Before we describe some of these developments, it is important to go over some of the major "failures" of VB theory and inspect them a bit more closely.

Are the Failures of VB Theory Real Ones?

All the so-called failures of VB theory are due to misuse and failures of very simplified versions of the theory. Simple resonance theory enumerates structures without proper consideration of their interaction matrix elements (or overlaps). It will fail whenever the matrix element is important as in the case of aromatic versus antiaromatic molecules, and so on.[52] The hybridization

bond-pairing theory assumes that the most important energetic effect for a molecule is the bonding, and hence one should hybridize the atoms and make the maximum number of bonds—henceforth "perfect pairing". The perfect-pairing approach will fail whenever other factors (see below) become equal to or more important than bond pairing.[53,54] The VBHL theory is based on covalent structures only, which become insufficient and require inclusion of ionic structures explicitly or implicitly (through delocalization tails of the atomic orbitals, as in the GVB method described later). In certain cases, like that of antiaromatic molecules, this deficiency of VBHL makes incorrect predictions.[55] Next, we consider four iconic "failures", and show that some of them tainted VB in unexplained ways.

1. **The O_2 "Failure":** It is doubtful that this so-called failure can be attributed to Pauling himself, because in his landmark paper,[18] he was very careful to state that the molecule does not possess a "normal" state, but rather one with two three-electron bonds (**3** in Scheme 1). Also see Wheland on page 39 of his book.[33] We also located a 1934 *Nature* paper by Heitler and Pöschl[56] who treated the O_2 molecule with VB principles and concluded that "the $^3\Sigma_g^-$ term ... [gives] the fundamental state of the molecule". It is not clear to us how the myth of this "failure" grew, spread so widely, and was accepted so unanimously. Curiously, while Wheland acknowledged the prediction of MO theory by a proper citation of Lennard-Jones' paper,[27] Pauling did not, at least not in his landmark papers,[18,19] nor in his book.[20] In these works, the Lennard-Jones paper is either not cited,[19,20] or is mentioned only as a source of the state symbols[18] that Pauling used to characterize the states of CO, CN, and so on. One wonders about the role of animosity between the MO and VB camps in propagating the notion of the "failures" of VB to predict the ground state of O_2. Sadly, scientific history is determined also by human weaknesses. As we have repeatedly stated, it is true that a naive application of hybridization and the perfect pairing approach (simple Lewis pairing) without consideration of the important effect of four-electron repulsion would fail and predict a $^1\Delta_g$ ground state. As we shall see later, in the case of O_2, perfect pairing in the $^1\Delta_g$ state leads to four-electron repulsion, which more than cancels the π-bond. To avoid the repulsion, we can form two three-electron π-bonds, and by keeping the two odd electrons in a high-spin situation, the ground state becomes $^3\Sigma_g^-$ that is further lowered by exchange energy due to the two triplet electrons.[53]
2. **The C_4H_4 "Failure":** This is a failure of the VBHL approach that does not involve ionic structures. Their inclusion in an all-electron VB theory, either explicitly,[55,57] or implicitly through delocalization tails of the atomic orbitals,[58] correctly predicts the geometry and resonance energy. In fact, even VBHL theory makes a correct assignment of the ground state of cyclo butadiene (CBD), as the $^1B_{1g}$ state. By contrast, monodeterminantal MO

theory makes an incorrect assignment of the ground state as the triplet $^3A_{2g}$ state.[38,39] Moreover, HMO theory succeeded for the wrong reason. Since the Hückel MO determinant for the singlet state corresponds to a single Kekulé structure, CBD exhibits zero resonance energy in HMO.[36]

3. **The $C_5H_5^+$ "Failure":** This is a failure of simple resonance theory, not of VB theory. Taking into account the sign of the matrix element (overlap) between the five VB structures shows that singlet $C_5H_5^+$ is Jahn–Teller unstable, and the ground state is, in fact, the triplet state. This is generally the case for all the antiaromatic ionic species having $4n$ electrons over $4n + 1$ or $4n + 3$ centers.[52]
4. **The "Failure" associated with the PES of methane (CH_4):** Starting from a naive application of the VB picture of CH_4, it follows that since methane has four equivalent localized bond orbitals (LBOs), the molecule should exhibit only one ionization peak in PES. However, since the PES of methane shows two peaks, VB theory "fails"! This argument is false for two reasons. First, as has been known since the 1930s, LBOs for methane or any molecule, can be obtained by a unitary transformation of the delocalized MOs.[59] Thus, both MO and VB descriptions of methane can be cast in terms of LBOs. Second, if one starts from the LBO picture of methane, the electron can come out of any one of the LBOs. A physically correct representation of the CH_4^+ cation would be a linear combination of the four forms that ascribe electron ejection to each of the four bonds. One can achieve the correct physical description, either by combining the LBOs back to canonical MOs,[48] or by taking a linear combination of the four VB configurations that correspond to one bond ionization.[60,61] As shall be seen later, correct linear combinations are $^2A_1$ and $^2T_2$, the latter being a triply degenerate VB state.

We conclude that those who reject VB theory cannot continue to invoke "failures", because a properly executed VB theory does not fail, just as a properly done MO-based calculation does not "fail". This notion of VB "failure" that is traced back to the VB–MO rivalry in the early days of quantum chemistry should now be considered obsolete, unwarranted, and counterproductive. A modern chemist should know that there are two ways of describing electronic structure, and that these two are not contrasting theories, but rather two representations of the same reality. Their capabilities and insights into chemical problems are complementary and the exclusion of either one of them undermines the intellectual heritage of chemistry. Indeed, theoretical chemists in the dynamics community continued to use VB theory and maintained an uninterrupted chain of VB usage from London, through Eyring, Polanyi, to Wyatt, Truhlar, and others in the present day. Physicists, too, continued to use VB theory, and one of the main proponents is the Nobel Laureate P.W. Anderson, who developed a resonating VB theory of superconductivity. And, in terms of the focus of this chapter, in mainstream chemistry too, VB

theory is beginning to enjoy a slow but steady renaissance in the form of modern VB theory.

Modern VB Theory: VB Theory Is Coming of Age

The renaissance of VB theory is marked by a surge in the following two-pronged activity: (a) creation of general qualitative models based on VB theory, and (b) development of new methods and software that enable applications to moderate-sized molecules. Below we briefly mention some of these developments without pretence of creating an exhaustive list.

A few general qualitative models based on VB theory started to appear in the late 1970s and early 1980s. Among these models we count also semiempirical approaches based, for example, on Heisenberg and Hubbard Hamiltonians,[62–70] as well as Hückel VB methods,[52,71–73] which can handle well ground and excited states of molecules. Methods that map MO-based wave functions to VB wave functions offer a good deal of interpretive insight. Among these mapping procedures we note the half-determinant method of Hiberty and Leforestier,[74] and the CASVB methods of Thorsteinsson et al.[75,76] and Hirao and co-worker.[77,78] General qualitative VB models for chemical bonding were proposed in the early 1980s and the late 1990s by Epiotis et al.[79,80] A general model for the origins of barriers in chemical reactions was proposed in 1981 by Shaik, in a manner that incorporates the role of orbital symmetry.[52,81] Subsequently, in collaboration with Pross[82,83] and Hiberty,[84] the model has been generalized for a variety of reaction mechanisms,[85] and used to shed new light on the problems of aromaticity and antiaromaticity in isoelectronic series.[57] Following Linnett's reformulation of three-electron bonding in the 1960s,[86] Harcourt[87,88] developed a VB model that describes electron-rich bonding in terms of increased valence structures, and showed its occurrence in bonds of main group elements and transition metals.

Valence bond ideas have also contributed to the revival of theories for photochemical reactivity. Early VB calculations by Oosterhoff and co-workers[89,90] revealed a possible general mechanism for the course of photochemical reactions. Michl and co-workers[91,92] articulated this VB-based mechanism and highlighted the importance of "funnels" as the potential energy features that mediate the excited-state species back into the ground state. Recent work by Robb and co-workers[93–96] showed that these "funnels" are conical intersections that can be predicted by simple VB arguments, and computed at a high level of sophistication. Similar applications of VB theory to deduce the structure of conical intersections in photoreactions were done by Shaik and Reddy[97] and recently generalized by Zilberg and Haas.[98]

Valence bond theory enables a very straightforward account of environmental effects, such as those imparted by solvents and/or protein pockets. A major contribution to the field was made by Warshel who created an empirical VB (EVB) method. By incorporating van der Waals and London interactions

using a molecular mechanics (MM) method, Warshel created the QM(VB)–MM method for the study of enzymatic reaction mechanisms.[99–101] His pioneering work inaugurated the now emerging QM–MM methodologies for studying enzymatic processes. Hynes and co-workers,[102–104] showed how to couple solvent models to VB and create a simple and powerful model for understanding and predicting chemical processes in solution. Shaik[105,106] showed how solvent effects can be incorporated in an effective manner in the reactivity factors that are based on VB diagrams.

All in all, VB theory is seen to offer a widely applicable framework for thinking about and predicting chemical trends. Some of these qualitative models and their predictions are discussed in the Application sections.

In the 1970s, a stream of nonempirical VB methods began to appear and were followed by many applications of accurate calculations. All these methods divide the orbitals in a molecule into inactive and active subspaces, treating the former as a closed-shell and the latter by a VB formalism. The programs optimize the orbitals, and the coefficients of the VB structures, but they differ in the manners by which the VB orbitals are defined. Goddard et al.[107–110] developed the generalized VB (GVB) method, which uses semilocalized atomic orbitals (having small delocalization tails), employed originally by Coulson and Fisher for the H_2 molecule.[111] The GVB method is incorporated now in GAUSSIAN and in most other MO-based software. Somewhat later, Gerratt, Raimondi, and Cooper developed their VB method known as the spin coupled (SC) theory and its follow up by configuration interaction using the SCVB method,[112–114] which is now incorporated in the MOLPRO software. The GVB and SC theories do not employ covalent and ionic structures explicitly, but instead use semilocalized atomic orbitals that effectively incorporate all the ionic structures, and thereby enable one to express the electronic structures in compact forms based on formally covalent pairing schemes. Balint-Kurti and Karplus[115] developed a multistructure VB method that utilizes covalent and ionic structures with localized atomic orbitals (AOs). In a later development by van Lenthe and Balint-Kurti[116,117] and by Verbeek and van Lenthe,[118,119] the multistructure method is referred to as a VB self-consistent field (VBSCF) method. In a subsequent development, van Lenthe, Verbeek, and co-workers[120,121] generated the multipurpose VB program called TURTLE, which has recently been interfaced with the MO-based program GAMESS-UK. Matsen,[122,123] McWeeny,[124] and Zhang and co-workers[125,126] developed their spin-free VB approaches based on symmetric group methods. Subsequently, Wu et al.[127,128] extended the spin-free approach, and produced a general purpose VB program called the XIAMEN-99 package. Soon after, Li and McWeeny[129] announced their VB2000 software, which is also a general purpose program, including a variety of methods. Another package incorporating multiconfigurational VB (MCVB) methods, called CRUNCH and based on the symmetric group methods of Young, was written by Gallup et al.[130,131] During the early 1990s, Hiberty et al.[132–137] developed the breathing orbital

VB (BOVB) method, which also utilizes covalent and ionic structures, but in addition allows them to have their own unique set of orbitals. This method is now incorporated into the programs TURTLE and XIAMEN-99. Very recently, Wu et al.[138] developed a VBCI method that is akin to BOVB, but which can be applied to larger systems. The recent biorthogonal VB method (bio-VB) of McDouall[139] has the potential to carry out VB calculations on systems with up to 60 electrons outside the closed shell. And finally, Truhlar and co-workers[140] developed the VB-based multiconfiguration molecular mechanics method (MCMM) to treat dynamical aspects of chemical reactions, while Landis and co-workers[141] introduced the VAL–BOND method that predicts the structures of transition metal complexes using Pauling's ideas of orbital hybridization. In the section dedicated to VB methods, we mention the main software and methods that we used, and outline their features, capabilities, and limitations.

This plethora of acronyms for VB software starts to resemble that which accompanied the ascent of MO theory. While this may sound like good news, certainly it is also a call for systematization much like what Pople and co-workers enforced on computational MO terminology. Nonetheless, at the moment the important point is that the advent of many good VB programs has caused a surge of applications of VB theory to problems ranging from bonding in main group elements to transition metals, conjugated systems, aromatic and antiaromatic species, and even excited states and full pathways of chemical reactions, with moderate to very good accuracies. For example, a recent calculation of the barrier for the identity hydrogen exchange reaction, $H + H{-}H' \rightarrow H{-}H + H'$, by Song et al.[142] shows that it is possible to calculate the reaction barrier accurately with just eight classical VB structures! Valence bond theory is coming of age.

BASIC VB THEORY

Writing and Representing VB Wave Functions

VB Wave Functions with Localized Atomic Orbitals

We illustrate the theory by using, as an example, the two-electron/two-center (2e/2c) bond. A VB determinant is an antisymmetrized wave function that may or may not also be a proper spin eigenfunction. For example, $|a\bar{b}|$ in Eq. [2] is a determinant that describes two spin-orbitals a and b having one electron each; the bar over the b orbital indicates a β spin, while its absence indicates an α spin:

$$|a\bar{b}| = \frac{1}{\sqrt{2}}\{a(1)b(2)[\alpha(1)\beta(2)] - a(2)b(1)[\alpha(2)\beta(1)]\} \qquad [2]$$

The parenthetical numbers *1* and *2* are the electron indices. By itself this determinant is not a proper spin-eigenfunction. However, by mixing with $|\bar{a}b|$ two spin-eigenfunctions will result, one having a singlet coupling as shown in Eq. [3], the other possessing a triplet coupling in (Eq. [4]); in both cases the normalization constants are omitted for the time being.

$$\Psi_{HL} = |a\bar{b}| - |\bar{a}b| \quad [3]$$

$$\Psi_{T} = |a\bar{b}| + |\bar{a}b| \quad [4]$$

If *a* and *b* are the respective AOs of two hydrogen atoms, Ψ_{HL} in Eq. [3] is just the historical wave function used in 1927 by Heitler and London[7] to treat the bonding in the H_2 molecule, hence the subscript descriptor HL. This wave function displays a purely covalent bond in which the two hydrogen atoms remain neutral and exchange their spins (the singlet pairing is represented, henceforth by the two dots connected by a line as shown in **7** in Scheme 3).

7 **8** **9** **10**

Scheme 3

The state Ψ_T in Eq. [4] represents a repulsive triplet interaction (see **8** in Scheme 3) between two hydrogen atoms having parallel spins. The other VB determinants that one can construct in this simple two-electron/two-center 2e/2c case are $|a\bar{a}|$ and $|b\bar{b}|$, corresponding to the ionic structures **9** and **10**, respectively. Both ionic structures are spin-eigenfunctions and represent singlet situations. Note that the rules that govern spin multiplicities and the generation of spin-eigenfunctions from combinations of determinants are the same in VB and MO theories. In a simple two-electron case, it is easy to distinguish triplet from singlet eigenfunctions by factoring the spatial function out from the spin function: the singlet spin eigenfunction is antisymmetric with respect to electron exchange, while the triplet is symmetric. Of course, the spatial parts behave in precisely the opposite manner. For example, the singlet is $\alpha(1)\beta(2) - \beta(1)\alpha(2)$, while the triplet is $\alpha(1)\beta(2) + \beta(1)\alpha(2)$ in Eqs. [3] and [4].

While the H_2 bond was considered as purely covalent in Heitler and London's paper[7] (Eq. [3] and Structure **7** in Scheme 3), the exact description of H_2 or any homopolar bond ($\Psi_{VB\text{-full}}$ in Eq. [5]) involves a small contribution from the ionic structures **9** and **10**, which mix by configuration interaction (CI) in the VB framework. Typically, and depending on the atoms that are bonded, the weight of the purely covalent structure is ~75%, while the ionic structures

share the remaining 25%. By symmetry, the wave function maintains an average neutrality of the two bonded atoms (Eq. [5]).

$$\Psi_{\text{VB-full}} = \lambda(|a\overline{b}| - |\overline{a}b|) + \mu(|a\overline{a}| + |b\overline{b}|) \quad \lambda > \mu \tag{5a}$$

$$H_a{-}H_b \approx 75\%(H_a{\bullet}{-}{\bullet}H_b) + 25\%(H_a^- H_a^+ + H_b^+ H_b^-) \tag{5b}$$

For convenience, and to avoid confusion, we shall symbolize a purely covalent bond between A and B centers as A•—•B, while the notation A—B will be employed for a composite bond wave function like the one displayed in Eq. [5b]. In other words, A—B refers to the "real" bond while A•—•B designates its covalent component (see **2** in Scheme 1).

VB Wave Functions with Semilocalized AOs

One inconvenience of using the expression $\Psi_{\text{VB-full}}$ (Eq. [5]) is its relative complexity compared to the simpler HL function (Eq. [3]). Coulson and Fischer[111] proposed an elegant way of combining the simplicity of Ψ_{HL} with the accuracy of $\Psi_{\text{VB-full}}$. In the Coulson–Fischer (CF) wave function, Ψ_{CF}, the two-electron bond is described as a formally covalent singlet coupling between two orbitals φ_a and φ_b, which are optimized with freedom to delocalize over the two centers. This is exemplified below for H_2 (dropping once again the normalization factors):

$$\Psi_{\text{CF}} = |\varphi_a\overline{\varphi_b}| - |\overline{\varphi_a}\varphi_b| \tag{6a}$$

$$\varphi_a = a + \varepsilon b \tag{6b}$$

$$\varphi_b = b + \varepsilon a \tag{6c}$$

Here a and b are purely localized AOs, while φ_a and φ_b are delocalized AOs. In fact, experience shows that the Coulson–Fischer orbitals φ_a and φ_b, which result from the energy minimization, are generally not very delocalized ($\varepsilon < 1$). As such they can be viewed as "distorted" orbitals that remain atomic-like in nature. However minor this may look, the slight delocalization renders the Coulson–Fischer wave function equivalent to the VB-full (Eq. [5]) wave function with the three classical structures. A straightforward expansion of the Coulson–Fischer wave function leads to a linear combination of classical structures in Eq. [7].

$$\Psi_{\text{CF}} = (1 + \varepsilon^2)(|a\overline{b}| - |\overline{a}b|) + 2\varepsilon(|a\overline{a}| + |b\overline{b}|) \tag{7}$$

Thus, the Coulson–Fischer representation keeps the simplicity of the covalent picture while treating the covalent–ionic balance by embedding the effect of the ionic terms in a variational way through the delocalization tails. The Coulson–Fischer idea was later generalized to polyatomic molecules and gave rise to the

generalized valence bond (GVB) and spin-coupled (SC) methods, which were mentioned in the introductory part and will be discussed later.

VB Wave Functions with Fragment Orbitals

Valence bond determinants may involve fragment orbitals (FOs) instead of localized or semilocalized AOs. These fragment orbitals may be delocalized (e.g., like some MOs of the constituent fragments of a molecule). The latter option is an economical way of representing a wave function that is a linear combination of several determinants based on AOs, just as MO determinants are linear combinations of VB determinants (see below). Suppose, for example, that one wanted to treat the recombination of the $CH_3^{\bullet}$ and $H^{\bullet}$ radicals in a VB manner. First, let ($\varphi_1 - \varphi_5$) be the MOs of the $CH_3^{\bullet}$ fragment (φ_5 being singly occupied), and b the AO of the incoming hydrogen. The covalent VB function that describes the active C–H bond in our study just couples the φ_5 and b orbitals in a singlet way, as expressed in Eq. [8]:

$$\Psi(H_3C\bullet\!-\!\bullet H) = |\varphi_1\overline{\varphi_1}\varphi_2\overline{\varphi_2}\varphi_3\overline{\varphi_3}\varphi_4\overline{\varphi_4}\,\varphi_5\overline{b}\,| - |\varphi_1\overline{\varphi_1}\varphi_2\overline{\varphi_2}\,\varphi_3\,\overline{\varphi_3}\varphi_4\overline{\varphi_4}\,\overline{\varphi_5}b| \quad [8]$$

Here, $\varphi_1 - \varphi_4$ are fully delocalized on the CH_3 fragment. Even the φ_5 orbital is not a pure AO, but may involve some tails on the hydrogens of the fragment. It is clear that this option is conceptually simpler than treating all the C–H bonds in a VB way, including the ones that remain unchanged in the reaction.

Writing VB Wave Functions Beyond the 2e/2c Case

Rules for writing VB wave functions in the polyelectronic case are just intuitive extensions of the rules for the 2e/2c case discussed above. First, let

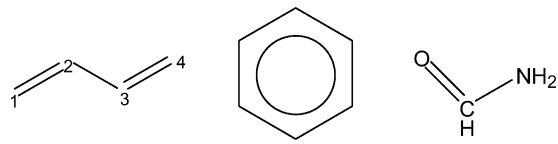

11 **12** **13**

Scheme 4

us consider butadiene, structure **11** in Scheme 4, and restrict the description to the π system.

Denoting the π AOs of the C_1–C_4 carbons by *a, b, c*, and *d*, respectively, the fully covalent VB wave function for the π system of butadiene displays two singlet couplings: one between *a* and *b*, and one between *c* and *d*. It follows that the wave function can be expressed in the form of Eq. [9], as a product of the bond wave functions.

$$\Psi(\mathbf{11}) = |(a\overline{b} - \overline{a}b)\,(c\overline{d} - \overline{c}d)| \quad [9]$$

Upon expansion of the product, one gets a sum of four determinants as in Eq. [10].

$$\Psi(\mathbf{11}) = |a\bar{b}c\bar{d}| - |a\bar{b}\bar{c}d| - |\bar{a}bc\bar{d}| + |\bar{a}b\bar{c}d| \qquad [10]$$

The product of bond wave functions in Eq. [9], involves so-called perfect pairing, whereby we take the Lewis structure of the molecule, represent each bond by a HL bond, and finally express the full wave function as a product of all these pair-bond wave functions. As a rule, such a perfect-pairing polyelectronic VB wave function having n bond pairs will be described by 2^n determinants, displaying all the possible 2×2 spin permutations between the orbitals that are singlet coupled.

The above rule can readily be extended to larger polyelectronic systems, like the π system of benzene **12**, or to molecules bearing lone pairs like formamide, **13**. In this latter case, using *n, c*, and *o*, respectively, to refer to the π AOs of nitrogen, carbon, and oxygen, the VB wave function describing the neutral covalent structure is given by Eq. [11]:

$$\Psi(\mathbf{13}) = |n\bar{n}c\bar{o}| - |n\bar{n}\,\bar{c}o| \qquad [11]$$

In any one of the above cases, improvement of the wave function can be achieved by using Coulson–Fischer orbitals that take into account ionic contributions to the bonds. Note that the number of determinants grows exponentially with the number of covalent bonds (recall, this number is 2^n, n being the number of bonds). Hence, 8 determinants are required to describe a Kekulé structure of benzene, and the fully covalent and perfectly paired wave function for methane is made of 16 determinants. This shows the benefit of using FOs rather than pure AOs as much as possible, as has been done above (Eq. [8]). Using FOs to construct VB wave functions is also appropriate when one wants to fully exploit the symmetry properties of the molecule. For example, we can describe all the bonds in methane by constructing group orbitals of the four Hs. Subsequently, we can distribute the eight bonding electrons of the molecule into these FOs as well as into the *2s* and *2p* AOs of carbon. Then we can pair up the electrons using orbital symmetry-matched FOs, as shown by the lines connecting these orbital pairs in Figure 1. The corresponding wave function can be written as follows:

$$\Psi(CH_4) = |(2s\overline{\varphi_s} - \overline{\varphi_s}2s)(2p_x\overline{\varphi_x} - \overline{\varphi_x}2p_x)(2p_y\overline{\varphi_y} - \overline{\varphi_y}\,2p_y)(2p_z\overline{\varphi_z} - \overline{\varphi_z}\,2p_z)| \qquad [12]$$

In this representation, each bond is a delocalized covalent two-electron bond, written as a HL-type bond. The VB method that deals with fragment orbitals

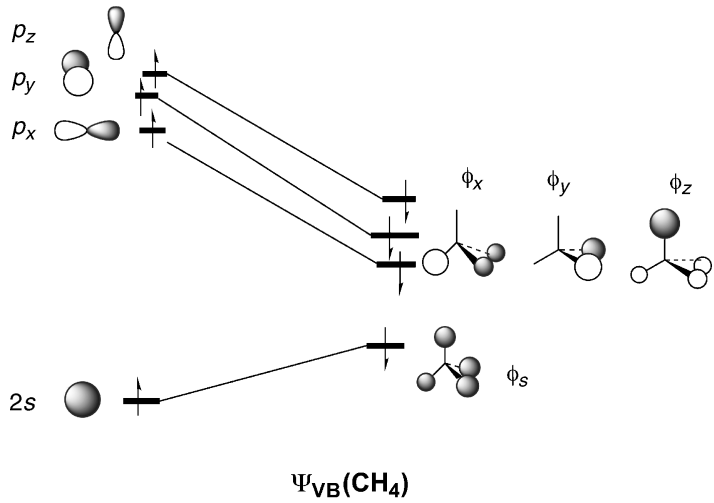

Figure 1 A VB representation of methane using delocalized FOs. Each line that connects the orbitals is a bond pair. The total wave function is given in Eq. 12.

(FO–VB) is particularly useful in high-symmetry cases such as ferrocene and other organometallic complexes.

Pictorial Representation of VB Wave Functions by Bond Diagrams

Since we argue that a bond need not necessarily involve only two AOs on two centers, we must provide an appropriate pictorial representation of such a bond. A possibility is the bond diagram in Figure 2, which shows two spin-paired electrons in general orbitals φ_1 and φ_2, with a line connecting these orbitals. This bond diagram represents the wave function in Eq. [13]

$$\Psi_{\text{bond}} = |\varphi_1\overline{\varphi_2}| - |\overline{\varphi_1}\varphi_2| \qquad [13]$$

where the orbitals can take any shape; it can involve two centers with localized AOs, or two Coulson–Fischer orbitals with delocalization tails, or FOs that span multiple centers.

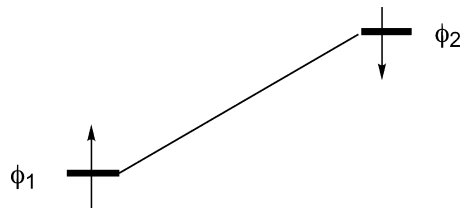

Figure 2 A bond diagram representation of two spin-paired electrons in orbitals ϕ_1 and ϕ_2. The bond pair is indicated by a line connecting the orbitals.

The Relationship between MO and VB Wave Functions

We now consider the difference between the MO and VB descriptions of an electronic system, at the simplest level of both theories. As we shall see, in the cases of one-electron, three-electron, and four-electron interactions between two centers, there is no real difference between the two theories, except for a matter of language. However, the two theories do differ in their description of the two-electron bond. Let us consider, once again, the example of H_2, with its two AOs *a* and *b,* and examine first the VB description, dropping normalization factors for simplicity.

As has been stated already, at equilibrium distance the bonding is not 100% covalent, and requires an ionic component to be accurately described. On the other hand, at long distances the HL wave function is the correct state, as the ionic components necessarily drop to zero and each hydrogen carries one electron away through the homolytic bond breaking. The HL wave function *dissociates correctly,* but is quantitatively inaccurate at bonding distances. Therefore, the way to improve the HL description is straightforward: simply mixing Ψ_{HL} with the ionic determinants and optimizing the coefficients variationally, by CI. One then gets the wave function $\Psi_{VB\text{-}full}$, in Eq. [5a] above, which contains a major covalent component and a minor ionic one.

Let us now turn to the MO description. Bringing together two hydrogen atoms leads to the formation of two MOs, σ and σ^* (bonding and antibonding, respectively); see Eq. [14].

$$\sigma = a + b \qquad \sigma^* = a - b \tag{14}$$

At the simple MO level, the ground state of H_2 is described by Ψ_{MO}, in which the bonding σ MO is doubly occupied. Expansion (see Appendix for details) of this MO determinant into its AO determinant constituents leads to Eq. [15]:

$$\Psi_{MO} = |\sigma\overline{\sigma}| = (|a\overline{b}| - |\overline{a}b|) + (|a\overline{a}| + |b\overline{b}|) \tag{15}$$

It is apparent from Eq. [15] that the first half of the expansion is just the Heitler–London function Ψ_{HL} (Eq. [3]), while the remaining part is ionic. It follows that the MO description of the two-electron bond will always be half-covalent, half-ionic, irrespective of the bonding distance. Qualitatively, it is already clear that in the MO wave function, the ionic weight is excessive at bonding distances, and becomes an absurdity at long distances, where the weight of the ionic structures should drop to zero in accord with homolytic cleavage. The simple MO description *does not dissociate correctly* and this is the reason why it is inappropriate for the description of stretched bonds as, for example, those found in transition states. The remedy for this poor description is CI, specifically the mixing of the ground configuration, σ^2, with the diexcited one, σ^{*2}. The reason this mixing resizes the covalent versus

ionic weights is the following: If one expands the diexcited configuration, Ψ_D, into its VB constituents (for expansion technique, see Appendix A.1), one finds the same covalent and ionic components as in Eq. [15], but coupled with a negative sign as in Eq. [16]:

$$\Psi_D = |\sigma^*\overline{\sigma^*}| = -(|a\bar{b}| - |\bar{a}b|) + (|a\bar{a}| + |b\bar{b}|) \qquad [16]$$

It follows that mixing the two configurations Ψ_{MO} and Ψ_D with different coefficients as in Eq. [17] will lead to a wave function Ψ_{MO-CI} in which the covalent and ionic components have

$$\Psi_{MO-CI} = c_1|\sigma\overline{\sigma}| - c_2|\sigma^*\overline{\sigma^*}| \qquad c_1, c_2 > 0 \qquad [17]$$

unequal weights, as shown by an expansion of Ψ_{MO-CI} into AO determinants in Eq. [18]:

$$\Psi_{MO-CI} = (c_1 + c_2)(|a\bar{b}| - |\bar{a}b|) + (c_1 - c_2)(|a\bar{a}| + |b\bar{b}|) \qquad [18a]$$

$$c_1 + c_2 = \lambda \qquad c_1 - c_2 = \mu \qquad [18b]$$

Since c_1 and c_2 are variationally optimized, expansion of Ψ_{MO-CI} should lead to exactly the same VB function as $\Psi_{VB-full}$ in Eq. [5], leading to the equalities expressed in Eq. [18b] and to the equivalence of Ψ_{MO-CI} and $\Psi_{VB-full}$. The equivalence also includes the Coulson–Fischer wave function Ψ_{CF} (Eq. [6]) which, as we have seen, is equivalent to the VB-full description.

$$\Psi_{MO} \neq \Psi_{HL} \quad \Psi_{MO-CI} \equiv \Psi_{VB-full} \equiv \Psi_{CF} \qquad [19]$$

To summarize, the simple MO treatment describes the bond as being too ionic, while the simple VB level (Heitler–London) defines it as being purely covalent. Both theories converge to the right description when CI is introduced. The accurate description of two-electron bonding is half-way between the simple MO and simple VB levels; elaborated MO and VB levels become equivalent and converge to the right description, in which the bond is mostly covalent but has a substantial contribution from ionic structures.

This equivalence clearly indicates that the MO–VB rivalry, discussed above, is unfortunate and senseless. VB and MO are not two diametrically different theories that exclude each other, but rather two representations of reality that are mathematically equivalent. The best approach is to use these two representations jointly and benefit from their complementary insight. In fact, from the above discussion of how to write a VB wave function, it is apparent that there is a spectrum of orbital representations that stretches between the fully local VB representations through semilocalized CF orbitals, to the use of delocalized fragment orbitals VB (FO–VB), and all the way to the fully

delocalized MO representation (in the MO–CI language). Based on the problem at hand, the best representation from this spectrum should be the one that gives the clearest and most portable insight into the problem.

Formalism Using the Exact Hamiltonian

Let us turn now to the calculation of energetic quantities using exact VB theory by considering the simple case of the H_2 molecule. The exact Hamiltonian is of course the same as in MO theory, and is composed in this case of two core terms and a bielectronic repulsion:

$$H = h(1) + h(2) + 1/r_{12} + 1/R \qquad [20]$$

where the h operator represents the attraction between one electron and the nuclei, r_{12} is the interelectronic distance and R is the distance between the nuclei and accounts for nuclear repulsion. In the VB framework, some particular notations are traditionally employed to designate the various energies and matrix elements:

$$Q = \langle |a\overline{b}||H||a\overline{b}| \rangle = \langle a|h|a\rangle + \langle b|h|b\rangle + \langle ab|1/r_{12}|ab\rangle \qquad [21]$$

$$K = \langle |a\overline{b}||H||b\overline{a}| \rangle = \langle ab|1/r_{12}|ab\rangle + 2S\langle a|h|b\rangle \qquad [22]$$

$$\langle (|a\overline{b}|)|(|b\overline{a}|) \rangle = S^2 \qquad [23]$$

Here Q is the energy of a single determinant $|a\overline{b}|$, K is the spin exchange term which will be dealt with later, and S is the overlap integral between the two AOs a and b.

The energy Q has an interesting property: It is quasiconstant as a function of the interatomic distance, from infinite distance to the equilibrium bonding distance R_{eq} of H_2. It corresponds to the energy of two hydrogen atoms when brought together without exchanging their spins. Such a pseudo-state (which is not a spin-eigenfunction) is called the "quasi-classical state" of H_2 (Ψ_{QC} in Fig. 3), because all the terms of its energy have an analogue in classical (not quantum) physics. Turning now to real states, that is, spin-eigenfunctions, the energy of the ground state of H_2, in the fully covalent approximation of HL, is readily obtained.

$$E(\Psi_{HL}) = \frac{\langle (|a\overline{b}| - |\overline{a}b|)|H|(|a\overline{b}| - |\overline{a}b|)\rangle}{\langle (|a\overline{b}| - |\overline{a}b|)|(|a\overline{b}| - |\overline{a}b|)\rangle} = \frac{Q+K}{1+S^2} \qquad [24]$$

Plotting the $E(\Psi_{HL})$ curve as a function of the distance now gives qualitatively correct Morse curve behavior (Fig. 3), with a reasonable bonding energy, even if a deeper potential well can be obtained by allowing further mixing with the

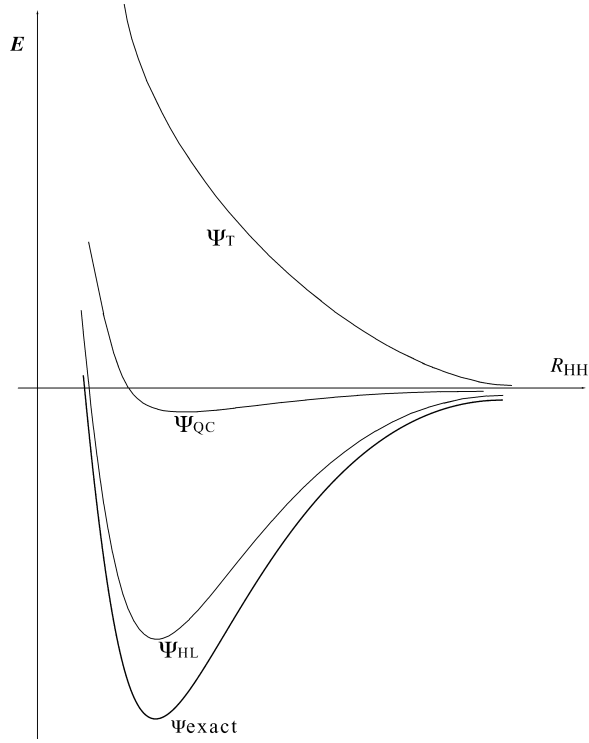

Figure 3 Energy curves for H_2 as a function of internuclear distance. The curves displayed, from top to bottom, correspond to the triplet state, Ψ_T, the quasi-classical state, Ψ_{QC}, the HL state, Ψ_{HL}, and the exact (full CI) curve, Ψ_{exact}.

ionic terms (Ψ_{exact} in Fig. 3). This shows that, in the covalent approximation, all the bonding comes from the *K* terms. Thus, *the physical phenomenon responsible for the bond is the exchange of spins between the two AOs, that is, the resonance between the two spin arrangements* (see **1**).

Examination of the *K* term in Eq. [22] shows that it is made of a repulsive exchange integral, which is positive but necessarily small (unlike Coulomb two-electron integrals), and of a negative term, given by the product of the overlap *S* and an integral that is called the "resonance integral", which is itself proportional to *S*.

Replacing Ψ_{HL} by Ψ_T in Eq. [24] leads to the energy of the triplet state, Eq. [25].

$$E(\Psi_T) = \frac{\langle (|\,a\bar{b}\,| + |\bar{a}b\,|)|\,H\,|(|\,a\bar{b}\,| + |\,\bar{a}b\,|)\,\rangle}{\langle (|\,a\bar{b}\,| + |\,\bar{a}b\,|)|(|\,a\bar{b}\,| + |\,\bar{a}b|)\rangle} = \frac{Q - K}{1 - S^2} \qquad [25]$$

Recalling that the Q integral is a quasi-constant from R_{eq} to infinite distance, Q remains nearly equal to the energy of the separated fragments and can serve, at any distance, as a reference for the bond energy. It follows from Eqs. [24] and [25] that, if we neglect overlap in the denominator, the triplet state (Ψ_T in Fig. 3) is repulsive by the same quantity ($-K$) as the singlet is bonding ($+K$). Thus, at any distance larger than R_{eq}, the bonding energy is about one-half of the singlet–triplet gap. This property will be used later in applications to reactivity.

Qualitative VB Theory

A VB calculation is just a configuration interaction in a space of AO or FO determinants, which are in general nonorthogonal to each other. It is therefore essential to derive some basic rules for calculating the overlaps and Hamiltonian matrix elements between determinants. The fully general rules have been described in detail elsewhere.[52] Examples will be given here for commonly encountered simple cases.

Overlaps between Determinants

Let us illustrate the procedure with VB determinants of the type Ω and Ω' below,

$$\Omega = N|a\bar{a}b\bar{b}| \quad \Omega' = N'|c\bar{c}d\bar{d}| \qquad [26]$$

where N and N' are normalization factors. Each determinant is made of a diagonal product of spin orbitals followed by a signed sum of all the permutations of this product, which are obtained by transposing the order of the spin orbitals. Denoting the diagonal products of Ω and Ω', by Ψ_d and Ψ'_d, respectively, the expression for Ψ_d reads

$$\Psi_d = a(1)\,\bar{a}(2)\,b(3)\,\bar{b}(4) \quad (1,2,\ldots \text{ are electron indices}) \qquad [27]$$

and an analogous expression can be written for Ψ'_d.

The overlap between the (unnormalized) determinants $|\,a\,\bar{a}\,b\,\bar{b}\,|$ and $|\,c\,\bar{c}\,d\,\bar{d}\,|$ is given by Eq. [28]:

$$\langle(|\,a\,\bar{a}\,b\,\bar{b}\,|)(|\,c\,\bar{c}\,d\,\bar{d}\,|)\rangle = \left\langle \Psi_d \middle| \sum_P (-1)^t P(\Psi'_d) \right\rangle \qquad [28]$$

where the operator P represents a *restricted subset of permutations*: The ones made of pairwise transpositions between spin orbitals of the same spin, and t determines the parity, odd or even, and hence also the sign of a given pairwise

transposition P. Note that the identity permutation is included. In the present example, there are four possible such permutations in the product Ψ'_d:

$$\sum_P (-1)^{t}P(\phi'_d) = c(1)\,\overline{c}(2)\,d(3)\,\overline{d}(4) - d(1)\,\overline{c}(2)\,c(3)\,\overline{d}(4) - c(1)\,\overline{d}(2)\,d(3)\,\overline{c}(4) + d(1)\,\overline{d}(2)\,c(3)\,\overline{c}(4) \quad [29]$$

One then integrates Eq. [28] electron by electron, leading to Eq. [30] for the overlap between $|\,a\,\overline{a}\,b\,\overline{b}\,|$ and $|\,c\,\overline{c}\,d\,\overline{d}\,|$:

$$\langle(|\,a\,\overline{a}\,b\,\overline{b}\,|)|(|\,c\,\overline{c}\,d\,\overline{d}\,|)\rangle = S_{ac}^2 S_{bd}^2 - S_{ad}S_{ac}S_{bc}S_{bd} - S_{ac}S_{ad}S_{bd}S_{bc} + S_{ad}^2 S_{bc}^2 \quad [30]$$

where S_{ac}, for example, is a simple overlap between two orbitals a and c.

Generalization to different types of determinants is trivial.[52] As an application, let us obtain the overlap of a VB determinant with itself, and calculate the normalization factor N of the determinant Ω in Eq. [26]:

$$\langle(|\,a\,\overline{a}\,b\,\overline{b}\,|)|(|\,a\,\overline{a}\,b\,\overline{b}\,|)\rangle = 1 - 2S_{ab}^2 + S_{ab}^4 \quad [31]$$

$$\Omega = (1 - 2S_{ab}^2 + S_{ab}^4)^{-1/2}|a\,\overline{a}\,b\overline{b}| \quad [32]$$

Generally, normalization factors for determinants are larger than unity. The exception is those VB determinants that do not have more than one spin orbital of each spin variety (e.g., the determinants that compose the HL wave function). For these latter determinants the normalization factor is unity (i.e., $N = 1$).

An Effective Hamiltonian

Using the exact Hamiltonian for calculating matrix elements between VB determinants would lead to complicated expressions involving numerous bielectronic integrals, owing to the $1/r_{ij}$ terms. Thus, for practical qualitative or semiquantitative applications, one uses an effective Hamiltonian in which the $1/r_{ij}$ terms are only implicitly taken into account, in an averaged manner. One then defines a Hamiltonian made of a sum of independent monoelectronic Hamiltonians, much like in simple MO theory:

$$H^{\text{eff}} = \sum_i h(i) \quad [33]$$

where the summation runs over the total number of electrons. Here the operator h has a meaning different from Eq. [20] since it is now an effective

monoelectronic operator that incorporates part of the electron–electron and nuclear–nuclear repulsions. Going back to the four–electron example above, the determinants Ω and Ω' are coupled by the following effective Hamiltonian matrix element:

$$\langle\Omega|H^{\text{eff}}|\Omega'\rangle = \langle\Omega|h(1) + h(2) + h(3) + h(4)|\Omega'\rangle \qquad [34]$$

It is apparent that the above matrix element is composed of a sum of four terms that are calculated independently. The calculation of each of these terms (e.g., the first one) is quite analogous to the calculation of the overlap in Eq. [30], except that the first monoelectronic overlap S in each product is replaced by a monoelectronic Hamiltonian term:

$$\langle(|\,\mathrm{a}\,\bar{\mathrm{a}}\,\mathrm{b}\,\bar{\mathrm{b}}\,|)|\,h(1)\,|(|\,\mathrm{c}\,\bar{\mathrm{c}}\,\mathrm{d}\,\bar{\mathrm{d}}\,|)\rangle = h_{ac}S_{ac}S_{bd}^2 - h_{ad}S_{ac}S_{bc}S_{bd} - h_{ac}S_{ad}S_{bd}S_{bc} + h_{ad}S_{ad}S_{bc}^2 \qquad [35a]$$

$$h_{\mathrm{ac}} = \langle\mathrm{a}|\mathrm{h}|\mathrm{c}\rangle \qquad [35b]$$

In Eq. [35b], the monoelectronic integral accounts for the interaction between two overlapping orbitals. A diagonal term of the type h_{aa} is interpreted as the energy of the orbital a, and will be noted ε_a in the following equations. By using Eqs. [34] and [35], it is easy to calculate the energy of the determinant $|\,\mathrm{a}\,\bar{\mathrm{a}}\,\mathrm{b}\bar{\mathrm{b}}\,|$:

$$E(|\mathrm{a}\bar{\mathrm{a}}\mathrm{b}\bar{\mathrm{b}}|) = N^2(2\varepsilon_a + 2\varepsilon_b - 2\varepsilon_a S_{ab}^2 - 2\varepsilon_b S_{ab}^2 - 4h_{ab}S_{ab} + 4h_{ab}S_{ab}^3) \qquad [36]$$

An interesting application of the above rules is the calculation of the energy of a spin-alternant determinant such as **14** in Scheme 5 for butadiene.

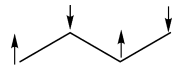

14

Scheme 5

Such a determinant, in which the spins are arranged so that two neighboring orbitals always display opposite spins is referred to as a "quasiclassical" (QC) state and is a generalization of the QC state that we already encountered above for H_2. The rigorous formulation of its energy involves some terms that arise from permutations between orbitals of the same spins, which are necessarily nonneighbors. Neglecting interactions between nonnearest neighbors, all these vanish, so that the energy of the QC state is given by the simple expression below.

$$E|\,\mathrm{a}\,\bar{\mathrm{b}}\,\mathrm{c}\,\bar{\mathrm{d}}\,| = \varepsilon_a + \varepsilon_b + \varepsilon_c + \varepsilon_d \qquad [37]$$

Generalizing, the energy of a spin-alternant determinant is always the sum of the energies of its constituent orbitals. In the QC state, the interaction between overlapping orbitals is therefore neither stabilizing nor repulsive. This is a nonbonding state, which can be used for defining a reference state, with zero energy, in the framework of VB calculations of bonding energies or repulsive interactions.

Note that the rules and formulas that are expressed above in the framework of qualitative VB theory are independent of the type of orbitals that are used in the VB determinants: purely localized AOs, fragment orbitals or Coulson–Fischer semilocalized orbitals. Depending on the kind of orbitals that are chosen, the h and S integrals take different values, but the formulas remain the same.

Some Simple Formulas for Elementary Interactions

In qualitative VB theory, it is customary to take the average value of the orbital energies as the origin for various quantities. With this convention, and using some simple algebra,[52] the monoelectronic Hamiltonian between two orbitals becomes β_{ab}, the familiar "reduced resonance integral":

$$\beta_{ab} = h_{ab} - 0.5(h_{aa} + h_{bb})S_{ab} \qquad [38]$$

It is important to note that these β integrals, used in the VB framework are the same as those used in simple MO models such as extended Hückel theory.

Based on the new energy scale, the sum of orbital energies is set to zero, that is:

$$\sum_i \varepsilon_i = 0 \qquad [39]$$

In addition, since the energy of the QC determinant is given by the sum of orbital energies, its energy then becomes zero:

$$E(|\,\mathrm{a}\,\overline{\mathrm{b}}\,\mathrm{c}\,\overline{\mathrm{d}}\,|) = 0 \qquad [40]$$

The Two-Electron Bond

By application of the qualitative VB theory, Eq. [41] expresses the HL-bond energy of two electrons in atomic orbitals a and b, which belong to the atomic centers A and B. The binding energy D_e is defined relative to the quasiclassical state $|\,a\overline{b}\,|$ or to the energy of the separate atoms, which are equal within the approximation scheme.

$$D_e(\mathrm{A{-}B}) = 2\beta S/(1 + S^2) \qquad [41]$$

Here, β is the reduced resonance integral that we have just defined and S is the overlap between orbitals a and b. Note that if instead of using purely localized AOs for a and b, we use semilocalized Coulson–Fischer orbitals, Eq. [41] will not be the simple HL-bond energy but would represent *the bonding energy of the real A—B bond* that includes its optimized covalent and ionic components. In this case, the origins of the energy would still correspond to the QC determinant with the localized orbitals. Unless otherwise specified, we will always use qualitative VB theory with this latter convention.

Repulsive Interactions

By using the above definitions, one gets the following expression for the repulsive energy of the triplet state:

$$\Delta E_T(\mathrm{A} \uparrow\uparrow \mathrm{B}) = -2\beta S/(1 - S^2) \qquad [42]$$

The triplet repulsion arises due to the Pauli exclusion rule and is often referred to as a Pauli repulsion.

For a situation where we have four electrons on the two centers, VB theory predicts a doubling of the Pauli repulsion, and the following expression is obtained in complete analogy to qualitative MO theory:

$$\Delta E(\mathrm{A}\!:\!:\!\mathrm{B}) = -4\beta S/(1 - S^2) \qquad [43]$$

One can, in fact, simply generalize the rules for Pauli repulsion. Thus, the electronic repulsion in an interacting system is equal to the quantity:

$$\Delta E_{\mathrm{rep}} = -2n\beta S/(1 - S^2) \qquad [44]$$

n being the number of electron pairs with identical spins.

Now, consider VB structures with three electrons on two centers, (A:$^{\bullet}$B) and (A$^{\bullet}$:B). The interaction energy of each one of these structures by itself is repulsive and following Eq. [42] will be given by the Pauli repulsion term in Eq. [45]:

$$\Delta E((\mathrm{A}\!:\!^{\bullet}\mathrm{B}) \quad \text{and} \quad (\mathrm{A}^{\bullet}\!:\!\mathrm{B})) = -2\beta S/(1 - S^2) \qquad [45]$$

Mixing Rules for VB Structures

Whenever a wave function is written as a normalized resonance hybrid between two VB structures of equivalent energies (e.g, as in Eq. [46], the energy of the hybrid is given by the normalized averaged self-energies of the constituent resonance structures and the interaction matrix element, H_{12},

between the structures in Eq. [47].

$$\Psi = N[\Phi_1 + \Phi_2]$$
$$\text{where} \quad N = 1/[2(1 + S_{12})]^{1/2} \qquad [46]$$
$$E(\Psi) = 2N^2 E_{\text{av}} + 2N^2 H_{12}$$
$$\text{where} \quad H_{12} = \langle \Phi_1 | \mathbf{H} | \Phi_2 \rangle \quad \text{and} \quad E_{\text{av}} = [(E_1 + E_2)/2] \qquad [47]$$

Such a mixed state is stabilized relative to the energy of each individual VB structure, by a quantity that is called the "resonance energy" (*RE*):

$$\text{RE} = [H_{12} - E_{\text{av}} S_{12}]/(1 + S_{12}) \quad S_{12} = \langle \Phi_1 | \Phi_2 \rangle \qquad [48]$$

Equation [48] expresses the RE in the case where the two limiting structures Φ_1 and Φ_2 have equal or nearly equal energies, which is the most favorable situation for maximum stabilization. However, if the energies E_1 and E_2 are different, then according to the rules of perturbation theory, the stabilization will still be significant, albeit than in the degenerate case.

A typical situation where the VB wave function is written as a resonance hybrid is odd-electron bonding (one-electron or three-electron bonds). For example, a one-electron bond A•B is a situation where only one electron is shared by two centers A and B (Eq. [49]), while three electrons are distributed over the two centers in a three-electron bond A.˙.B (Eq. [50]):

$$\text{A•B} = \text{A}^{+}\text{•B} \leftrightarrow \text{A•}^{+}\text{B} \qquad [49]$$
$$\text{A}.\dot{.}\text{B} = \text{A•:B} \leftrightarrow \text{A:•B} \qquad [50]$$

Simple algebra shows that the overlap between the two VB structures is equal to S (the $\langle \text{a}|\text{b} \rangle$ orbital overlap)[a] and that resonance energy follows Eq. [51]:

$$\text{RE} = \beta/(1 + S) = D_e(\text{A}^{+}\text{•B} \leftrightarrow \text{A•}^{+}\text{B}) \qquad [51]$$

Equation [51] also gives the bonding energy of a one-electron bond. Combining Eqs. [45] and [51], we get the bonding energy of the three-electron bond, Eq. [52]:

$$D_e(\text{A•:B} \leftrightarrow \text{A:•B}) = -2\beta S/(1 - S^2) + \beta/(1 + S)$$
$$= \beta(1 - 3S)/(1 - S^2) \qquad [52]$$

[a] Writing ϕ_1 and ϕ_2 so that their positive combination is the resonance-stabilized one.

These equations for odd-electron bonding energies are good for cases where the forms are degenerate or nearly so. In cases where the two structures are not identical in energy, one should use the perturbation theoretic expression.[52]

For more complex situations, general guidelines for derivation of matrix elements between polyelectronic determinants are given in Appendix A.2. Alternatively, one could follow the protocol given in the original literature.[52,143]

Nonbonding Interactions in VB Theory

Some situations are encountered where one orbital bears an unpaired electron in the vicinity of a bond, such as **15** in Scheme 6:

15

Scheme 6

Since A•B•—•C displays a singlet coupling between orbitals *b* and *c*, Eq. [53] gives its wave function:

$$\text{A•B•—•C} = \text{N}(|\text{a b}\,\overline{\text{c}}| - |\text{a}\,\overline{\text{b}}\,\text{c}|) \qquad [53]$$

in which it is apparent that the first determinant involves a triplet repulsion with respect to the electrons in a and b while the second one is a spin-alternant determinant. The energy of this state, relative to a situation where A and BC are separated, is therefore:

$$E(\text{A•B•—•C}) - E(\text{A}) - E(\text{B•—•C}) = -\beta S/(1 - S^2) \qquad [54]$$

which means that bringing an unpaired electron into the vicinity of a covalent bond results in half of the full triplet repulsion. This property will be used below when we discuss VB correlation diagrams for radical reactions. The

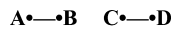

16

Scheme 7

repulsion is the same if we bring two covalent bonds, A•—•B and C•—•D, close to each other, as in **16** (Scheme 7):

$$E(\text{A•—•B}\cdots\text{C•—•D}) - E(\text{A•—•B}) - E(\text{C•—•D}) = -\beta S/(1 - S^2) \qquad [55]$$

Equation [55] can be used to calculate the total π energy of one canonical structure of a polyene, for example, structure **17** of butadiene (Scheme 8).

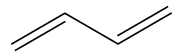

17

Scheme 8

Since there are two covalent bonds and one nonbonded repulsion in this VB structure, its energy is expressed simply as follows:

$$\Psi(\mathbf{17}) = 4\beta S/(1 + S^2) - \beta S/(1 - S^2) \qquad [56]$$

As an application, let us compare the energies of two isomers of hexatriene. The linear s-trans conformation can be described as a resonance between the canonical structure **18** and "long bond" structures **19–21** (Scheme 9)

18 **19** **20** **21**

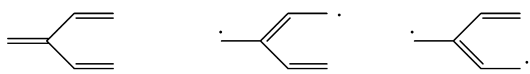

22 **23** **24**

Scheme 9

where one short bond is replaced by a long bond. On the other hand, the branched isomer is made only of structures **22–24**, since it lacks an analogous structure to **21**.

It is apparent that the canonical structures **18** and **22** have the same electronic energies (three bonds, two nonbonded repulsions), and that structures **19–21**, **23**, and **24** are also degenerate (two bonds, three nonbonded repulsions). Furthermore, if one omits structure **21**, the matrix elements between the remaining long-bond structures and the canonical ones are all the same. Thus, elimination of structure **21** will make both isomers isoenergetic. If, however, we take structure **21** into account, it will mix and increase, however, slightly, the RE of the linear polyene that becomes thermodynamically more stable than the branched one. This subtle prediction, which is in agreement with experiment, will be demonstrated again below in the framework of Heisenberg Hamiltonians.

Table 1 Elementary Interaction Energies in the Qualitative MO and VB Models

Type of Interaction	Stabilization (MO Model)	Stabilization (VB Model)
1-Electron	$\beta/(1+S)$	$\beta/(1+S)$
2-Electron	$2\beta/(1+S)$	$2\beta S/(1+S^2)$
3-Electron	$\beta(1-3S)/(1-S^2)$	$\beta(1-3S)/(1-S^2)$
4-Electron	$-4\beta S/(1-S^2)$	$-4\beta S/(1-S^2)$
Triplet repulsion	$-2\beta S/(1-S^2)$	$-2\beta S/(1-S^2)$
3-Electron repulsion		$-2\beta S/(1-S^2)$

Comparison with Qualitative MO Theory

Some (but not all) of the elementary interaction energies that are discussed above also have qualitative MO expressions, which may or may not match the VB expressions. In qualitative MO theory, the interaction between two overlapping AOs leads to a pair of bonding and antibonding MOs, the former being stabilized by the quantity $\beta/(1+S)$ and the latter destabilized by $-\beta/(1-S)$ relative to the nonbonding level. The stabilization–destabilization of the interacting system relative to the separate fragments is then calculated by summing up the occupancy-weighted energies of the MOs. A comparison of the qualitative VB and MO approaches is given in Table 1, where the energetics of the elementary interactions are calculated with both methods. It is apparent that both qualitative theories give identical expressions for the odd-electron bonds, the four-electron repulsion, and the triplet repulsion. This is not surprising if one notes that the MO and VB wave functions for these four types of interaction are identical. On the other hand, the expressions for the MO and VB two-electron-bonding energies are different; the difference is related to the fact, discussed above, that MO and VB wave functions are themselves different in this case. Therefore, we suggest a rule that may be useful if one is more familiar with MO theory than VB: *Whenever the VB and MO wave functions of an electronic state are equivalent, the VB energy can be estimated using qualitative MO theory.*

INSIGHTS OF QUALITATIVE VB THEORY

This section demonstrates how the simple rules of the above VB approach can be utilized to treat a variety of problems. Initially, we treat a series of examples, which were mentioned in the introduction as "failures" of VB theory, and show that properly done VB theory leads to the right result for the right reason. Subsequently, we proceed with a relatively simple problem in chemical bonding of one-electron versus two-electron bonds and demonstrate that VB theory can make surprising predictions that stand the

test of experiment. Finally, we show how VB theory can lead to a general model for chemical reactivity, the VB diagram. Since these subtopics cover a wide range of chemical problems we cannot obviously treat them in-depth, and wherever possible we refer the reader to more extensive reviews.

Are the "Failures" of VB Theory Real?

As mentioned in the introduction, VB theory has been accused of a few "failures" that are occasionally used to dismiss the theory, and have caused it to have an unwarranted reputation. The next few subsections use the simple VB guidelines drawn above to demonstrate that VB theory is free of these "failures".

Dioxygen

One of the major "failures" that has been associated with VB theory concerns the ground state of the dioxygen molecule, O_2. It is true that a naive application of hybridization followed by perfect pairing (simple Lewis pairing) would predict a $^1\Delta_g$ ground state, that is, the diamagnetic doubly bonded molecule O=O. This is likely the origin of the notion that VB theory makes a flawed prediction that contradicts experiment (see, e.g., references [50] and [51]). However, this conclusion is not valid, since in the early 1970s Goddard et al.[107] performed GVB calculations and demonstrated that VB theory predicts a triplet $^3\Sigma_g^-$ ground state. This same outcome was reported in papers by McWeeny[144] and Harcourt.[145] In fact, any VB calculation, at whatever imagined level, would lead to the same result, so the myth of "failure" is definitely baseless.

Goddard et al.[107] and subsequently the present two authors[53] also provided a simple VB explanation for the choice of the ground state. Let us reiterate this explanation based on our qualitative VB theory, outlined above.

Apart from one σ bond and one σ lone pair on each oxygen atom, the dioxygen molecule has six π electrons to be distributed in the two π planes, say π_x and π_y. The question is What is the most favorable mode of distribution? Is it **25** in which three electrons are placed in each π plane, or perhaps is it **26** where two electrons are allocated to one plane and four to the other (Scheme 10)? Obviously, **25** is a diradical structure displaying one three-electron bond

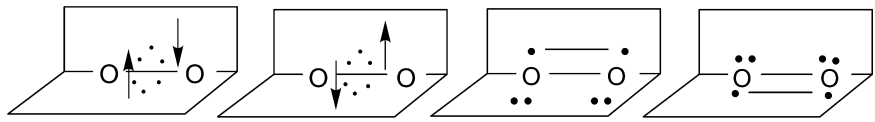

25 **25'** **26** **26'**

Scheme 10

in each of π planes, whereas **26** exhibits a singlet π bond, in one plane, and a four-electron repulsion, in the other. A naive application that neglects the repulsive three-electron and four-electron interactions would predict that structure **26** is preferred, leading to the above-mentioned legendary failure of VB theory, namely, that VB predicts the ground state of O_2 to be the singlet closed-shell structure, O=O. Inspection of the repulsive interactions shows that they are of the same order of magnitude or even larger than the bonding interactions, that is, the neglect of these repulsion is unjustified. The right answer is immediately apparent, if we carry out the VB calculation correctly, including the repulsion and bonding interactions for structures **25** and **26**. The resulting expressions and the respective energy difference, which are shown in Eqs. [57–59], demonstrate clearly that the diradical structure **25** is more stable than the doubly bonded Lewis structures **26**.

$$E(\mathbf{25}) = 2\beta(1 - 3S)/(1 - S^2) \quad [57]$$

$$E(\mathbf{26}) = 2\beta S/(1 + S^2) - 4\beta S/(1 - S^2) \quad [58]$$

$$E(\mathbf{26}) - E(\mathbf{25}) = -2\beta(1 - S)^2/(1 - S^4) > 0 \quad [59]$$

Thus far we have not considered the set of Slater determinants **25′** and **26′**, which are symmetry-equivalent to **25** and **26** by inversion of the π_x and π_y planes. The interactions between the two sets of determinants yield two pairs of resonant–antiresonant combinations that constitute the final low-lying states of dioxygen, as represented in Figure 4. Of course, our effective VB theory was chosen to disregard the bielectronic terms and, therefore, the theory, as

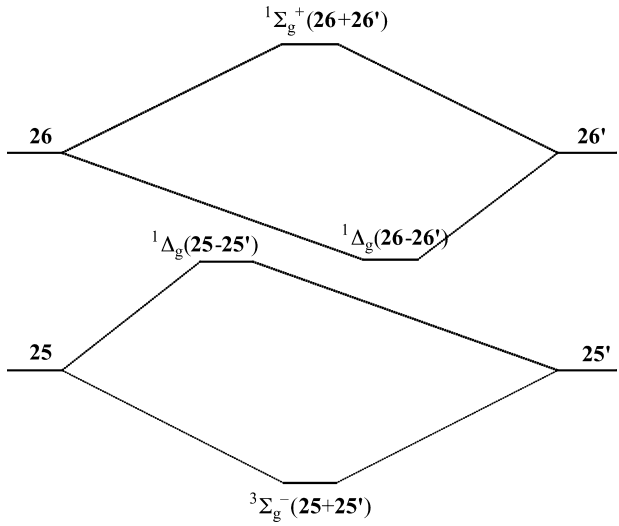

Figure 4 Formation of the symmetry adapted states of O_2 from the biradical (**25**, **25′**) and perfectly-paired (**26**, **26'**) structures.

such, will not tell us what the lowest spin state in the O_2 diradical is. This, however, is a simple matter, because further considerations can be made by appealing to Hund's rule, which is precisely what qualitative MO theory must do in order to predict the triplet nature of the O_2 ground state. Accordingly, the in-phase and out-of-phase combinations of the diradical determinants **25** and **25′** lead to triplet ($^3\Sigma_g^-$) and singlet ($^1\Delta_g$) states, respectively, the former being the lowest state by virtue of favorable exchange energy.

Similarly, **26** and **26′** yield a resonant $^1\Delta_g$ combination and an antiresonant $^1\Sigma_g^+$ one. Thus, it is seen that simple qualitative VB considerations not only predict the ground state of O_2 to be a triplet, but also yield a correct energy ordering for the remaining low-lying excited states.

The Valence Ionization Spectrum of CH_4

As discussed in the introduction, the development of PES showed that the spectra could be simply interpreted if one assumed that electrons occupy delocalized molecular orbitals.[47,48] By contrast, VB theory, which uses localized bond orbitals (LBOs), seems completely useless for interpretation of PES. Moreover, since VB theory describes equivalent electron pairs that occupy LBOs, the PES results seem to be in disagreement with this theory. An iconic example of this "failure" of VB theory is the PES of methane that displays two different ionization peaks. These peaks correspond to the a_1 and t_2 MOs, but not to the four equivalent C—H LBOs in Pauling's hybridization theory.

Let us now examine the problem carefully in terms of LBOs to demonstrate that VB gives the right result for the right reason. A physically correct representation of the CH_4^+ cation would be a linear combination of the four forms such that the wave function does not distinguish the four LBOs that are related by symmetry. The corresponding VB picture, more specifically an FO–VB picture, is illustrated in Figure 5, which enumerates the VB structures and their respective determinants. Each VB structure involves a localized one-electron bond situation, while the other bonds are described by doubly occupied LBOs. To make life easier, we can use LBOs that derive from a unitary transformation of the canonical MOs. As such, these LBOs would be orthogonal to each other and one can calculate the Hamiltonian matrix element between two such VB structures by simply setting all overlaps to zero in the VB expressions, or by using the equivalent rules of qualitative MO theory. Thus, to calculate the Φ_1–Φ_2 interaction matrix element, one first puts the orbitals of both determinants in maximal correspondence, by means of a transposition in Φ_2. The resulting two transformed determinants differ by only one spin orbital, $c \neq d$, so that their matrix element is simply β. Going back to the original Φ_1 and Φ_2 determinants, it appears that their matrix element is negatively signed (Eq. [60]),

$$\begin{aligned}\langle\Phi_1|H^{\text{eff}}|\Phi_2\rangle &= \langle(|\,\mathrm{a}\,\overline{\mathrm{a}}\,\mathrm{b}\,\overline{\mathrm{b}}\,\mathrm{c}\,\overline{\mathrm{c}}\,\mathrm{d}\,|)|\,H^{\text{eff}}\,|(|\,\mathrm{d}\,\overline{\mathrm{d}}\,\mathrm{a}\,\overline{\mathrm{a}}\,\mathrm{b}\,\overline{\mathrm{b}}\,\mathrm{c}\,|)\rangle \\ &= -\langle(|\,\mathrm{a}\,\overline{\mathrm{a}}\,\mathrm{b}\,\overline{\mathrm{b}}\,\mathrm{c}\,\overline{\mathrm{c}}\,\mathrm{d}\,|)|\,H^{\text{eff}}\,|(|\,\mathrm{a}\,\overline{\mathrm{a}}\,\mathrm{b}\,\overline{\mathrm{b}}\,\mathrm{c}\,\overline{\mathrm{d}}\,\mathrm{d}\,|)\rangle = -\beta \qquad [60]\end{aligned}$$

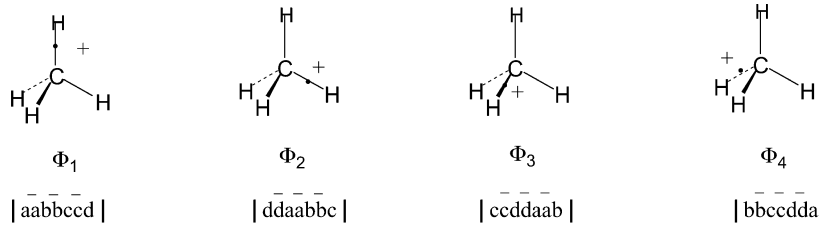

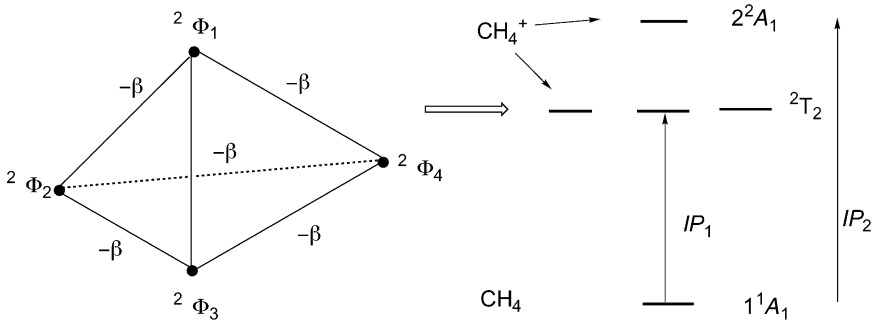

Figure 5 Generation of the $^2T_2$ and 2^2A_1 states of CH_4^+, by VB mixing of the four localized structures. The matrix elements between the structures, shown graphically, leads to the three-below-one splitting of the states, and to the observations of two ionization potential peaks in the PES spectrum (adapted from Ref. 61 with permission of Helvetica Chemica Acta).

and this can be generalized to any pair of Φ_i–Φ_j VB structure in Figure 5.

$$\langle \Phi_i | H^{\text{eff}} | \Phi_j \rangle = -\beta \qquad [61]$$

There remains to diagonalize the Hamiltonian matrix in the space of the four configurations, Φ_1–Φ_4, to get the four states of CH_4^+. This can be done by diagonalizing a matrix of Hückel type, with the only difference being that the β matrix elements have a negative sign, as shown below in Scheme 11.

$$\begin{vmatrix} -E & -\beta & -\beta & -\beta \\ -\beta & -E & -\beta & -\beta \\ -\beta & -\beta & -E & -\beta \\ -\beta & -\beta & -\beta & -E \end{vmatrix} = 0$$

Scheme 11

The diagonalization can be done using a Hückel program; however, the result can be found even without any calculation (e.g, by use of symmetry projection operators of the T_d point group). Diagonalization of the above Hückel matrix, with negatively signed β leads to the final states of CH_4^+, shown alongside the interaction graph in Figure 5. These cationic states exhibit a three-below-one splitting (i.e., a low-lying triply degenerate $^2T_2$ state and above it a $^2A_1$ state). The importance of the sign of the matrix element can be appreciated by diagonalizing the above Hückel matrix using a positively signed β. Doing that would have reversed the state ordering to one-below-three, which is of course incorrect. Thus, simple VB theory correctly predicts that methane will have two ionization peaks, one (IP_1) at lower energy corresponding to transition to the degenerate $^2T_2$ state and one (IP_2) at a higher energy corresponding to transition to the $^2A_1$ state. The facility of making this prediction and its agreement with experiment show once more that, here, too, the "failure" of VB theory is due more to a myth that caught on due to the naivety of the initial argument than to any true failure of VB.

Aromaticity–Antiaromaticity

As discussed in the introduction, simple resonance theory completely fails to predict the fundamental differences between $C_5H_5^+$ and $C_5H_5^-$, $C_3H_3^+$, and $C_3H_3^-$, $C_7H_7^+$, and $C_7H_7^-$, and so on. Hence, a decisive defeat was dealt to VB theory when, during the 1950–1960s, organic chemists were finally able to synthesize these transient molecules and establish their stability patterns (which followed Hückel rules) with no guide or insight coming from resonance theory. We shall now demonstrate (which has been known for quite a while[52,146,147]) that the simple VB theory outlined above is capable of deriving the celebrated $4n + 2/4n$ dichotomy for these ions.

As an example, we compare the singlet and triplet states of the cyclopropenium molecular ions, $C_3H_3^+$ and $C_3H_3^-$, shown in Figures 6 and 7. The VB configurations needed to generate the singlet and triplet states of the equilateral triangle $C_3H_3^+$ are shown in Figure 6. It is seen that the structures can be generated from one another by shifting single electrons from a singly occupied p_π orbital to a vacant one. By using the guidelines for VB matrix elements (see Appendix A.2), we deduce that the leading matrix element between any pair of structures with singlet spins is $+\beta$, while for any pair with triplet spin the matrix element is $-\beta$. The corresponding configurations of $C_3H_3^-$ are shown in Figure 7. In this case, the signs of the matrix elements are inverted compared with the case of the cyclopropenium cation, and are $-\beta$ for any pair of singlet VB structures, and $+\beta$ for any pair of triplet structures.

If we symbolize the VB configurations by heavy dots we can present these resonance interactions graphically, as shown in the mid-parts of Figures 6 and 7. These interaction graphs are all triangles and have the topology of corresponding Hückel and Möbius AO interactions.[148] Of course, one could diagonalize the corresponding Hückel–Möbius matrices and obtain energy levels

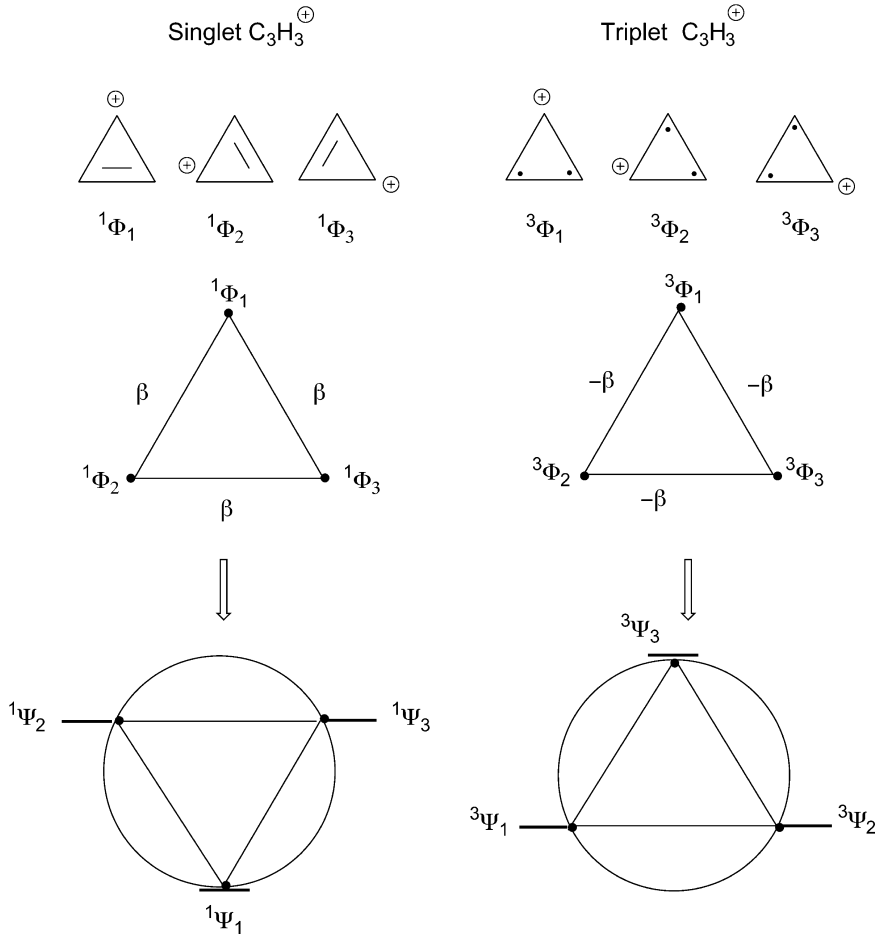

Figure 6 The VB structures for singlet and triplet states of $C_3H_3^+$, along with the graphical representation of their interaction matrix elements (adapted from Ref. 61 with permission of Helvetica Chemica Acta). The spread of the states is easily predicted from the circle mnemonic used in simple Hückel theory. The expressions for the VB structures are deduced from each other by circular permutations: $^1\Phi_1 = |a\bar{b}| - |\bar{a}\,b|$, $^1\Phi_2 = |b\bar{c}| - |\bar{b}\,c|$, $^1\Phi_3 = |c\bar{a}| - |\bar{c}\,a|$, $^3\Phi_1 = |ab|$, $^3\Phi_1 = |bc|$, $^3\Phi_1 = |ca|$.

and wave functions, but a shortcut based on the well-known mnemonic of Frost and Musulin[149] exists. A triangle is inscribed within a circle having a radius $2|\beta|$, and the energy levels are obtained from the points where the vertices of the triangle touch the circle. Using this mnemonic for the VB mixing shows that the ground state of $C_3H_3^+$ is a singlet state, while the triplet state is higher lying and doubly degenerate. By contrast, the ground state of $C_3H_3^-$ is a triplet state, while the singlet state is higher lying, doubly degenerate, and

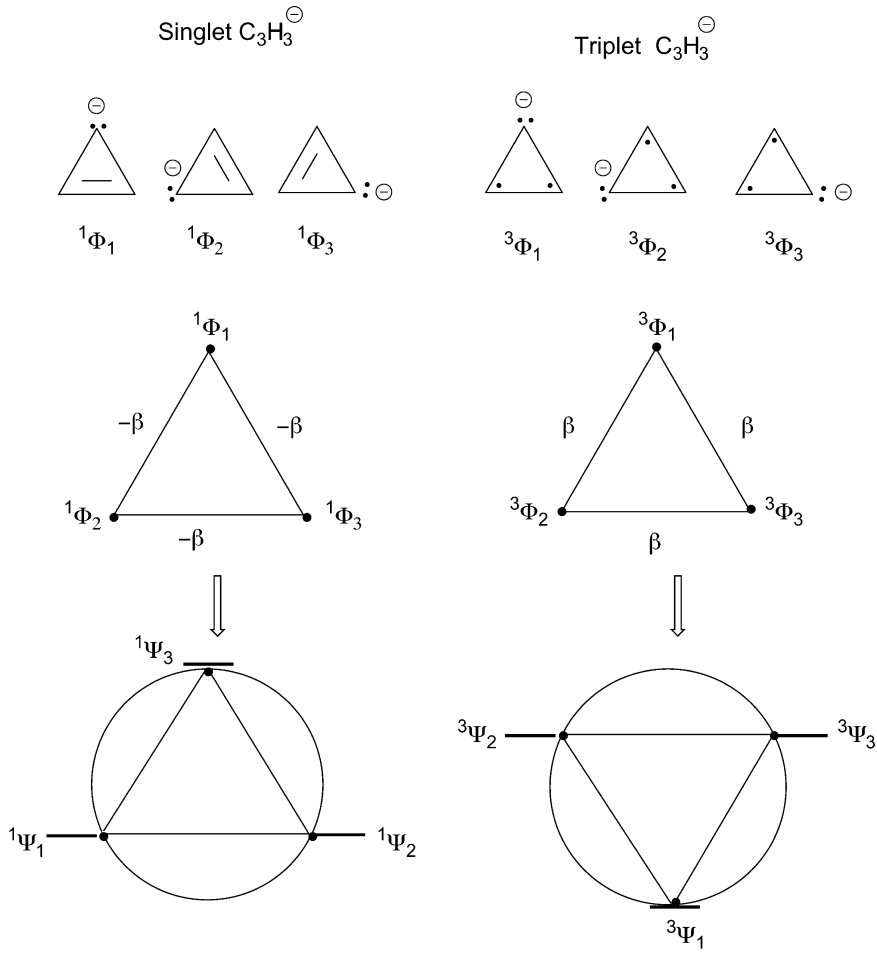

Figure 7 The VB structures for singlet and triplet states of $C_3H_3^-$, along with the graphical representation of their interaction matrix elements (adapted from Ref. 61 with permission of Helvetica Chemica Acta). The spread of the states is easily predicted from the circle mnemonic used in simple Hückel theory. The expressions for the VB structures are deduced from each other by circular permutations: $^1\Phi_1 = |a\bar{b}\,c\bar{c}| - |\bar{a}\,bc\bar{c}|$, $^1\Phi_2 = |b\bar{c}\,a\bar{a}| - |\bar{b}\,c\,a\,\bar{a}|$, $^1\Phi_3 = |c\bar{a}\,b\bar{b}| - |\bar{c}\,a\,b\bar{b}|$, $^3\Phi_1 = |a\,b\,c\bar{c}|$, $^3\Phi_1 = |bc\,a\bar{a}|$, $^3\Phi_1 = |ca\,b\bar{b}|$.

hence Jahn-Teller unstable. Thus, $C_3H_3^+$ is aromatic, while $C_3H_3^-$ is antiaromatic.[52]

In a similar manner, the VB states for $C_5H_5^+$ and $C_5H_5^-$ can be constructed. Restricting the treatment to the lowest energy structures, there remain five structures for each spin state, and the sign of the matrix elements will be inverted compared to the $C_3H_3^{-,+}$ cases. The cation will have $-\beta$ matrix

elements for the singlet configurations and $+\beta$ for the triplets, while the anion will have the opposite signs. The VB-mnemonic shows that $C_5H_5^-$ possesses a singlet ground state, and by contrast, $C_5H_5^+$ has a triplet ground state, whereas its singlet state is higher in energy and Jahn–Teller unstable. Thus, in the cyclopentadienyl ions, the cation is antiaromatic while the anion is aromatic.

Moving next to the $C_7H_7^{+,-}$ species, the sign patterns of the matrix element will invert again and agree with those in the $C_3H_3^{+,-}$ case. As such, the VB-mnemonic will lead to similar conclusions, that is, that the cation is aromatic, while the anion is antiaromatic with a triplet ground state. Thus, the sign patterns of the β-matrix element, and hence also the ground state's stability obey the $4n/4n+2$ dichotomy.

Clearly, a rather simple VB theory is all that is required to reproduce the rules of aromaticity and antiaromaticity of the molecular ions, and to provide the correct relative energy levels of the corresponding singlet and triplet states. This VB treatment is virtually as simple as HMO theory itself, with the exception of the need to know the sign of the VB matrix element. But, with some practice, this can be learned.

Another highly cited "failure" of VB theory concerns the treatments of antiaromatic molecules such as CBD and COT versus aromatic ones like benzene. The argument goes as follows: Since benzene, CBD, and COT can all be expressed as resonance hybrids of their respective Kekulé structures, they should have similar properties, and since they do not, this must mean that VB theory fails. As we have already stressed, this is a failure of resonance theory that simply enumerates resonance structures, but not of VB theory. Indeed, at the ab initio level, Voter and Goddard[58] demonstrated that GVB calculations, predict correctly the properties of CBD. Subsequently, Gerratt and coworkers[150,151] showed that spin-coupled VB theory correctly predicts the geometries and ground states of CBD and COT. Recently, in 2001, the present authors and their co-workers used VB theory to demonstrate[57] that (a) the vertical *RE* of benzene is larger than that of CBD and COT, and (b) the standard Dewar resonance energy (DRE) of benzene is 21 kcal/mol, while that for CBD is negative, in perfect accord with experiment. Thus, properly done ab initio VB theory indeed succeeds with CBD, COT, or with any other antiaromatic species. A detailed analysis of these results for benzene CBD and COT, has been given elsewhere[55,152] but is beyond the scope of this chapter.

Can VB Theory Bring New Insight into Chemical Bonding?

The idea that a one-electron bond might be stronger than a two-electron bond between the same atoms sounds unnatural in simple-MO theory. How could two bonding electrons stabilize a molecular interaction less than a single one? If we take a common interatomic distance for the two kinds of bonds, the one-electron bonding energy should be half the two-electron bonding energy

according to the qualitative MO formulas in Table 1. Relaxing the bond length should disfavor the one-electron bond even more than the two-electron one, since the latter is shorter and enjoys larger overlap between the fragments' orbitals.

The simple VB model makes a very different prediction. By using VB formulas, an overlap-dependent expression is found for the ratio of one-electron to two-electron bonding energies (Table 1 and Eq. [62]):

$$\frac{D_e(1-\mathrm{e})}{D_e(2-\mathrm{e})} = \frac{1+S^2}{2S(1+S)} \qquad [62]$$

According to Eq. [62], the one-electron bond is weaker than the two-electron bond in the case of strong overlap (typically the H_2^+/H_2 case), but the reverse is true if the overlap S is smaller than a critical value of 0.414. There are many chemical species that possess smaller overlap than this critical value (e.g., alkali dimers and other weak binders). By contrast, strong binders like H, C, and so on, usually maintain larger overlaps, $S \geq 0.5$. The qualitative prediction based on Eq. [62], compares favorably with experimental and computational data. Indeed the binding energy of the two-electron bond in H_2 (4.75 eV) is somewhat less than twice that of the one-electron bond in H_2^+ (2.78 eV). In contrast, comparing Li_2^+ and Li_2 leads to the intriguing experimental result that the binding energy for Li_2^+ (1.29 eV) is *larger* than that for Li_2 (1.09 eV), which is in agreement with the VB model but at variance with qualitative MO theory.

What is the reason for the discrepancy of the MO and VB approaches? As we have seen, the qualitative expression for the odd-electron bonding energies is the same in both theories. However, the two-electron bonding energies are different. Assuming that the β integral is proportional to the overlap S, the two-electron bonding energy is a linear function of S in the MO model, but a quadratic function of S in the VB model. It follows that, for large overlaps, the VB and MO models more or less agree with each other, while they qualitatively differ for weak overlaps. In this latter case, the VB model predicts a larger one-electron versus two-electron ratio of bonding energies than the MO model. Note that the reasoning can be extended to three-electron bonds as well: for weakly overlapping binders, the VB model predicts that three-electron bonds might approach the strength of the corresponding two-electron bonds. In comparison, application of simple MO theory would have predicted that any three-electron bond energy should always be less than one-half of the corresponding two-electron bond energy, for any overlap. In agreement with the VB prediction, the three-electron bond in F_2^-, in which the two interacting orbitals have a typically weak overlap (~0.10), has a binding energy of 1.31 eV, not much smaller than the two-electron bonding energy of F_2 which is no larger than 1.66 eV.

Insight into bonding is not limited to this example. In fact, VB theory gives rise to new bonding paradigms that are discussed in the literature but are not reviewed here for lack of space. One such paradigm is called "charge-shift bonding" and concerns two-electron bonds that are neither covalent nor ionic but whose bonding energy is dominated by the covalent–ionic resonance interaction; for example, F—F and O—O are charge-shift bonds.[153–155] Another paradigm is the "ferromagnetic-bonding" that occurs in high-spin clusters (e.g., $^{n+1}Li_n$) that are devoid of electron pairs.[156,157]

VB Diagrams for Chemical Reactivity

One advantage of representing reactions in terms of VB configurations is the unique and unified insight that it brings to reactivity problems. The centerpiece of the VB diagram model is the VB correlation diagram that traces the energy of the VB configurations along the reaction coordinate. The subsequent configuration mixing reveals the cause of the barrier, the nature of the transition state, and the reasons for occurrence of intermediates. Furthermore, the diagram allows qualitative and semiquantitative predictions to be made about a variety of reactivity problems, ranging from barrier heights, stereo- and regio-selectivities, and mechanistic alternatives. Since its derivation, via the projection of MO-based wave functions along the reaction coordinate,[81] the VB diagram model has been applied qualitatively[53,83–85,158] as well as quantitatively by direct computation of the VB diagram;[159–168] as such this is a qualitative model with an isomorphic quantitative analogue.

The straightforward representation of the VB diagram focuses on the "active bonds", those that are being broken or made during the reaction. Of course, it is the localized nature of the electron pairs in the VB representation that makes this focusing possible. The entire gamut of reactivity phenomena requires merely two generic diagrams, which are depicted schematically in Figure 8, and that enable a systematic view of reactivity. The first is a diagram of two interacting states, called a VB state correlation diagram (VBSCD), which describes the formation of a barrier in a single chemical step due to avoided crossing or resonance mixing of the VB states that describe reactants and products. The second is a three-curve diagram (or generally a many-curve diagram), called a VB configuration-mixing diagram (VBCMD), which describes a stepwise mechanism derived from the avoided crossing and VB mixing of the three curves or more. The ideas of curve crossing and avoided crossing were put to use in the early days of VB theory by London, Eyring, Polanyi, and Evans, who pioneered the implementation of VB computation as a means of generating potential energy surfaces and locating transition states. In this respect, the VB diagrams (VBSCD and VBCMD) are developments of these early ideas into a versatile system of thought that allows prediction of a variety of reactivity patterns from properties of the reactants and products.

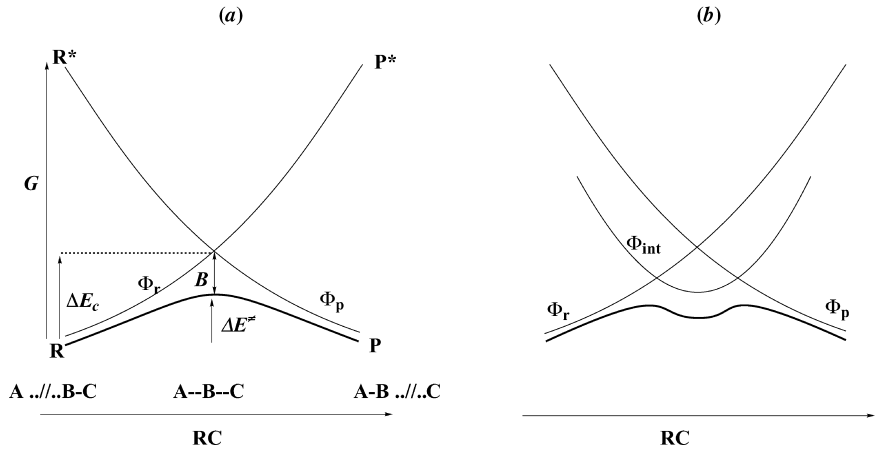

Figure 8 The VB diagrams for conceptualizing chemical reactivity: (*a*) VBSCD showing the mechanism of barrier formation by avoided crossing of two curves of reactant and product type state curves. (*b*) VBCMD showing the formation of a reaction intermediate. The final adiabatic states are drawn in bold curves.

A review of both kinds of VB diagrams has recently appeared,[85] and we refer the reader to this review paper for comprehensive information. Here we will concentrate on diagrams of the first type, VBSCD, and give a brief account of their practical use.

The VBSCDs apply to the general category of reactions that can be described as the interplay of two major VB structures, that of the reactants (A/B—C in Fig. 8*a*) and that of the products (A—B/C). The diagram displays the ground state energy profile of the reacting system (bold curve), as well as the energy profile of each VB structure as a function of the reaction coordinate (thin curves). Thus, starting from the reactant's geometry on the left, the VB structure that represents the reactant's electronic state, *R*, has the lowest energy and merges with the supersystem's ground state. Then, as one deforms the supersystem towards the products' geometry, the latter VB structure gradually rises in energy and finally reaches an excited state *P** that represents the VB structure of the reactants in the products' geometry. A similar diabatic curve can be traced from *P*, the VB structure of the products in its optimal geometry, to *R**, the same VB structure in the reactants' geometry. Consequently, the two curves cross somewhere in the middle of the diagram. The crossing is of course avoided in the adiabatic ground state, owing to the resonance energy *B* that results from the mixing of the two VB structures. The barrier is thus interpreted as arising from avoided crossing between two diabatic curves, which represent the energy profiles of the VB structures of the reactants and products.

The VBSCD is a handy tool for making predictions by relating the magnitudes of barriers to the properties of reactants. Thus, the barrier $\Delta E^{\neq}$ of a

reaction can be expressed as a function of some fundamental parameters of the diagrams. The first of these parameters is the vertical energy gap G (Fig. 8*a*) that separates the ground state of the reactant, R, from the excited state R^*. This parameter can take different expressions, depending on which reaction is considered, but is always related to simple and easily accessible energy quantities of the reactants. Another important factor is the height of the crossing point, ΔE_c, of the diabatic curves in the diagram, relative to the energy of the reactants. For predictive purposes, this quantity can, in turn, be expressed as a fraction f, smaller than unity, of the gap G (Eq. [63]).

$$\Delta E_c = f\,G \qquad [63]$$

This parameter is associated with the curvature of the diabatic curves, large upward curvatures meaning large values of f, and vice versa for small upward curvature. The curvature depends on the descent of R^* and P^* toward the crossing point and on the relative pull of the ground states, R and P, so that f incorporates various repulsive and attractive interactions of the individual curves along the reaction coordinate. The last parameter is the resonance energy B arising from the mixing of the two VB structures in the geometry of the crossing point. The barrier $\Delta E^{\neq}$ can be given a rigorous expression as a function of the three physical quantities f, G, and B as in Eq. [64]:

$$\Delta E^{\neq} = f\,G - B \qquad [64]$$

A similar expression can be given for the barrier of the reverse reaction as a function of the product's gap and its corresponding f factor. One then distinguishes between the reactant's and product's gaps, G_r and G_p, and their corresponding f factors f_r and f_p. A unified expression for the barrier as a function of the two promotion gaps and the endo- or exothermicity of the reaction can be derived by making some simplifying approximations.[85,169,170] One such simplified expression has been derived recently[168] and is given in Eq. [65].

$$\Delta E^{\neq} = f_0 G_0 + 0.5\Delta E_{rp} - B \qquad f_0 = 0.5(f_r + f_p) \quad G_0 = 0.5(G_r + G_p) \qquad [65]$$

Here, the first term is an intrinsic factor that is determined by the averaged f and G quantities, the second term gives the effect of the reaction thermodynamics, and the third term is the resonance energy of the transition state, due to the avoided crossing.

Taken together the barrier expressions describe the interplay of three effects. The intrinsic factor $f_0 G_0$ describes the energy cost due to unpairing of bonding electrons in order to make new bonds, the ΔE_{rp} factor accounts for the classical rate-equilibrium effect, while B involves information about the preferred stereochemistry of the reaction. Figure 9 outlines pictorially

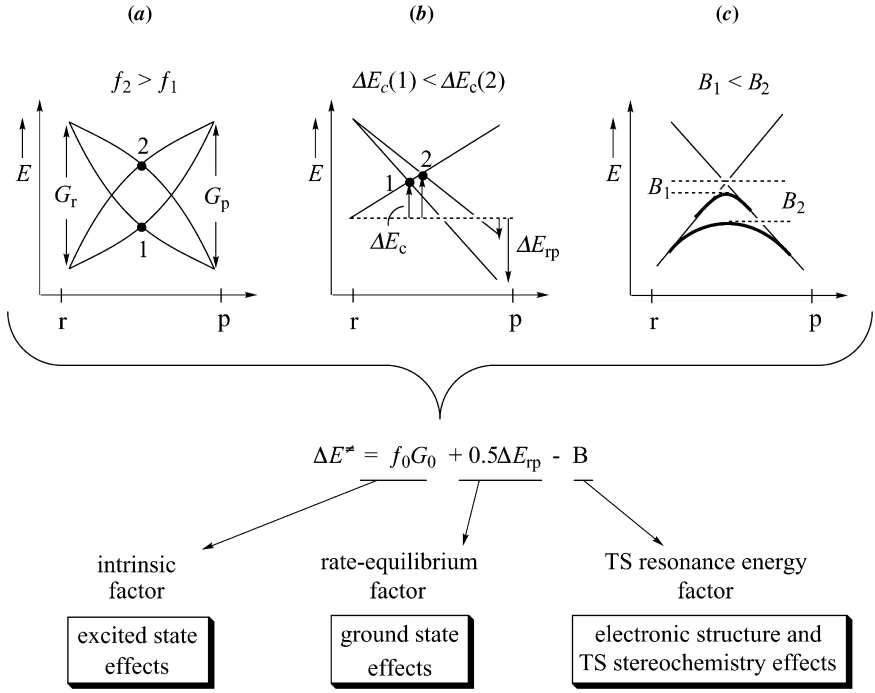

Figure 9 Illustration of the factors that control the variation of the barrier height in the VBSCD.

the impact of the three factors on the barrier. As such, the VB diagram constitutes in principle a unified and general structure–reactivity model.

A quantitative application of the diagram requires calculations of either ΔE_c and B or of f, G, and B. The energy gap factor, G, is straightforward to obtain for any kind of process. The height of the crossing point incorporates effects of bond deformations (bond stretching, angular changes, etc.) in the reactants and nonbonded repulsions between them at the geometry corresponding to the crossing point of the lowest energy on the seam of crossing between the two state curves (Fig. 8*a*). This, in turn, can be computed by means of ab initio calculations (e.g., straightforwardly by use of a VB method [159,166–168] or with any MO-based method), by determining the energy of the reactant wave function at zero iteration (see Appendix A.3) or by constrained optimization of block-localized wave functions.[171] Alternatively, the height of the crossing point can be computed by molecular mechanical means.[172–174] Except for VB theory that calculates B explicitly, in all other methods this quantity is obtained as the difference between the energy of the transition state and the computed height of the crossing point. In a few cases, it is possible to use analytical formulas to derive expressions for the

parameters f and B.[53,85,167] Thus, in principle, the VBSCD is computable at any desired accuracy.[142]

The purpose of this section is to teach an effective way for using the diagrams in a qualitative manner. The simplest way starts with the G parameter, which is the origin of the barrier, since it serves as a promotion energy needed to unpair the bonds of the reactants and pair the electrons in the mode required by the products. In certain families of related reactions both the curvatures of the diabatic curves (parameter f) and the avoided crossing resonance energy (parameter B) can be assumed to be nearly constant, while in other reaction series f and B vary in the same manner as G. In such cases, the parameter G is the crucial quantity that governs the reaction barriers in the series: the larger the gap G, the larger the barrier. Let us proceed with a few applications of this type.

Radical Exchange Reactions

Figure 10 describes the VB correlation diagram for a reaction that involves cleavage of a bond A—Y by a radical $X^{\bullet}$ (X, A, Y = any atom or molecular fragment):

$$X^{\bullet} + A{-}Y \rightarrow X{-}A + Y^{\bullet} \qquad [66]$$

Since R^{*} is just the VB image of the product in the geometry of the reactants, this excited state displays a covalent bond coupling between the infinitely

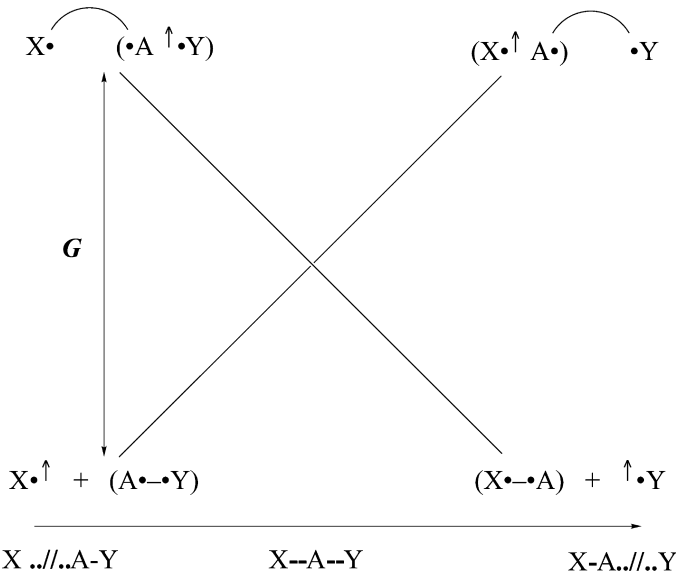

Figure 10 The state correlation in the VBSCD that describes a radical exchange reaction. Avoided crossing as in Figure 8*a* will generate the final adiabatic profile.

separated fragments X and A, and an uncoupled fragment $Y^{\bullet}$ in the vicinity of A. The VB wave function of such a state reads (dropping normalization factors):

$$\psi(R^*) = |\,x\,\bar{a}\,y\,| - |\,\bar{x}\,a\,y\,| \qquad [67]$$

where *x*, *a*, and *y* are, respectively, the active orbitals of the fragments X, A, Y. By using the rules of qualitative VB theory (Eqs. [40] and [42] where S^2 is neglected), the energy of R^* relative to the separated X, A, Y fragments becomes $-\beta_{ay}S_{ay}$, while the energy of *R* is just the bonding energy of the A—Y fragment (i.e., $2\beta_{ay}S_{ay}$). It follows that the energy gap *G* for any radical exchange reaction of the type in Eq. [66] is $-3\beta_{ay}S_{ay}$, which is just three quarters of the singlet–triplet gap ΔE_{ST} of the A—Y bond, namely,

$$G \approx 0.75\,\Delta E_{ST}(\text{A—Y}) \qquad [68]$$

The state R^* in Eq. [67] keeps strictly the wave function of the product *P*, and is hence a quasi-spectroscopic state that has a finite overlap with *R*. If one orthogonalizes the pair of states *R* and R^*, by for example, a Graham–Schmidt procedure, the excited state becomes a pure spectroscopic state in which the A—Y is in a triplet state and is coupled to $X^{\bullet}$ to yield a doublet state. In such an event, one could simply use, instead of Eq. [68], the gap G' in Eq. [69] that is simply the singlet–triplet energy gap of the A—Y bond:

$$G' = \Delta E_{ST}(\text{A—Y}) \qquad [69]$$

Each formulation of the state R^* has its own advantages,[175] but what is essential for the moment is that both use a gap that is either the singlet–triplet excitation of the bond that is broken during the reaction, or the same quantity scaled by approximately a constant 0.75. As mentioned above, a useful way of understanding this gap is as a promotion energy that is required in order to enable the A—Y bond to be broken before it can be replaced by another bond, X—A.

As an application, let us consider a typical class of radical exchange reactions, the hydrogen abstractions from alkanes. Eq. [70] describes the identity process of hydrogen abstraction by an alkyl radical:

$$R^{\bullet} + H\text{—}R \rightarrow R\text{—}H + R^{\bullet} \qquad [70]$$

Identity reactions proceed without a thermodynamic driving force, and project therefore the role of promotion energy as the origin of the barrier.

The barriers for a series of radicals have been computed by Yamataka and Nagase,[176] and were found to increase as the R—H bond energy *D*

increases; the barrier is the largest for $R = CH_3$ and the smallest for $R = C(CH_3)_3$. This trend has been interpreted by Pross et al.[177] using the VBSCD model. The promotion gap G that is the origin of the barrier (Eq. [68]) involves the singlet–triplet excitation of the R—H bond. Now, according to Eqs. [41] and [42], this singlet–triplet gap is proportional to the bonding energy of the R—H bond, that is, $\Delta E_{ST} \approx 2D$. Therefore, the correlation of the barrier with the bond strength is equivalent to a correlation with the singlet–triplet promotion energy (Eq. [68]), a correlation that reflects the electronic reorganization that is required during the reaction. In fact, the barriers for the entire series calculated by Pross et al.[177] can be fitted very well to the barrier equation, as follows:

$$\Delta E^{\neq} = 0.3481G - 50\,\text{kcal/mol} \quad G = 2D_{RH} \qquad [71]$$

which indicates that this is a reaction family with constant $f = 0.3481$ and $B = 50$ kcal/mol.

Recently, ab initio VB computations demonstrated that the ΔE_{ST} quantity[167] is the factor that organizes the trends for the barriers for the hydrogen exchange identity reaction, $R^{\bullet} + RH \rightarrow RH + {}^{\bullet}R$, when R varies down the column of the periodic table, that is, $R = CH_3$, SiH_3, GeH_3, and PbH_3. Thus, in this series, the barriers decrease down the column since the ΔE_{ST} quantity decreases.

Similar reaction series abound.[53,85] Thus, in a series of Woodward–Hoffmann forbidden 2 + 2 dimerizations, the promotion gap is proportional to the sum of the ΔE_{ST} ($\pi\pi^*$) quantities of the two reactants. Consequently, the barrier decreases from 42.2 kcal/mol for the dimerization of ethylene, where $\Sigma\Delta E_{ST}$ ($\pi\pi^*$) is large ($\sim$200 kcal/mol) down to $<$10 kcal/mol for the dimerization of disilene for which $\Sigma\Delta E_{ST}(\pi\pi^*)$ is small ($\sim$80 kcal/mol). A similar trend was noted for Woodward–Hoffmann allowed reactions (4 + 2 or 2 + 2 + 2), where the barrier jumps from 22 kcal/mol for the Diels–Alder reaction where $\Sigma\Delta E_{ST}(\pi\pi^*)$ is small ($\sim$173 kcal/mol) to 62 kcal/mol for the trimerization of acetylene where $\Sigma\Delta E_{ST}(\pi\pi^*)$ is very large ($\sim$297 kcal/mol).

Reactions between Nucleophiles and Electrophiles

Figure 11 illustrates the formation of the VB correlation diagram for a reaction between a nucleophile and an electrophile, Eq. [72]:

$$X^- + A{-}Y \rightarrow X{-}A + Y^- \qquad [72]$$

Equation [72] represents a typical S_N2 reaction where the nucleophile, X^-, shifts an electron to the A—Y electrophile, forms a new X—A bond, while the leaving group Y departs with the negative charge.

Let us now examine the nature of the R^* excited state for this process. Geometrically, A and Y are close together (as in the ground state R) and

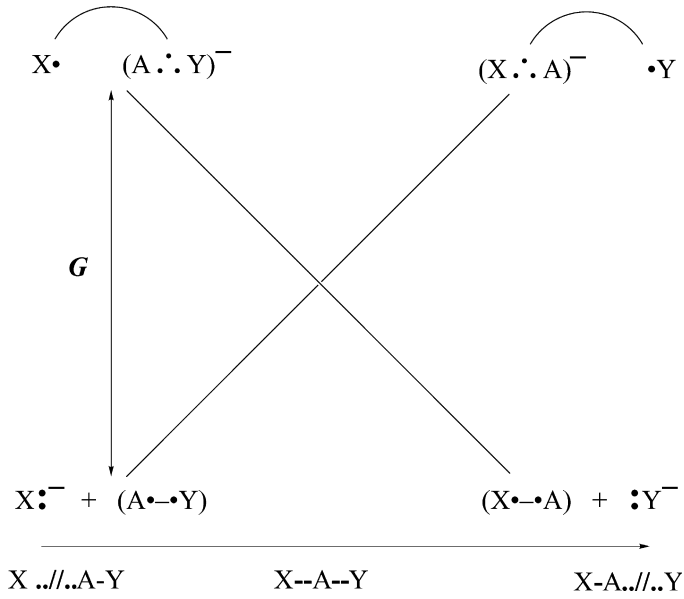

Figure 11 The state correlation in the VBSCD that describes a nucleophilic substitution reaction. Avoided crossing as in Figure 8*a* will generate the final adiabatic profile.

separated from X by a long distance. The X fragment, which is neutral in the product *P*, must remain neutral in R^*, and therefore carries a single active electron. As a consequence, the negative charge is located on the A—Y complex, so that the R^* state is the result of a charge transfer from the nucleophile to the electrophile, and can be depicted as $X^{\bullet}/(A.\therefore Y)^{-}$. It follows that the promotion from *R* to R^* is made of two terms: An electron detachment from the nucleophile (e.g., $X:^{-}$) and an electron attachment to the electrophile (e.g, A—Y). The promotion energy *G* is therefore the difference between the vertical ionization potential of the nucleophile, $I^*_{X:}$, and the vertical electron affinity of the electrophile, A^*_{A-Y}, given by Eq. [73],

$$G = I^*_{X:} - A^*_{A-Y} \qquad [73]$$

where the asterisk denotes a vertical quantity with respect to molecular as well as solvent configurations.[105,106] Thus, the mechanism of a nucleophilic substitution may be viewed as an electron transfer from the nucleophile to the electrophile, and a coupling of the supplementary electron of the electrophile to the remaining electron of the nucleophile.

A whole monograph and many reviews were dedicated to discussion of S_N2 reactivity based on the VBSCD model, and the interested reader may consult these.[85,169,170,178] One important feature that emerges from these

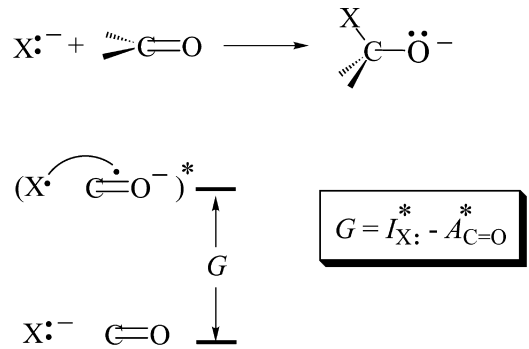

Figure 12 The ground and vertical charge-transfer states in the VBSCD that describes a nucleophilic attack on a carbonyl group.

treatments is the insight into variations of f. Thus, whether or not the single electrons in the R^* state are easily accessible to couple to a bond determines the size of the f factor; the easier the bond coupling along the reaction coordinate, the smaller the f and vice versa. For example, in delocalized nucleophiles (acetate, phenyl thiolate, etc.), the active electron is not 100% located on the atom that is going to be eventually linked to the fragment A in the reaction in Eq. [72]. So the diabatic curve will slowly descend from R^* to P and one may expect a large f factor. On the other hand, localized nucleophiles will correspond to smaller f factors. Of course, the same distinction can be made between localized and delocalized electrophiles, leading to the same prediction regarding the magnitude of f.

In general, all reactions between closed-shell electrophiles and nucleophiles subscribe to the same diagram type[85] with R^* and P^* states, which are vertical charge-transfer states that involve an electron transfer from the nucleophile to the electrophile, while coupling the single electron on the oxidized nucleophile to that on the reduced electrophile to form a bond pair. An example is the nucleophilic cleavage of an ester where the rate-determining step is known[179,180] to involve the formation of a tetrahedral intermediate, as depicted in Figure 12.

The promotion energy for the rate-determining step is, accordingly, the difference between the vertical ionization potential of the nucleophile and the electron attachment energy of the carbonyl group. The latter quantity is a constant for a given ester, and therefore the correlation of barriers with the promotion energy becomes a correlation with the vertical ionization energy of the nucleophiles. Figure 13 shows a structure–reactivity correlation for the nucleophilic cleavage of a specific ester based on the VBSCD analysis of Buncel et al.[181] It is seen that the free energies of activation correlate with the vertical ionization energies of the nucleophile in the reaction solvent. Furthermore, localized and delocalized nucleophiles appear to generate correlation lines of

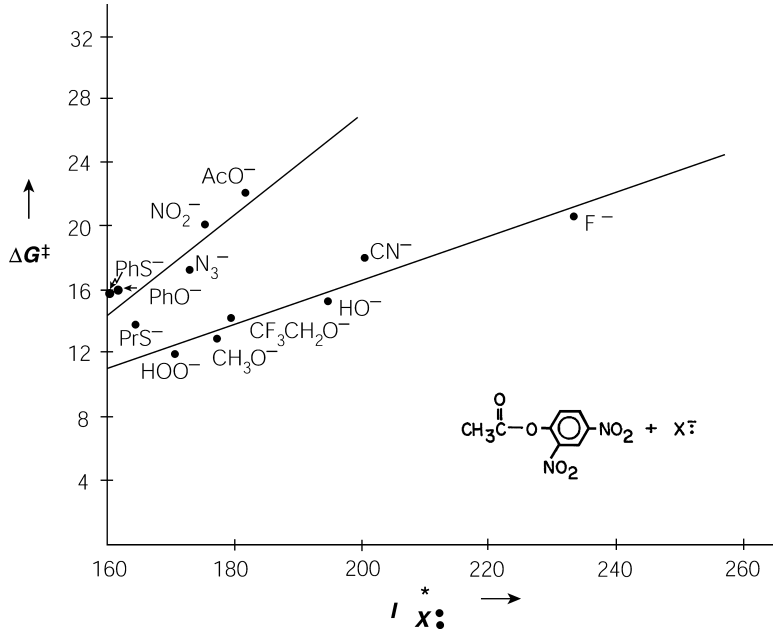

Figure 13 A plot of the free energy of activation for nucleophilic cleavage of an ester vs. the vertical ionization potential of the nucleophile (adapted from Ref. 85).

different slopes. The two correlation lines obtained for the experimental data in Figure 13 are readily understood based on Eq. [64] as corresponding to different f values, where the localized nucleophiles possess the smaller f value and hence a smaller structure–reactivity slope in comparison with the delocalized nucleophiles.

Significance of the f Factor

The f factor defines the intrinsic selectivity of the reaction series to a change in the vertical gap,[85,169] that is,

$$f = \partial(\Delta E^{\neq})/\partial G \qquad [74]$$

In reactions of electrophiles and nucleophiles, we just indicated that f increases as the nucleophile becomes more delocalized. Thus, the series of delocalized nucleophiles, in Figure 13, is more selective to changes (of any kind) that affect the gap, G, compared with the series of localized nucleophiles. This would be general for other processes as well; delocalization of the single electrons in the R^* states of the diagram results in higher f values, and vice versa. Such trends abound in electrophile–nucleophile combinations;

they were analyzed for radical addition to olefins,[182] and are likely to be a general feature of reactivity.

Another factor that raises f is the steric bulk of the substrate or the nucleophile.[169] For example in S_N2 reactions the bulkier the alkyl group in A—Y (Eq. [72]) the larger will be the value of f, and vice versa.[169] As a result, bulkier substrates will exhibit higher sensitivity to changes in the vertical gap. One such variation occurs when the reaction conditions change from gas phase to solution, in which case the promotion gap, $G = I^*_{X:} - A^*_{A-Y}$, increases by a significant amount. If we now compare two A—Y substrates such as methyl chloride and neopentyl chloride, the latter will possess a larger f value. *The consequence is that the steric effect that is observed in the gas phase will be amplified and become more significant in a solvent*. This exciting finding was recently published by Ren and Brauman.[183]

Making Stereochemical Predictions with the VBSCD Model

Making stereochemical predictions is easy using FO–VB configurations.[52,81,85] To illustrate the manner by which this can be practiced, let us take a simple example with well-known stereochemistry, the nucleophilic substitution reaction, Eq. [72]. The corresponding R^* state is depicted in Figure 14 in its FO–VB formulation, where the nucleophile appears here in its one-electron reduced form $X^{\bullet}$, with a single electron in ϕ_X, while the substrate has an extra electron in its σ^*_{CY} orbital. The two single electrons are coupled into a $\phi_X - \sigma^*_{CY}$ bond pair.

The R^* state correlates to product, $X—C/:Y^-$, since it contains a $\phi_X - \sigma^*_{CY}$ bond-pair that becomes the X—C bond, and at the same time the occupancy of the σ^*_{CY} orbital causes the cleavage of the C—Y bond to release

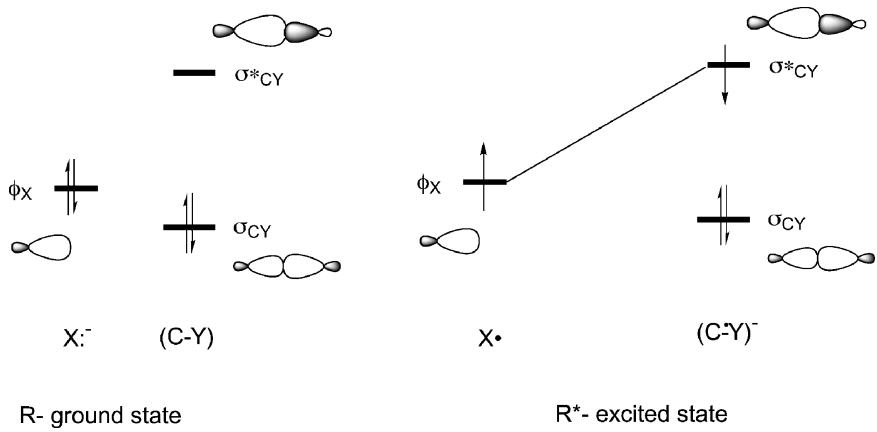

Figure 14 The ground (R) and charge-transfer (R^*) states in the VBSCD of the S_N2 reaction $X^- + C - Y \rightarrow X - C + Y^-$. The R^* state has a bond pair shown by the line connecting the orbitals ϕ_x and σ^*_{cy}.

the: Y^- anion. Furthermore, the R^* state contains information about the stereochemical pathway. Since the bond pair involves a $\phi_X - \sigma^*_{CY}$ overlap, due to the nodal properties of the σ^*_{CY} orbital the bond pair will be optimized when the $X^\bullet$ is coupled to the substrate in a colinear X—C—Y fashion. Thus, the steepest descent of the R^* state, and the lowest crossing point will occur along a backside trajectory of the nucleophile toward the substrate.

If we assume that the charge-transfer state remains the leading configuration of R^* near the crossing point, then the matrix element between R and R^* will dominate the size of the resonance energy B, and will enable making predictions about B. Since these two VB configurations differ by the occupancy of one spin orbital (ϕ_X in R is replaced by σ^*_{CY} in R^*) then following the qualitative rules for matrix elements (see Appendix A.2), the resonance energy of the transition state (TS) will be proportional to the overlap of these orbitals, that is,

$$B \propto \langle \phi_X | \sigma^*_{CY} \rangle \qquad [75]$$

It follows therefore, that in a backside trajectory, we obtain both the lowest crossing point as well as the largest TS resonance energy. Computationally, the back-side barrier is smaller by ~10–20 kcal/mol compared with a front-side attack.[184] Equation [75] constitutes an orbital selection rule for an S_N2 reaction. Working out this rather trivial prediction is nevertheless necessary since it constitutes a prototypical example for deriving orbital selection rules in other reactions, using FO–VB configurations. *Thus, the intrinsic bonding features of R^* provide information about the reaction trajectory, while the $\langle R|R^* \rangle$ overlap provides information about the geometric dependence of the resonance energy of the TS, B.*

By using this approach, it is possible to *derive orbital selection rules* for cases that are ambiguous in qualitative MO theory. For example, for radical cleavage of σ bonds, using the R^* with a triplet $\sigma^1\ \sigma^{*1}$ configuration on the substrate leads to prediction that the course of the reaction and the resonance interaction in the transition state will be determined by the product of overlaps between the orbital of the attacking radical, ϕ_R, and the σ and σ* orbitals of the substrate, namely, $\langle \phi_R|\sigma \rangle \langle \phi_R|\sigma^* \rangle$. This product is optimized once again in a back-side attack, and therefore one can predict that radical cleavage of σ bonds will proceed with inversion of configuration. All known experimental data[185–190] conform to this prediction. Another area where successful predictions have been made involves nucleophilic attacks on radical cations. Here using the corresponding R and R^* states,[191] it was predicted that stereoselectivity and regioselectivity of nucleophilic attack should be controlled by the lowest unoccupied molecular orbital (LUMO) of the radical cation. Both regioselectivity and stereospecificity predictions were verified by experiment[192,193] and computational means.[184] For a more in depth discussion the reader may consult the most recent review of the VBSCD and VBCMD models.[85]

VBSCD: A GENERAL MODEL FOR ELECTRONIC DELOCALIZATION AND ITS COMPARISON WITH THE PSEUDO-JAHN–TELLER MODEL

The valence bond state correlation diagram (VBSCD) serves as a model for understanding the status of electronic delocalization in isoelectronic series. Consider, for example, the following exchange process between monovalent atoms, which exchange a bond while passing through an $X_3^\bullet$ cluster in which three electrons are delocalized over three centers.

$$X^\bullet + X{-}X \rightarrow [X_3^\bullet] \rightarrow X{-}X +^\bullet X \qquad [76]$$

We can imagine a variety of such species (e.g., X = H, F, Cl, Li, Na, Cu), and ask ourselves the following question: When do we expect the $X_3^\bullet$ species to be a transition state for the exchange process, and when will it be a stable cluster, an intermediate en-route to exchange? In fact, the answer to this question comes from the VBSCD model, that describes all these process in a single diagram where G is given by Eq. [68], that is, $G \approx 0.75\ \Delta E_{ST}(X{-}X)$. Thus, as shown in Figure 15 a very large triplet promotion energy for X = H (250 kcal/mol) results in an $H_3^\bullet$ transition state, while the small promotion energy for X = Li (32 kcal/mol) results in a stable $Li_3^\bullet$ cluster. The VB computations of Maître et al.[166] in Figure 15 show that, as the promotion gap drops drastically, the avoided crossing state changes from a transition state for $H_3^\bullet$ to a stable cluster for $Li_3^\bullet$. Moreover, this transition from a barrier to an intermedi-

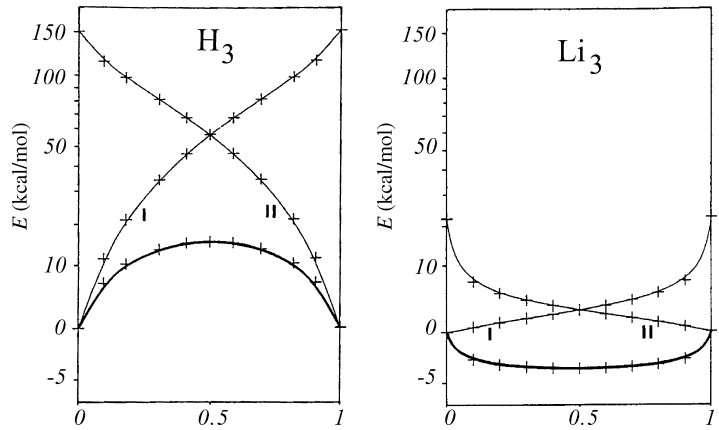

Figure 15 Ab initio computations of VBSCDs for the exchange processes, X•+ $X{-}X \rightarrow X{-}X + \bullet X$, for X = H and Li (adapted from Ref. 166). The abscissa is a reaction progress coordinate that stretches between zero and one (using the normalized reaction coordinates, $0.5(n_1 - n_2 + 1)$, where n_1 and n_2 are the X–X bond orders in X–X–X).

ate can in fact be predicted quantitatively from the barrier equation, by deriving explicit expressions for G, f, and B.[167]

The spectacular relationship between the nature of the $X_3^\bullet$ species and the promotion energy shows that the VBSCD is in fact a general model of the pseudo-Jahn–Teller effect (PJTE). A qualitative application of PJTE would predict all the $X_3^\bullet$ species to be transition state structures that relax to the distorted $X^\bullet{-}X{-}X$ and $X{-}X{-}^\bullet X$ entities. The VBSCD makes a distinction between strong binders that form transition states and weak binders that form stable intermediate clusters.

The variable nature of the $X_3^\bullet$ species in the isoelectronic series form a general model for electronic delocalization, enabling one to classify the species either as distortive or as stable. By using the isoelectronic analogy, one might naturally ask about the isoelectronic π-species in allyl radical; does it behave by itself like $H_3^\bullet$ or like $Li_3^\bullet$? Moreover, the same transformation displayed for $X_3^\bullet$ in Figure 15 can be shown for X_3^+, X_3^-, X_4, and X_6 species.[57] Likewise one might wonder about the status of the corresponding isoelectronic π components in allyl cation, anion, cyclobutadiene, or benzene. These questions were answered in detail elsewhere and the reader is advised to consult a recent review,[57] while here we deal only with the intriguing question concerning the π-electrons of benzene.

What Is the Driving Force, σ or π, Responsible for the D_{6h} Geometry of Benzene?

The regular hexagonal structure of benzene can be considered as a stable intermediate in a reaction that interchanges two distorted Kekulé-type isomers, each displaying alternating C—C bond lengths as shown in Figure 16. It is well known that the D_{6h} geometry of benzene is stable against a Kekuléan distortion (of b_{2u} symmetry), but one may still wonder which of the two sets of bonds, σ or π, is responsible for this resistance to a b_{2u} distortion. The σ frame, which is just a set of identical single bonds, is by nature symmetrizing and prefers a regular geometry. It is not obvious whether the π electronic component, by itself, is also symmetrizing or on the contrary distortive, with a weak force constant that would be overwhelmed by the symmetrizing driving force of the σ frame. To answer this question, consider in Figure 16 the VBSCD that represents the interchange of Kekulé structures along the b_{2u} reaction coordinate; the middle of the b_{2u} coordinate corresponds to the D_{6h} structure, while its two extremes correspond to the bond-alternated mirror-image Kekulé geometries. Part a of the figure considers π *energies only*. Starting at the left-hand side, Kekulé structure K_1 correlates to the excited state K_2^* in which the π bonds of the initial K_1 structure are elongated, while the repulsive nonbonding interactions between the π bonds are reinforced. The same argument applies if we start from the right-hand side, with structure K_2 and follow it along the b_{2u} coordinate; K_2 will then rise

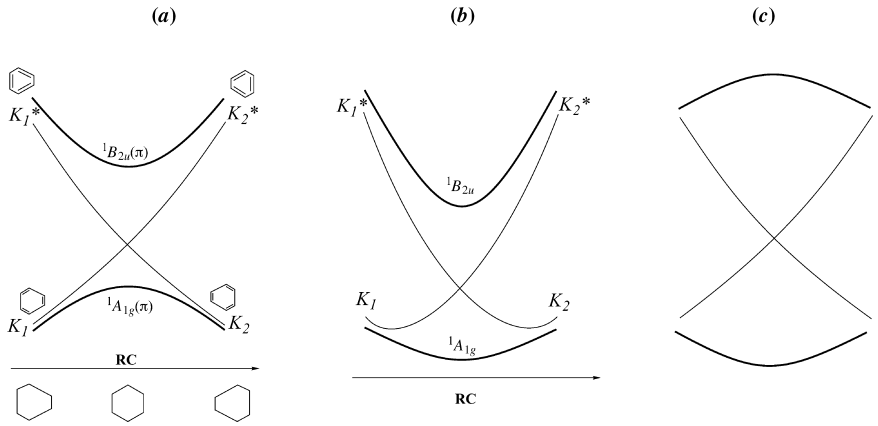

Figure 16 The VBSCDs showing the crossing and avoided crossing of the Kekulé structures of benzene along the bond alternating mode, b_{2u} for: (*a*) π-only curves, (*b*) full π + σ curves, and (c) π-only curves in a putative situation where the avoided crossing leads to a ground state with a π-symmetrizing tendency. In this latter case, the excited state will have a distortive π-state and hence, a low frequency for the b_{2u} mode.

and correlate to K_1^*. To get an estimate for the gap, we can extrapolate the Kekulé geometries to a complete distortion, in which the π bonds of K_1 and K_2 would be completely separated (which in practice is prevented by the σ frame that limits the distortion). At this asymptote, the promotion energy, $K_i \rightarrow K_i^*(i = 1, 2)$, is due to the unpairing of three π bonds in *the ground state*, K_i, and replacing them, in K_i^*, by three nonbonding interactions. As we recall the latter are repulsive triplet interactions. The fact that such a distortion can never be reached is of no concern. What matters is that this constitutes an asymptotic estimate of the energy gap G that correlates the two Kekulé structures, and that eventually determines if their mixing results in a barrier or in a stable situation, in the style of the X_3 problem in Figure 15 above. According to the VB rules, G is given by Eq. [77]:

$$G(K \rightarrow K^*) = 9/4\Delta_{ST}(C{=}C) \qquad [77]$$

Since the ΔE_{ST} value for an isolated π bond is of the order of 100 kcal/mol, Eq. [77] places the π electronic system in the region of large gaps. Consequently, the π component of benzene is predicted by the VBSCD model to be an *unstable transition state*, as illustrated in Figure 16*a*. This ''π-transition state'' prefers a distorted Kekuléan geometry with bond alternation, but is forced by the σ frame, with its strong symmetrizing driving force, to adopt the regular D_{6h} geometry. This proposal, which appeared as a daring prediction at the time, was made by Shaik and Bar on the basis of a qualitative VB diagram and semiempirical calculations.[194] It was later confirmed by rigorous

ab initio calculations, using different techniques of σ–π separations, by the present authors and their co-workers[195–198] and by others.[199–202] It was further linked, by the work of Haas and Zilberg,[203] to experimental data associated with the vibrational frequencies of the excited states of benzene.

The experimental data discussed by Haas and Zilberg,[203] as well as those of pioneering assignments[204–206] show a peculiar phenomenon. This phenomenon is both state specific to the $^1B_{2u}$ excited state, as well as vibrationally mode specific, to the bond-alternating mode, that is, *the Kekulé mode* b_{2u}. Thus, upon excitation from the $^1A_{1g}$ ground state to the $^1B_{2u}$ excited state, with exception of b_{2u} all other vibrational modes behave "normally" and undergo frequency lowering in the excited state, as expected from the decrease in π bonding and disruption of aromaticity following a $\pi \rightarrow \pi^*$ excitation. By contrast, the Kekulé b_{2u} mode, undergoes an upward shift of 257–261 cm^{-1}. As explained below, this phenomenon is predictable from the VBSCD model and constitutes a critical test of π distortivity in the ground state of benzene.

Indeed, the VBSCD model is able to lead to predictions not only on the ground state of an electronic system, but also on some selected excited state. Thus, the mixing of the two Kekulé structures K_1 and K_2 in Figure 16*a* leads to a pair of resonant and antiresonant states $K_1 \pm K_2$; the $^1A_{1g}$ ground state $K_1 + K_2$ is the resonance-stabilized combination, and the $^1B_{2u}$ excited state $K_1 - K_2$ is the antiresonant mixture (this is the first excited state of benzene[207]). In fact, the VBSCD in Figure 16*a* predicts that the curvature of the $^1A_{1g}(\pi)$ ground state (restricted to the π electronic system) is negative, whereas by contrast, that of the $^1B_{2u}(\pi)$ state is positive. Of course, when the energy of the σ frame is added as shown in Figure 16*b*, the net total driving force for the ground state becomes symmetrizing, with a small positive curvature. By comparison, the $^1B_{2u}$ excited state displays now a steeper curve and is much more symmetrizing than the ground state, having more positive curvature. As such, the VBSCD model predicts that an $^1A_{1g} \rightarrow {}^1B_{2u}$ excitation of benzene should result in the reinforcement of the symmetrizing driving force, which will be manifested as a frequency increase of the Kekulean b_{2u} mode. We may consider an alternative scenario, displayed in Figure 16*c* where now we assume that the π component for the ground state is symmetrizing (positive curvature) as might have been dictated by common wisdom. In such an event, the π component would be distortive in the $^1B_{2u}$ state, and consequently, the excitation would have resulted in the lowering of the b_{2u} frequency. Since this is clearly not the case, the finding of an enhanced b_{2u} frequency in the excited state constitutes an experimental proof of the π distortivity in the ground state of benzene.

In order to show how delicate the balance is between the σ and π opposing tendencies, we recently[57] derived an empirical equation, Eq. [78], for $4n + 2$ annulenes:

$$\Delta E_{\pi+\sigma} = 5.0(2n + 1) - 5.4(2n) \quad \text{kcal/mol} \qquad [78]$$

Here $\Delta E_{\pi+\sigma}$ stands for the total (π and σ) distortion energies, the terms $5.0(2n+1)$ represent the resisting σ effect, which is 5.0 kcal/mol for an adjacent pair of σ bond, whereas the negative term, $-5.4(2n)$, accounts for the π distortivity. This expression predicts that for $n = 7$, namely, the $C_{30}H_{30}$ annulene, the $\Delta E_{\pi+\sigma}$ becomes negative and the annulene undergoes bond localization. If we increase the π distortivity coefficient a tiny bit, namely, to

$$\Delta E_{\pi+\sigma} = 5.0(2n+1) - 6.0(2n) \quad \text{kcal/mol} \qquad [79]$$

the equation would now predict that the annulene with $n = 3$, namely, $C_{14}H_{14}$, will undergo bond localization. This extreme sensitivity, which is predicted to manifest in computations and experimental data of annulenes, is a simple outcome of the VBSCD prediction that the π component of these species behaves as a transition state with a propensity toward bond localization.

VBSCD: THE TWIN-STATE CONCEPT AND ITS LINK TO PHOTOCHEMICAL REACTIVITY

Photochemistry is an important field for future applications. The pioneering work of van Der Lugt and Oosterhoff[89] and Michl[91] highlighted the importance of avoided crossing regions as decay channels in photochemistry. Köppel and co-workers[208,209] showed that conical intersections, rather than avoided crossing regions, are the most efficient decay channels, from excited to ground states. Indeed, this role of conical intersections in organic photochemistry has been extensively investigated by Robb and co-workers,[93,96] and conical intersections are calculated today on a routine basis using software such as GAUSSIAN. Bernardi et al.[93] further showed that VB notions can be useful to rationalize the location of conical intersections and their structure.

As was subsequently argued by Shaik and Reddy,[97] the VBSCD is a straightforward model for discussing the relation between thermal and photochemical reactions and between the avoided crossing region and a conical intersection. Thus, the avoided crossing region of the VBSCD leads to the twin-states $\Psi^{\ddagger}$ and Ψ^{*} (Fig. 17); one corresponds to the resonant state of the VB configurations and the other to the antiresonant state.[85] Since the extent of this VB mixing is a function of geometry, there should exist in principle, *a specific distortion mode that converts the avoided crossing region into a conical intersection* where the twin-states $\Psi^{\ddagger}$ and Ψ^{*} become degenerate, and thereby enable the excited reaction complex to decay into the ground-state surface. In this manner, the conical intersection will be anchored at three structures; two of them are the reactant (R) and product (P_1) of the thermal reaction, and the third is the product (P_2) generated by the distortion mode that causes the degeneracy of the twin-states $\Psi^{\ddagger}$ and Ψ^{*}. *The new product would therefore*

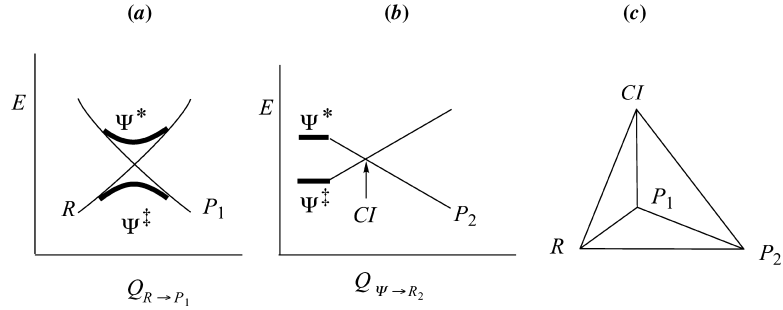

Figure 17 (*a*) The VBSCD showing the twin-states formed by avoided crossing along the reaction coordinate of the thermal reaction leading to product P_1. (*b*) The crossover of the twin-states to generate a conical intersection (CI) along a coordinate that stabilizes the twin excited state, and leading to product P_2. (*c*) The conical intersection will be anchored in three minima (or more): reactants (R), P_1, and P_2.

be characteristic of the distortion mode that is required to convert the avoided crossing region into a conical intersection. Assuming that most of the excited species roll down eventually to the Ψ^* funnel, then P_2 would be a major photoproduct.[a]

A trivial example is the celebrated hydrogen exchange reaction, $H_a - H_b + H_c \rightarrow H_a + H_b - H_c$, where the transition state has a colinear geometry, $H_a - H_b - H_c$. In this geometry, the ground state $\Psi^{\ddagger}$ is the resonating combination of R and P and the transition state for the thermal reaction, while the twin-excited state Ψ^* is the corresponding antiresonating combination:

$$\Psi^{\ddagger} = R - P;$$

$$R = |a\bar{b}c| - |\bar{a}bc| \quad P = |ab\bar{c}| - |a\bar{b}c| \qquad [80]$$

$$\Psi^* = R + P = |ab\bar{c}| - |\bar{a}bc| \qquad [81]$$

where the orbitals *a, b*, and *c* belong to H_a, H_b, and H_c, respectively.

It is clear from Eq. [81] that Ψ^* involves a bonding interaction between H_a and H_c and will be lowered by the bending mode that brings H_a and H_c together. Furthermore, the expression for the avoided crossing interaction B (Eq. [82]) shows that this quantity shrinks to zero in an equilateral triangular

$$B = \langle R|H^{\text{eff}}|P\rangle = -2\beta_{ab}S_{ab} - 2\beta_{bc}S_{bc} + 4\beta_{ac}S_{ac} \qquad [82]$$

[a] If, however, there exist other excited-state funnels near the twin excited state, Ψ^*, other products will be formed, which are characteristic of these other excited states and can be predicted in a similar manner provided one knows the identity of these excited states.

structure where the $H_a - H_c$, $H_a - H_b$, and $H_b - H_c$ interactions are identical. As such, the equilateral triangle defines a conical intersection with a doubly degenerate state, in the crossing point of the VBSCD. This D_{3h} structure will relax to the isosceles triangle with short $H_a - H_c$ distance that will give rise to a "new" product $H_b + H_a - H_c$. The photocyclization of allyl radical to cyclopropyl radical is precisely analogous. The ground state of allyl is the resonating combination of the two Kekulé structures, while the twin-excited state, Ψ^*, is their antiresonating combination with the long bond between the allylic terminals.[52] As such, rotation of the two allylic terminals will lower Ψ^*, raise the ground state, and establish a conical intersection that will channel the photoexcited complex to the cyclopropyl radical, and vice versa.

The photostimulation of S_N2 systems such as $X^- + A{-}Y$ (A = Alkyl) was analyzed before, using VBSCD-based rationale, for predicting the location of conical intersections.[97] Here, the transition state for the thermal reaction is the colinear $[X{-}A{-}Y]^-$ structure, which is the $\Psi^{\neq}(A')$ resonating combination of the two Lewis structures, while the twin-excited state, $\Psi^*(A'')$, is their antiresonating combination; the symmetry labels refer to C_s symmetry. This latter excited state is readily written as an A″ symmetry-adapted combination of Lewis structures, Eq. [83]:

$$\Psi^* = (|\, x\overline{x}\, a\overline{y}\,| - |\, x\overline{x}\, \overline{a}\, y\,|) - (|\, y\overline{y}\, x\, \overline{a}\,| - |\, y\overline{y}\, \overline{x}\, a\,|) \qquad [83]$$

where the orbitals *x, a*, and *y* belong to the fragments X, A, and Y, respectively.

Rearranging Eq. [83] to Eq. [84] reveals a stabilizing three-electron bonding interaction between X and Y, of the type $(X^{\bullet}\ {:}Y^- \rightarrow X{:}^-\ {}^{\bullet}Y)$.

$$\Psi^* = (|\, \overline{x}\, x\overline{y}\, a\,| + |\, \overline{x}\, y\overline{y}\, a\,|) - (|\, x\overline{x}\, y\overline{a}\,| + |\, x\overline{y}\, y\overline{a}\,|) \qquad [84]$$

As such, the bending mode that brings the X and Y groups together destabilizes the $[X{-}A{-}Y]^-$ structure and stabilizes the twin-excited state, until they establish a conical intersection that correlates down to $X\therefore Y^-$ and $R^{\bullet}$, as shown in Figure 18. This analysis is supported by experimental observation that the irradiation of the I^-/CH_3I cluster at the charge-transfer band leads to I_2^- and $CH_3^{\bullet}$, while for $I^-/\ CH_3Br$ such excitation generates IBr^- and $CH_3^{\bullet}$.[210]

The notion of twin-states of the VBSCD and the phase inversion rule of Longuet–Higgins were utilized by Zilberg and Haas[98] to delineate unified selection rules for conical intersections, and rationalize the outcome of a variety of photochemical reactions.

The presence of excited-state minima above the thermal transition state is a well known phenomenon.[89,91–93] The VBSCD model merely gives this ubiquitous phenomenon a simple mechanism in terms of the avoided crossing of

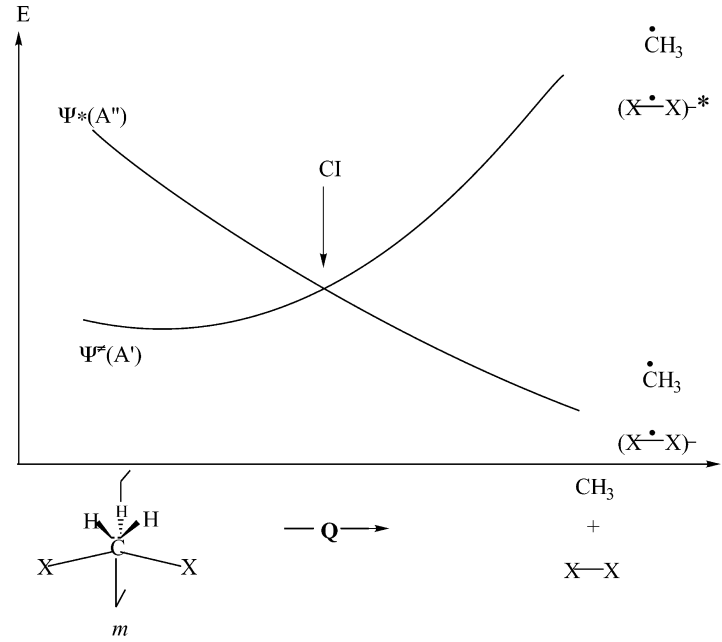

Figure 18 Generation of a conical intersection (*CI*) by crossing of the twin states along the bending distortion mode, in S_N2 systems. Symmetry labels refer to the mirror plane *m*.

VB structures, and hence enables one to make predictions in a systematic manner. Other important applications of the twin states concern the possibility of spectroscopic probing or accessing the twin excited state that lies directly above the transition state of a thermal reaction. Thus, much like the foregoing story of benzene, any chemical reaction will possess a transition state, $\Psi^{\ddagger}$ and a twin excited state, Ψ^*.[81,211] For most cases, albeit not all, the twin excited state should be stable, and hence observable; its geometry will be almost coincident with the thermal transition state and its electronic state symmetry should be identical to the symmetry of the reaction coordinate of the ground-state process,[212] namely,

$$\Gamma(\Psi^*) = \Gamma(Q_{RC}) \qquad [85]$$

In addition, the twin excited state will possess a real and greatly increased frequency of the reaction coordinate mode, by analogy to the benzene story where the b_{2u} mode was enhanced in the $^1b_{2u}$ twin excited state. Thus, since the twin pair has coincident geometry, a spectroscopic characterization of Ψ^* will provide complementary information on the transition state $\Psi\ddagger$ and will enable resolution of the transition state structure.

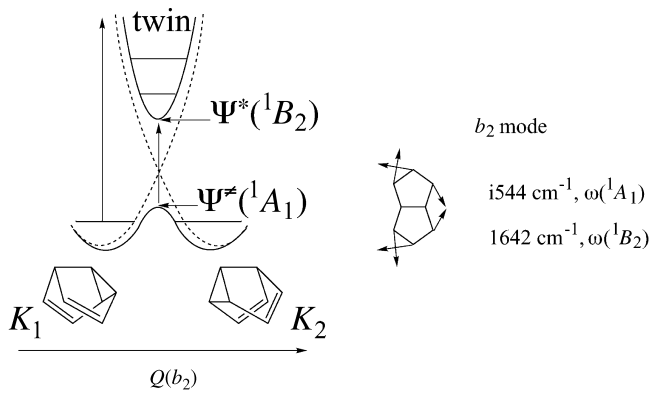

Figure 19 The twin states along the b_2 reaction coordinate for the semibullvalene rearrangement. When the thermal barrier is NOT much higher than the zero-point levels of the two isomers, the transition state ($\Psi^{\neq}$) region becomes available thermally. Absorption in the transition state region is in the visible, leading to thermochromism at elevated temperature.

As a proof of principle, the twin states were characterized for the semibullvalene rearrangement[212] and found to possess virtually identical geometries. As shown in Figure 19, the twin excited state possesses B_2 symmetry as the symmetry of the reaction coordinate of the thermal process. And the transition state mode, b_2, which is imaginary for $\Psi^{\neq}(A_1)$ was shown to be real for $\Psi^*(B_2)$.[212] These calculations match the intriguing findings of Quast et al.[213] in the semibullvalene and barbaralene systems. Thus, these authors[213,214] have designed semibullvalene and barbaralene derivatives in which the barrier for the rearrangement could be lowered drastically, to a point where it almost vanishes. Quast[213,214] found that these molecules exhibit thermochromism without having a chromophore; they are colorless at low temperatures but highly colored at 380 K. According to Quast, the thermochromism arises due to the low energy transition from the transition state ($\Psi^{\neq}$) to the twin excited state (Ψ^*), Figure 19. Thus, since the thermal barrier is exceptionally low, at elevated temperatures the transition state becomes thermally populated. Since the $\Psi^{\neq}$-Ψ^* gap is small, one observes color due to absorption within the visible region. However, at low temperatures, the molecules reside at the bottom of the reactant–product wells, where the gap between the ground and excited state is large and hence, the absorption is in the ultraviolet (UV) region and the color is lost. To quote Quast, ''thermochromic ... semibullvalene allow the observation of transition states even with one's naked eye''.[214] Of course, identifying appropriate systems where the twin excited state is observable is required for the eventual ''observation'' of the transition states of thermal reactions.

Coherent control[215] is a powerful new chemical method that makes use of the availability of the twin excited state to control the course of chemical reactions by laser excitation. Thus, laser excitation from $\Psi^{\ddagger}$ to Ψ^{*}(Fig. 17*a*), using two different and complementary photons causes the decay of Ψ^{*} to occur in a controlled manner either to the reactant or products. In the case where the reactants and products are two enantiomers, the twin excited state is achiral, and the coherent control approach leads to chiral resolution.

In summary, the twin excited state plays an important role in photochemistry as well as in thermal chemistry.

THE SPIN HAMILTONIAN VB THEORY

Quite a different brand of VB theory comes from physics, and is rooted in the phenomenological Hamiltonians that are called magnetic- or spin-Hamiltonians after their first formulation by Heisenberg.[9] Unlike the theory used above, which relies on VB structures that are eigenfunctions of both the S_z and S^2 operators, this theory relies on VB determinants, which are eigenfunctions of only the S_z operator. The following section describes the type of insight that can be gained from this VB approach.

Theory

The spin-Hamiltonian VB theory uses the same approximations as the qualitative theory presented above to calculate the Hamiltonian matrix elements, but with a few simplifications. The theory is restricted to determinants having one electron per AO; this restriction excludes ionic structures or molecules bearing lone pairs. As such, the theory has mainly been applied to conjugated polyenes. Another simplification is the zero-differential overlap approximation, which means that all overlaps are neglected in the formulas.

Apart from these simplifying assumptions, a fundamental difference between qualitative VB theory and spin-Hamiltonian VB theory is that the basic constituent of the latter theory is the AO determinant, without any a priori bias for a given electronic coupling into bond pairs. Instead of an interplay between VB structures, a molecule is viewed then as a collective spin-ordering: The electrons tend to occupy the molecular space (i.e., the various atomic centers) in such a way that *an electron of* α *spin will be surrounded by as many* β *spin electrons as possible, and vice versa*. Determinants having this property, called the "most spin-alternated determinants" (MSAD) have the lowest energies (by virtue of the VB rules, in *Qualitative VB Theory*) and play the major role in electronic structure. As a reminder, the reader should recall from our discussion above that the unique spin-alternant determinant, which we called the quasiclassical state, is used as a reference for the interaction energy.

The usefulness of such a magnetic description in chemistry has been demonstrated by Malrieu and his co-workers.[64,65,216] Without any numerical computations, the method can be used to deduce qualitative rules, regarding the spin multiplicity of the ground-states of polyenes (especially for diradicals), the spin distribution in free radicals and triplet states, differences in bond lengths, and relative stabilities of isomers. It can also be used quantitatively, through CI, leading to ground-state equilibrium geometries, rotational barriers, excited-states ordering (for neutral excited states), and so on.

We now briefly describe the principles of the method and simple rules for the construction of the Hamiltonian matrix. For the sake of consistency, rather than the original formulation of Malrieu,[64,65,216] we use here a formulation[52,71–73] that is in harmony with the qualitative VB theory above. The method can be summarized with a few principles:

1. All overlaps are neglected.
2. The energy of a VB determinant Ψ_D is proportional to the number of Pauli repulsions that take place between adjacent AOs having electrons with identical spins:

$$E(\Psi_D) = \sum_{r\uparrow,s\uparrow} g_{rs} \qquad [86]$$

   where g_{rs} is a parameter that is quantified either from experimental data, or is ab initio (DFT) calculated as one-half of the singlet–triplet gap of the r—s bond. In terms of the qualitative theory above, g_{rs} is therefore just the key quantity $-2\beta_{rs}S_{rs}$. (We, however, avoid the integral S in the present theory since the overlaps are neglected).
3. The Hamiltonian matrix element between two determinants differing by one spin permutation between orbitals r and s is equal to g_{rs}. Any other off-diagonal matrix elements are set to zero (see Scheme 12).

$\lvert\bar{a}bc\bar{d}\rvert$	$\lvert a\bar{b}c\bar{d}\rvert$	$\lvert a\bar{b}\bar{c}d\rvert$	$\lvert\bar{a}bcd\rvert$	$\lvert abc\bar{d}\rvert$	$\lvert\bar{a}\bar{b}cd\rvert$
0	0	g_{ab}	g_{cd}	0	g_{bc}
	0	g_{cd}	g_{ab}	g_{bc}	0
		g_{bc}	0	0	0
			g_{bc}	0	0
				$g_{ab}+g_{cd}$	0
					$g_{ab}+g_{cd}$

Scheme 12

Diagonalization of this matrix gives the energy of the ground state relative to the nonbonding state (the spin-alternant determinant), and in addition leads to the entire spectrum of the lowest neutral excited states. Note that applying the spin-Hamiltonian model to ethylene leads to a π bonding energy $-g$, which is equivalent to the $2\beta S$ used in the qualitative VB theory above.

Applications

Ground States of Polyenes and Hund's Rule Violations

A simple principle of the spin-Hamiltonian VB theory is that *the lowest state of a molecule will have the multiplicity associated with the S_z value of its MSAD*, that is, it will be a singlet if $n_\alpha = n_\beta$ in the MSAD, a doublet if $n_\alpha = n_\beta + 1$, a triplet if $n_\alpha = n_\beta + 2$, and so on.[217] For example, the MSAD of orthoxylylene **27** and paraxylylene **28** (Scheme 13) both have $S_z = 0$ while that of metaxylylene (**29**) has $S_z = 1$.

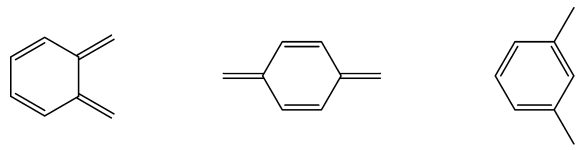

27 **28** **29**

Scheme 13

It follows that ortho- and para-xylylenes will have singlet ground states while metaxylylene has a triplet ground state. The prediction is correct but not particularly surprising, since **27** and **28** can be described by a perfectly paired Kekulé structure while **29** cannot and is therefore a diradical that will be a triplet state based on Hund's rule. More intriguing are the predictions of Hund's rule *violations*. Let us consider, for example, 2,3-dimethylene-butadiene and 1,3-dimethylene-butadiene.These are two polyenes for which it is impossible to draw a Kekulé structure, and which are therefore diradicaloids. Now the MSAD of these two species (**30** and **31** in Scheme 14) have different S_z values, $S_z = 0$ for **30** versus $S_z = 1$ for **31**.

30 **31**

Scheme 14

In this case, the spin-Hamiltonian predicts 2,3-dimethylene-butadiene to be a singlet diradicaloid (in violation of Hund's rule) and 1,3-dimethylene-butadiene to be a triplet, in agreement with experiment. By contrast, monodeterminantal MO calculations predict that all these diradicaloids have triplet ground states. It is only after CI that one gets the correct assignments.[218] Violations of Hund's rule can be explained by the phenomenon of dynamic spin-polarization and predicted to take place when the degenerate singly occupied MOs form a disjointed set.[218,219] In such a case, the advantage of the triplet over the singlet becomes very weak owing to a small exchange integral, and when CI is applied, it preferentially stabilizes the singlet, and reverses the singlet–triplet energy order. Comparison of the spin-polarization argument to the present VB analysis, shows the VB method to be faster, physically intuitive, and independent of any numerical calculation.

Relative Stabilities of Polyenes

Subtle predictions can be made about the relative energies of two isomers having comparable Kekulé structures, such as the linear s-trans conformation and branched conformation of hexatriene, **18** and **22** in Scheme 9 above. For each of these isomers, we shall consider that the total π energy is a perturbation of

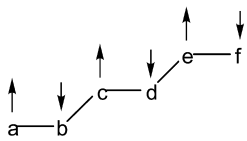

32

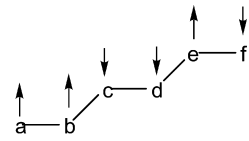

33

Scheme 15

the energy of the MSAD (e.g., **32** for the linear conformation in Scheme 15) by less ordered determinants. Each of the latter determinants is generated from the MSAD by the inversion of two spins along a given linkage (e.g., **33** vs. **32** in Scheme 15), while keeping the total S_z constant. According to the above rules, the Hamiltonian matrix element between **32** and **33** is the integral g_{bc}, and the energy of **32** relative to **33** is $g_{ab} + g_{cd}$, since the spin reorganization introduces two Pauli repulsions along the *a-b* and *c-d* linkages.

More generally, the number of Pauli repulsions that one introduces, relative to the MSAD, by inverting the spins in a linkage *r-s* is equal to the number of linkages that are adjacent to *r-s*. Thus, assuming that all the *g* integrals are the same for the sake of simplicity, the energy of a determinant Ψ_{rs} generated by spin inversion relative to a MSAD Ψ is given by Eq. [87]:

$$E(\psi_{rs}) - E(\psi) = g \times n_a(rs) \qquad [87]$$

where n_a is the number of linkages that are adjacent to *r*-*s*. We now consider all determinants displaying a spin transposition between two adjacent atoms with respect to the MSAD. The matrix elements between the determinants Ψ_{rs} and Ψ will be the same and all equal to the *g* integral. Hence, the total π energy that arises from a second order perturbation correction ($PT2$) will be given by Eq. [88]:

$$E(PT2) = \sum_{rs} \frac{g^2}{g n_a(rs)} \quad = \quad g \sum_{rs} \frac{1}{n_a(rs)} \qquad [88]$$

where the energy is calculated relative to the MSAD. Therefore, it appears that the energy of a polyene is a simple topological function that is related to the shape of the molecule and to the way the various linkages are connected to each other. Calculating the energies of the two isomers of hexatriene is thus

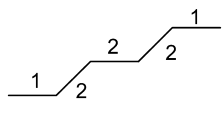

34

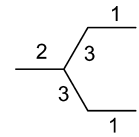

35

$E(\text{PT2}) = -(2/1 + 3/2)g$ $E(\text{PT2}) = -(2/1 + 1/2 + 2/3)g$

Scheme 16

a simple matter. In Scheme 16, each linkage in **34** and **35** is labeled by the number of bonds that are adjacent it. From these numbers, the expressions for the total energies of each isomer are immediately calculated (Scheme 16), and clearly show that the linear isomer is more stable than the branched one, in agreement with experimental facts.

AB INITIO VB METHODS

A number of ab initio VB methods have been implemented to calculate VB wave functions and their associated energies and molecular properties. Once the general scheme for writing VB wave functions is established (see *Basic VB Theory* above), an important task is the optimization of the orbitals that are used to construct the AO or FO determinants of the VB structures. Historically, the classical VB method used the atomic orbitals of the free atoms, without any further change. This crude approximation, which is no longer employed, resulted in highly inaccurate energies, since it does not take into account the considerable rearrangements in size and shape that an

AO undergoes when fragments assemble to a molecule. Accordingly, we shall restrict ourselves here to modern VB methods that perform orbital optimization.

Orbital-Optimized Single-Configuration Methods

A great step forward in accuracy and compactness was made when optimized orbitals of Coulson–Fischer (CF) type were employed in VB calculations. As shown above (*Basic VB Theory*), describing a two electron bond as formally covalent singlet coupling between two CF orbitals φ_a and φ_b (Eqs. [6b] and [6c]), which are optimized and free to delocalize over the two centers, is an ingenious way to include both the covalent and ionic components of the bond in an implicit way in a wave function of the Heitler–London type. Thus, the CF representation has the advantage of keeping the well-known picture of perfect pairing while treating the left–right electron correlation associated with any given bond in a variational way.

The CF proposal, generalized to polyatomic molecules, gave rise to the "separated electron pair" theory that was initiated by Hurley et al.[220] and later developed as the GVB method by Goddard and co-workers,[109,221,222] and as the SC method by Gerratt and co-workers.[112–114,223–225] In both these latter methods the valence electrons are described by a single configuration of singly occupied orbitals, and the various spin-coupled structures—generated so as to form a complete and linearly independent set of spin-eigenfunctions—are allowed to mix to generate the final state. In the SC method, both the orbitals and the mixing coefficients are optimized simultaneously, while in the most general form of GVB theory they are optimized sequentially. It is important to note that, while no constraint of any kind is applied to the shapes of the orbitals during the optimization, they are generally obtained in a form that is pretty much localized, as will be exemplified below. Thus, each bond in a polyatomic VB structure is viewed as a pair of singlet-coupled orbitals that are quasi-atomic and display a strong mutual overlap.

The Generalized VB Method

The GVB method is generally used in its restricted perfectly paired form, referred to as GVB–PP, which pairs the atoms as in the most important Lewis structure. The GVB–PP method introduces two simplifications. The first one is the Perfect-Pairing (PP) approximation, by which only one VB structure is generated in the calculation. The wave function may then be expressed in the simple form of Eq. [89], where each term in parentheses is a so-called "geminal" two-electron function, which takes the form of a singlet-coupled GVB pair (φ_{ia}, φ_{ib}) and is associated with one particular bond or lone pair.

$$\psi_{GVB} = |\,(\varphi_{1a}\overline{\varphi}_{1b} - \overline{\varphi}_{1a}\varphi_{1b})(\varphi_{2a}\overline{\varphi}_{2b} - \overline{\varphi}_{2a}\varphi_{2b})\cdots(\varphi_{na}\overline{\varphi}_{nb} - \overline{\varphi}_{na}\varphi_{nb})\,| \quad [89]$$

The second simplification, which is introduced for computational convenience, is the *strong orthogonality* constraint, whereby all the orbitals in Eq. [89] are required to be orthogonal to each other unless they are singlet paired, that is,

$$\langle \varphi_{ia} | \varphi_{ib} \rangle \neq 0 \qquad [90a]$$

$$\langle \varphi_i | \varphi_j \rangle = 0 \text{ otherwise} \qquad [90b]$$

This strong orthogonality constraint is, of course, a restriction, however, usually not a serious one, since it applies to orbitals that are not expected to overlap significantly. By contrast, the orbitals that are coupled together in a given GVB pair display, of course, a strong overlap.

For further mathematical convenience, each geminal in Eq. [89] can be rewritten, by simple orbital rotation, as an expansion in terms of natural orbitals,

$$|(\varphi_{1a}\overline{\varphi}_{1b} - \overline{\varphi}_{1a}\varphi_{1b})| = C_i |\phi_i \overline{\phi}_i| + C_i^* |\phi_i^* \overline{\phi_i^*}| \qquad [91]$$

This alternative form of the geminal contains two closed-shell terms. The natural orbitals ϕ_i *and* ϕ_i^*, in Eq. [91], have the shapes of localized bond MOs, respectively bonding and antibonding, and are orthogonal to each other. They are connected to the GVB pairs by the simple transformation below:

$$\varphi_{ia} = \frac{\phi_i + \lambda \phi_i^*}{(1+\lambda^2)^{1/2}} \qquad [92a]$$

$$\varphi_{ib} = \frac{\phi_i - \lambda \phi_i^*}{(1+\lambda^2)^{1/2}} \qquad [92b]$$

$$\lambda^2 = -\frac{C_i^*}{C_i} \qquad [92c]$$

The use of natural orbitals, which constitute an orthogonal set, avoids the $N!$ problem, resulting in a great computational advantage over the use of the GVB pairs in the effective equations that have to be solved for self-consistency. A GVB–PP calculation is thus just a special case of a low-dimensional MCSCF calculation, with all the CPU advantages of MO calculations and the additional interpretability of a wave function that is transformed eventually to a VB form.

The perfect-pairing and strong-orthogonality restrictions result in considerable computer time savings and no great loss of accuracy, as long as the computed molecule is made of clearly separated local bonds (e.g., methane).[226] On the other hand, it is clear that these restrictions would be

highly inappropriate for delocalized electronic species like benzene, for which the PP approximation is not meaningful, and all electron-pairing schemes have to be considered to provide a reasonable state wave function.[207,227]

The GVB method takes care of all the left–right correlation in molecules, but does not include the totality of the "nondynamical" electron correlation since the various local ionic situations are constrained to be equal with this method (e.g., two adjacent local ionic forms $+-/-+$ and $+-/+-$ will be found to possess the same weight). Accounting for the full nondynamical correlation, requires a "Complete Active Space" MCSCF calculation (CASSCF,which involves all possible configurations that can be constructed within the space of valence orbitals). Having said that, we nevertheless emphasize that as a rule, the GVB method provides results that are much closer to CASSCF quality than to Hartree–Fock.

As a VB method, GVB ensures correct homolytic dissociation as a bond is broken. However, the calculated dissociation energy is generally too low, due to lack of dynamical electron correlation, although far better than the value computed at the Hartree–Fock level. For example, while Hartree–Fock gives a negative bond dissociation energy of F_2, GVB yields a positive bond energy, but one that is less than one-half of the experimental value.[132] As shown below, better accuracy can be reached by going beyond the one-configuration VB model.

The perfect-pairing GVB wave function is a good starting point for further CI, called "Correlation-Consistent Configuration Interaction" (CCCI). Thus, Carter and Goddard defined a general method employing a relatively small but well-defined CI expansion for calculating accurate bonding energies.[228] In this method, one first generates a restricted CI expansion (RCI) in which each GVB pair is allowed to have all three possible occupancies for two electrons distributed among the orbitals of that bond pair. Then, the CI is extended by including all single and double excitations from each bond pair that undergoes dissociation to all other orbitals. Further, since bond dissociation generally leads to geometric and hybridization changes in the resultant fragments, the change in shape of the orbitals adjacent to the dissociating bond(s) is also taken into account. This is done by adding, from each RCI configuration, all single excitations from the valence space to all orbitals. The GVB–CCCI approach has been successfully applied to single and double bonds and to transition metal complexes.[228]

The Spin-Coupled Method

The spin-coupled method of Gerratt and co-workers[112–114,223–225] differs from the GVB–PP method in that it removes any orthogonality and perfect-pairing restrictions. The method is still of the single-configuration type, but all the modes of spin-pairing are included in the wave functions and the orbitals are allowed to overlap freely with each other. The SC method has often been used to provide firm theoretical support to some basic concepts

like orbital hybridization, or resonance between Kekulé structures, which were qualitative postulates in the early days of VB theory. The chemical picture that emerges from the SC method has the following features: (a) the SC method deals with correlated electrons; (b) no preconceptions or constraints are imposed on the spin-couplings nor on the shapes of the orbitals, which are determined by the variational principle alone; (c) the set of orbitals arising from such calculations is unique. As such, the SC method represents the ultimate level of accuracy compatible with the orbital approximation that describes the molecule as a single configuration with fixed orbital occupancies. Thus, it is clear that the shape of the orbitals and the relative importance of the various spin-couplings determined by this method, should have strong relevance to the nature of chemical bonding.

The methane molecule, as the archetypal system displaying hybridization, has been studied by Cooper et al.[229] in the framework of SC theory. It appears that the spin-coupled description of methane resembles very closely our intuitive view of four localized C—H bonds. The eight spin-coupled orbitals that arise from the variational principle fall into two groups of four. Four of the orbitals are each localized on a hydrogen atom. The other four degenerate orbitals are localized on carbon, and each represents a slightly distorted, approximately sp^3 hybrid pointing toward one of the H atoms. All the hybrid orbitals are identical in shape and mutually related by symmetry operations of the T_d point group. The full spin-coupled wave function, with its 14 different spin-couplings, lies 65 mh below the Hartree–Fock wave function and only 12 mh above the full valence CASSCF wave function with its 1764 spin functions. The perfect-pairing function is the dominant mode of spin-coupling, only 3 mh above the full spin-coupled wave function. It is noted that the strong orthogonality restriction that is often used in GVB theory is an excellent approximation that barely raises the total energy, by < 2 mh.[226] The hybridization picture is of course very general, and allows any type of hybridization beyond the classical sp^3, sp^2 and sp types. For example, according to a GVB calculation by Goddard,[221] the hybrids involved in the O—H bonds of H_2O have more p character than the lone pairs (82 and 59%, respectively, as compared to the 75% expected for sp^3 hybrids), in agreement with the fact that the HOH angle is smaller than the standard tetrahedral angle.

Calculations of SC[230] or GVB[231,232] types have also been able to provide a simple picture for the electronic structure of lithium clusters Li_n ($n = 3$–8). In these cases, once again a single spin-coupling is found to be sufficient, but the optimized orbitals, though being localized, are not atomic but interstitial, that is, localized between two nuclei or more. The rhomboid structure **36** of Li_4, for example, is easily explained by the single spin-coupling displaying two bonds between interstitial orbitals, as illustrated in Scheme 17.

The SC method has also been used to probe the validity of the traditional description of conjugated molecules, and in particular aromatic systems, as sets of resonating Kekulé structures. Taking benzene as an example and using

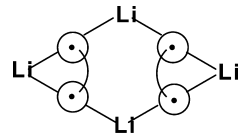

36

Scheme 17

the σ–π separation, the converged spin-coupled wave function[207] displays two dominant spin functions, which correspond to the traditional Kekulé structures. The orbitals that arise from the calculation are highly localized and have the form of slightly distorted *2p* AOs perpendicular to the molecular plane. The three remaining spin functions that are necessary to form a complete basis set of neutral VB structures, the so-called Dewar structures, contribute only 20% to the ground state. This one-configuration wave function is considerably lower in energy than the Hartree–Fock level, by 75 mh, and only 7 mh higher than the full valence CI within the π-valence space. The description of benzene as a mixture of limiting Kekulé structures is thus given a firm foundation that proves to be generally valid for other aromatic and antiaromatic systems.

The spin-coupled valence bond (SCVB) theory is an extension of the spin-coupled method, in which further CI is performed after the one-configuration calculation. At the simplest level, the CI includes all the configurations that can possibly be generated by distributing the electrons within the set of the active orbitals that were optimized in the preliminary SC calculation; both covalent and "ionic" type configurations are considered. When applied to the π system of benzene,[207] this level of calculation was found to provide a satisfactory account of the valence states, and showed that the first excited state, $^1B_{2u}$, is made of the antiresonant combination of the two Kekulé structures. A higher level of SCVB theory includes additional excitations, for example, from the orbitals of the σ core, or to orbitals that are virtual in the one-configuration calculation. To preserve the valence bond character of the wave function, the virtual orbitals have to be localized as much as possible. This condition is met in the SCVB method,[223] in which each occupied orbital of the ground configuration is made to correspond to a stack of virtual orbitals localized in the same region of space, by means of an effective operator representing the field created by the remaining occupied orbitals. There remains to perform a simple CI (of nonorthogonal type) among the space of the configurations so generated. By experience, the excited configurations generally bring very little stabilization as far as ground states are concerned. This is easily explained by the fact that the orbitals are optimized precisely so as to concentrate all important physical effects in the reference single configuration. On the other

hand, excited configurations are important for satisfactory state ordering and transition energies.[207]

Orbital-Optimized Multiconfiguration VB Methods

VBSCF

The VBSCF method of van Lenthe and Balint-Kurti[117] is a general method of multiconfiguration self-consistent field (MCSCF) type, which is able to deal with nonorthogonal orbitals. The VBSCF wave function is, in principle, a linear combination of VB structures, in which both orbitals and coefficients are optimized simultaneously. It is therefore a generalization of the above one-configuration methods to the multiconfiguration case, with the interesting advantage that no particular configuration is favored during the course of the orbital optimization. The orbitals can be optimized freely as in GVB or SC methods, but may also be constrained to be localized each on a single atom or fragment. The method has been efficiently implemented[118,119,233,234] by the Utrecht group in the TURTLE program.[120] A program having similar capabilities, XIAMEN 99, has been developed by Wu and co-workers, based on the spin-free formulation of VB theory.[128] Being a multiconfigurational method, the VBSCF theory, in TURTLE and XIAMEN99, is an ideal tool for studying problems that involve resonance energies and avoided crossing situations. Some examples of this usage are discussed below.

The VBSCF method has been used to probe the validity of the resonance model in organic chemistry following some controversies that appeared in the literature, regarding the presence or absence of resonance stabilization, for example, in the peptide bond, carboxylic acids, and enols. The enhanced acidity of carboxylic acids relative to alcohols is traditionally attributed to the stabilization of the carboxylate anion by delocalization of its π electrons via resonance structures **37–39** in Scheme 18.

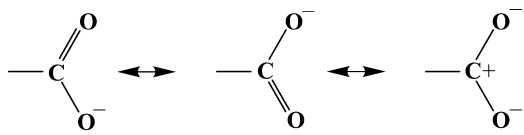

37 **38** **39**

Scheme 18

A similar resonating scheme can be applied to the enolate anion. On the other hand, not being a conjugated system, this does not apply to the alkoxide anion. However successful, this traditional view was challenged by several authors[235–238] who advanced the idea that the enhanced acidities originate from the high polaritizabilities of the carbonyl and vinyl groups. To resolve

the controversy, one must answer the key question: how much does π electron delocalization stabilize the carboxylate and enolate anions relative to a reference situation in which the delocalization would be "turned off"? Clearly, a meaningful answer to this question would emerge only when the orbitals in the VB wave function are strictly localized, as in the VBSCF method.

A direct estimate of the stabilization energy due to delocalization is very simple, as illustrated with the following example of the carboxylate anion, in Scheme 18. First, a localized reference state is calculated, in which the geometry and the orbitals are optimized with the unique restriction that the π atomic orbital of one of the oxygens cannot delocalize over the other atoms and remains doubly occupied, as in **37**. Second, the ground state is calculated at the same level of theory, but with electron delocalization being fully allowed. The results of the calculations[239] give a clear-cut answer: In all cases the delocalization of the oxygen π lone pair stabilizes the anion more than the parent acids. These excess values are 23 kcal/mol for carboxylic acids and 21 kcal/mol for enols compared with only 8 kcal/mol for alcohols. It follows that, in accord with the traditional view, π electron delocalization plays an important role in the acidity enhancement of carboxylic acids and enols relative to alcohols. By comparison with the experimental acidities, it was concluded[239] that a lower limit for the contribution of electron delocalization to the total acidity enhancement is 48% for the carboxylic acids and 62% for the enols, values that clearly establish the importance of resonance effects, while leaving some room for nonnegligible inductive effects.

The peptide and thio-peptide bonds have some specific properties like coplanarity, substantial rotational barrier and kinetic stability towards nucleophilic attack or hydrolysis. All these properties are easily rationalized by the

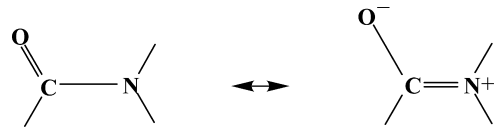

40 **41**

Scheme 19

classical resonance hybrid model, illustrated in Scheme 19 for an amide. According to this resonating picture, the peptide bond is mainly described by **40**, with a significant contribution from the charge-transfer structure **41**, and this resonance contribution is the root cause of both the low basicity of the nitrogen's lone pair and the barrier to rotation around the C—N bond.

As in the preceding case, the simple resonance picture was criticized[240–242] on the basis of electron population analyses using the AIM method,[243] to the extent that (thio)amides were proposed to be viewed as special

cases of amines with a carbonyl substituent.[242] At the heart of the debate[244–247] was the role of the π electron delocalization energy in the barrier to rotation (16 kcal/mol for formamide, 18 kcal/mol for thioformamide[248]) around the C—N bond. To settle the question, the adiabatic energy difference between the localized form **40**, with the π lone pair localized on the nitrogen atom, and the fully delocalized ground state, was calculated[249] for formamide and thioformamide with the VBSCF method,[117] and the same type of calculation was repeated for the 90° rotated conformations. As a result, the contribution of resonance stabilization to the rotational barrier, estimated as that quantity by which electron delocalization stabilizes the planar conformation more than the 90° rotated conformation, was found to be 7.3 and 13.7 kcal/mol, respectively, for formamide and thioamide. While this indicates that other factors do contribute to the rotational barrier, resonance stabilization in amides and thioamides emerges as an important factor, in agreement with the traditional view and the common wisdom that allylic resonance is an important driving force in organic chemistry.

Clearly, therefore, VBSCF constitutes a handy tool for studies of the role of electronic delocalization, in molecules that possess more than one Lewis structure.

VBCI: A Post VBSCF Method that Involves Dynamic Correlation

The VBCI method, recently developed by Wu et al.[138] is a post-VBSCF calculation that uses configuration interaction to supplement the VBSCF energy with dynamic correlation. At the same time, the method preserves the interpretability of the final wave function in terms of a minimal number of VB structures, each having a clear chemical meaning. The VB structures that are used in the VBSCF calculations are referred to as fundamental structures, denoted as Φ_K^0, and the orbitals that appear in the VBSCF calculation are referred to as occupied orbitals. Depending on the problem at hand, the VBSCF calculation may use semidelocalized CF orbitals, or orbitals that are each localized on a single atom or fragment; in the latter case the fundamental structures will explicitly involve the covalent and ionic components of the bonds.

The CI calculation that follows the VBSCF step requires the definition of virtual orbitals. To keep the interpretability of the final wave function, the virtual orbitals are defined, by use of a projector, so as to be localized on the same fragments as the corresponding occupied orbitals. After generating the virtual orbitals, the excited VB structures are created in the following way. Given a fundamental structure Φ_K^0, an excited VB structure Φ_K^i is built-up by replacing occupied orbital(s) φ_i with virtual orbital(s) φ_j^*. By restricting the replacement of virtual orbital φ_j^* to the same fragment as φ_i, the excited structure Φ_K^i retains the same electronic pairing pattern and charge distribution as Φ_K^0. In other words, both Φ_K^0 and Φ_K^i describe the same classical VB structure. Thus, the collection of excited VB structures nascent from a given fundamental VB structure serves to relax the latter and endow it with dynamic correlation.

Several levels of CI can be employed. The starting point always involves single excitations and is referred to as VBCIS. This can be followed by VBCISD, VBCISDT, and so on, where D stands for double excitations and T for triples. The level at which truncation is made will depend on the size of the problem and the desired accuracy. In practice, the VBCISD level has been tested for some dissociation energies and reaction barriers for hydrogen exchange reactions[138,142] and has been shown to match the accuracy of the molecular orbital based coupled cluster CCSD and CCSD(T) methods, while retaining the interpretability of simpler VB methods. In the case of the hydrogen exchange reaction[142] of $H + H_2$, the method gave a barrier of 10 kcal/mol, compatible with the corresponding experimental data (9.6–9.8 kcal/mol). In summary: The VBCI method can be used like the VBSCF method for problems involving resonance and for calculating VBSCDs. The accuracy of VBCI is comparable to CCSD and CCSD(T) methods.

Different Orbitals for Different VB Structures

There are many molecules, in particular some radicals, that are naturally described in terms of two or more resonance structures, and for which the one-configuration approximation is not appropriate. Such molecules are generally subject to the well-known broken-symmetry artifact, whereby a wave function calculated at an insufficient level of theory is of lower symmetry than the nuclear framework, which results in erroneous energetics and discontinuities of the calculated potential surface. The formyloxyl radical (**42** ↔ **43** in Scheme 20) is a typical example, but the problem is very general and includes

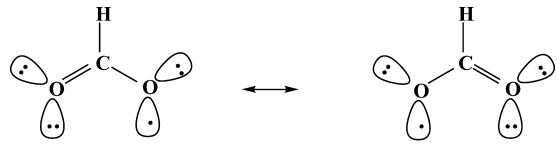

42 **43**

Scheme 20

an enormous variety of open-shell electronic states, as, for example, allyl radicals[250] or radicals of allylic type,[251–256] core-ionized diatoms,[257] n–π^* excited molecules containing two equivalent carbonyl groups,[258] n-ionized molecules having equivalent remote lone pairs,[259] and charged clusters.[260–263] The same problem arises in localized versus mixed-valent organometallic species with two metal ions that can have different oxidation states, in doped stacks of aromatic conductors and semiconductors, and in electron-transfer processes between two identical species (e.g., metal ion centers separated by a bridge). Clearly, this is a ubiquitous problem in chemistry.

The problem has been lucidly rationalized by McLean et al.[255] in VB terms. It arises from a competition between two VB-related effects. The first is the familiar resonance effect whereby a mixture of two resonance structures is lower in energy than either one taken separately. The other is the so-called orbital size effect, whereby each VB structure gains stabilization if it can have its particular set of orbitals, which are specifically optimized for that VB structure and not the other. The two effects cannot be taken into account simultaneously in any one-configuration theory, be it of VB or MO type, because it employs a common set of orbitals. In the (frequent) case where the orbital size effect is the important factor, the wave function takes more or less the form of one particular VB structure, thereby resulting in an artefactual symmetry-breaking. In the MO-based framework, the remedy consists of performing MCSCF calculations in a rather large space of configurations.[255] On the other hand, the remedy is very simple in the VB framework, and consists of allowing different orbitals for different VB structures in the course of the orbital optimization, as illustrated in Scheme 21, by **44** and **45** for the formyloxyl radical,

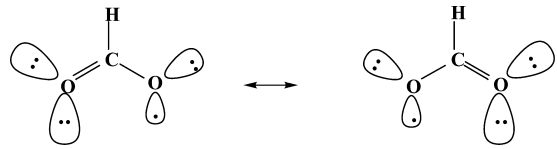

44 **45**

Scheme 21

in which the doubly occupied orbitals are diffuse and hence drawn larger than the more compact singly occupied ones. Note that *all* the orbitals of **44** are different from those of **45**, although the major differences are seen between the two orbitals that are involved in the electron transfer.

In the spirit of the above described method, Jackels and Davidson[252] cured the symmetry-breaking problem in the NO_2 radical by using a symmetry-adapted combination of two symmetry-broken Hartree–Fock wave functions, by means of a 2×2 nonorthogonal CI. The generalized multistructural (GMS) method of Hollauer and Nascimento[264,265] includes both the symmetry broken structures and the symmetry-adapted one in the same calculation, followed by subsequent CI. The symmetry-broken subwave functions are optimized at the GVB level in the R-GVB (Resonating-GVB) method of Voter and Goddard.[257] In all these methods, the subwave functions representing the individual resonance structures are optimized separately, which may lead to an underestimation of the resonance energy since the orbital optimization only takes care of the size effect. To remedy this defect, Voter and Goddard subsequently improved their method by allowing the subwave functions

to be optimized in the presence of each other, leading to the final generalized resonating valence bond method (GRVB).[258]

Breathing Orbitals: A Post VBSCF Method that Involves Dynamic Correlation

The breathing orbital valence bond (BOVB) method[132–137] is a generalization of the principle of "different orbitals for different structures" to the description of the elementary bond, be it of the one-electron, two-electron, or three-electron type. The objective of the method is threefold: (a) yielding accurate bond dissociation energy curves, which is a necessary condition for a meaningful description of the elementary events of a reaction, bond breaking and bond formation; (2) keeping the wave function compact and transparent in terms of structural formulas; (3) being suitable for calculations of diabatic states. In order to achieve these requirements, the method rests on the basic principle that if all relevant structural formulas for a given electronic system are generated, and if their VB description is made optimal by a proper orbital optimization, then a variational combination of the corresponding VB structures would accurately reproduce the energetics of this electronic system throughout a reaction coordinate. Accordingly, the composite VB structures of CF type are abandoned and the wave function takes a classical VB form in which all possible structural formulas (e.g., covalent and ionic) are generated. Then, each structural formula is made to correspond to a single VB structure that displays the appropriate orbital occupancy.

Since the ionic and covalent components of the bonds are explicitly included in the wave function, it is not necessary (and in fact, not useful) to let the orbitals of the VB structures be delocalized. This exclusion permits a better interpretability of the wave function in terms of unambiguous structural formulas, by dealing with VB structures defined with orbitals that are each strictly localized on a single atom or fragment. Within this constraint, the orbitals are optimized with the freedom to be different for different VB structures, so as to minimize the energy of the full multistructure wave function. It is important to note that the different VB structures are not optimized separately but in the presence of each other, so that the orbital optimization not only lowers the energies of each individual VB structure but also maximizes the resonance energy resulting from their mixing. As such, the BOVB wave function is a post-VBSCF method that incorporates dynamic correlation.

The difference between the BOVB and GVB or SC philosophies is best appreciated by comparing their respective descriptions of the two-electron bond. The classical representation for the GVB or SC wave function, obtained after expansion of the CF expression into AO determinants as in Eq. [7], takes the form of a linear combination of covalent and ionic classical VB structures (**46–48**), for which both coefficients and orbitals are optimized. However, there is the penalizing restriction that the same common set of AOs is used for all three structures, as shown in Scheme 22 for the F_2 molecule.

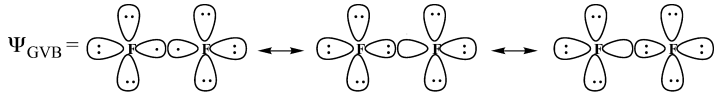

F•–•F **F⁻ F⁺** **F⁺ F⁻**

46 **47** **48**

Scheme 22

On the other hand, the BOVB method assumes the three-structure classical form of the wave function right at the outset. Like the GVB or SC methods, it optimizes the coefficients and the orbitals simultaneously, but with the important feature that each VB structure (**49–51**) may now have its specific set of orbitals, different from one structure to the other, as pictorially represented in Scheme 23, for the same F—F bond.

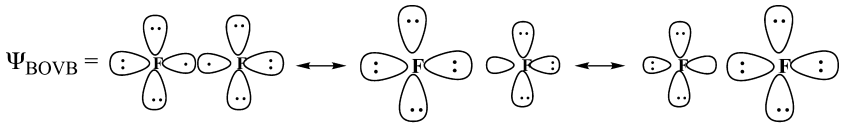

49 **50** **51**

Scheme 23

As a consequence of the BOVB procedure, the active orbitals (those involved in the bond) can use this extra degree of freedom to adapt themselves to their instantaneous occupancies. The spectator orbitals (not involved in the bond) can fit the instantaneous charges of the atoms to which they belong. Thus, all the orbitals follow the charge fluctuation that is inherent to any bond by undergoing instantaneous changes in size and shape, hence the name "breathing orbitals". The same philosophy underlies the description of odd-electron bonds, in terms of two VB structures.

Since the BOVB wave function takes a classical VB form, it is not practical for the VB description of large electronic systems, because a large number of VB structures would have to be generated in such a case. As such, the usual way of applying BOVB is to describe with it only those orbitals and electrons that undergo significant changes in the reaction, like bond breaking or formation, while the remaining orbitals and electrons are described as doubly occupied MOs. Thus, even though the spectator electrons reside in doubly occupied MOs, these orbitals too are allowed to optimize freely, but are otherwise left uncorrelated.

The BOVB method has several levels of accuracy. At the most basic level, referred to as L-BOVB, all orbitals are strictly localized on their respective fragments. One way of improving the energetics by allowing more degrees of freedom is to let the inactive orbitals get delocalized. This option, which does not alter the interpretability of the wave function, accounts better for the nonbonding interactions between the fragments and is referred to as D-BOVB. Another improvement can be achieved by incorporating radial electron correlation in the active orbitals of the ionic structures, by allowing the doubly occupied orbitals to split into two singly occupied orbitals that are spin-paired. This option carries the label "S" (for split), leading to the SL-BOVB, and SD-BOVB levels of calculation, the latter being the most accurate.

The BOVB method has been successfully tested for its ability to reproduce dissociation energies and/or dissociation energy curves close to full CI results or other highly accurate calculations performed with the same basis sets. A variety of two-electron and odd-electron bonds, including difficult test cases as F_2, FH, or F_2^-,[133–135] and the H_3M—Cl series (M = C, Si, Ge, Sn, Pb)[137,155,266] were investigated. Owing to its use of strictly localized active orbitals, the method is suitable for calculating clearly defined diabatic states that are supposed to retain the physical features of a given asymptotic state at any point of a reaction coordinate without collapsing to the ground state by virtue of uncontrolled orbital optimization.

It is interesting to interpret the improvement of BOVB with respect to a CASSCF, GVB, or SC calculation of a two-electron bond. These four methods account for all the nondynamic correlation associated with the formation of the bond from separate fragments, but differ in their dynamic correlation content. In a medium-sized basis set, say 6-31+G(d), CASSCF, GVB, or SC account for less than one-half of the bonding energy of F_2, 14–16 kcal/mol.[133] On the other hand, an SD-BOVB calculation yields a bonding energy of 36.2 kcal/mol,[a] versus an experimental value of 38.2 kcal/mol.[137] Where does this difference come from? It appears that the BOVB method brings just what is missing in the CASSCF calculation, that is, dynamical correlation, not all of it but just *that part that is associated to the bond that is being broken or formed*. In other words, the BOVB method takes care of the differential dynamical correlation. In this respect it is approximately equivalent to the VBCI method.

The importance and physical nature of dynamic correlation is even better appreciated in the case of three-electron bonds, a type of bond in which the electron correlation is entirely dynamic, since there is no left–right correlation

[a]Note that this bonding energy is overestimated with respect to a full CI calculation for the same basis set, which is estimated as close to 30 kcal/mol. The SD-BOVB systematically overestimates bonding energies relative to full CI and yields values that are intermediate between full CI and experiment, a "fortunate" systematic error that compensates for basis set insufficiency.

associated with odd-electron bonds. As has been noted above, the Hartree–Fock and simple VB functions for three-electron bonds (hence GVB, SC, or VBSCF) are nearly equivalent and yield similar bonding energies. If we take the F_2^- radical anion as an example, it turns out that the Hartree–Fock bonding energy is exceedingly poor, only 4 kcal/mol at the spin-unrestricted Hartree–Fock level (UHF), and even worse at the restricted Hartree–Fock (RHF) level, while the experimental bonding energy is 30.3 kcal/mol. By contrast, the SD-BOVB calculation, which involves only two VB structures (**52**, **53**) with breathing orbitals as in Scheme 24 below, yields an excellent bonding energy of 28.0 kcal/mol.

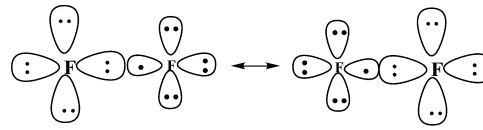

52 **53**

Scheme 24

Looking at **52** and **53** in Scheme 24 allows a clear understanding of the nature of the dynamic correlation effect. Indeed, with respect to a Hartree–Fock or VBSCF calculation, the BOVB wave function brings the additional effect that the orbitals adapt themselves to the net charge of each fragment, for example, being more diffuse when the fragment is negatively charged and less so when the fragment is neutral. This effect, which we have called the "breathing orbital effect" but which is called "size effect" by others, corresponds to the differential dynamic correlation associated with the bond, and is just *the instantaneous adaptation of the orbitals to the dynamic charge fluctuations that transpire in the bond*. This interpretation of dynamic correlation, which is particularly apparent in the three-electron bond, carries over to the two-electron bond (e.g., F_2 above) that also undergoes some charge fluctuation through its ionic components.

The BOVB method has been used for many applications relevant to bonding in organic, inorganic, and organometallic chemistry.[133,134,155,167,168,266–274] Recently, the L-BOVB method was applied to compute the barriers to hydrogen abstraction in the series $X\bullet + H{-}X' \rightarrow X{-}H + \bullet X'$, and gave results comparable with CCSD at the same basis set.[167]

In summary, the VBSCF,[117–120] VBCI,[138] and BOVB[133–137] methods are ideal tools for studying bonding and for generating VBSCDs for chemical reactions. However, while VBSCF will provide a qualitatively correct picture, both VBCI and BOVB methods will give quantitatively good results in addition to a lucid chemical picture.

PROSPECTIVE

The many examples included in this chapter clearly demonstrate that far from being dead, VB theory is a vibrant field of research that produces many new methods and key paradigms of chemical bonding and reactivity. It is hoped that this chapter will serve its intended purpose of teaching some elements of this theory.

This review of VB theory and its applications is by no means exhaustive. The two most important omissions are the applications of this theory to the study of chemical dynamics and to enzymatic chemistry. Ever since the pioneering paper of London on the potential energy surface of H_3,[275] and the paper of Eyring and Polanyi[276] on elementary reactions, most of the surfaces used in the studies of chemical dynamics are based on VB formalisms and thinking, for example, LEPS surfaces, and those generated by application of DIM theory or the BEBO methods.[277,278] This kind of thinking was recently extended to the treatment of large molecules in the molecular mechanics-based VB method, called MCMM.[140,173] The empirical VB (EVB) method, initiated by Warshel and Weiss,[99] has gradually evolved into a general QM(EVB)/MM method[100,101] for the study of enzymatic reactions within their native protein environment. Owing to its lucid insight into chemical reactivity the prospects of this VB-based method are far reaching, and an example is a recent analysis of the role of near-attack-configuration (NAC) in enzymatic catalysis.[279] Elsewhere, in the field of enzymatic reactions, the use of VB ideas led to new paradigms, such as the notion of a chameleon oxidant, for the active species of the enzyme cytochrome P450.[280] Thus, in many respects, VB theory is coming of age, with the development of faster, and more accurate ab initio VB methods,[142] and with generation of new post-Pauling concepts. As these activities flourish further, so will the usage of VB theory spread among practicing chemists.

APPENDIX

A.1 Expansion of MO Determinants in Terms of AO Determinants

Let D_{MO} be a single determinant involving molecular spin orbitals φ_i and φ_j, which can be of α or β spins:

$$D_{\mathrm{MO}} = |\cdots \varphi_i \cdots \varphi_J \cdots| \qquad [A1]$$

$$\varphi_i = \sum_{\mu} C_{\mu i} \chi_{\mu} \qquad [A2]$$

$$\varphi_j = \sum_{\nu} C_{\nu j} \chi_{\nu} \qquad [A3]$$

Replacing φ_i and φ_j in Eq. [A1] by their expansions in terms of AOs, D_{MO} can be expanded into a linear combination of AO-based determinants. The procedure is carried out in the same manner by which one would expand a simple product of orbitals, as long as one remembers that the ordering of the orbitals is important in the AO determinants, and that two determinants that differ by permutation of two of their orbitals are equivalent but of opposite sign. Thus, many AO determinants in Eq. [A4] can be regrouped after permuting their orbitals and changing their signs.

$$\begin{aligned} |\cdots\varphi_i\cdots\varphi_j\cdots| &= \left|\left(\sum_{\mu} C_{\mu i}\chi_{\mu}\right)\cdots\left(\sum_{\nu} C_{\nu j}\,\chi_{\nu}\right)\right| \\ &= \sum_{\mu} C_{\mu i}\cdots\sum_{\nu}\; C_{\nu j}\cdots|\cdots\chi_{\mu}\cdots\chi_{\nu}\cdots| \end{aligned} \qquad [A4]$$

While this is a trivial matter for small determinants, larger ones require a bit of algebra and a systematic method[74] that is shown below.

Let us consider the determinant D_{MO} below as being composed of two "half-determinants", h^{α}_{MO} and h^{β}_{MO}, one regrouping the spin-orbitals of α spins and the other those of β spins.

$$D_{\mathrm{MO}} = (h^{\alpha}_{\mathrm{MO}}, h^{\beta}_{\mathrm{MO}}) \qquad [A5]$$

Half-determinants have no physical meaning but are defined here as a convenient mathematical intermediary. Each of these MO-based half-determinants can be expanded into AO-based half-determinants, just as has been done for the determinants in Eq. [A4]. After orbital permutations the AO-based half-determinants that are equivalent are regrouped, and we are left with some AO-based half-determinants h^{α}_{r}, each having a unique collection of AOs

$$h^{\alpha}_{\mathrm{MO}} = \sum_{r} C^{\alpha}_{r} h^{\alpha}_{r} \qquad [A6]$$

where the label r designates a given set of AOs.

The coefficients of each of these AO half-determinants in the expansion is given by Eq. [A7]:

$$C^{\alpha}_{r} = \sum_{P}(-1)^{t} P(\cdots\times C_{\mu i}\times\cdots\times C_{\nu j}\cdots) \qquad [A7]$$

where P is a permutation between indices μ and ν and t is the parity of the permutation. By associating two AO half-determinants h^{α}_{r} and h^{β}_{s}, one gets the full AO-based determinant $(h^{\alpha}_{r}, h^{\beta}_{s})$ whose coefficient in the expansion of

D_{MO} is just the product of the coefficients of its two half-determinants:

$$D_{\mathrm{MO}} = \sum_{r,s} C_r^{\alpha} C_s^{\beta} (h_r^{\alpha}, h_s^{\beta}) \qquad [A8]$$

A.2 Guidelines for VB Mixing

Derivation of matrix elements between polyelectronic VB determinants follows from the discussion in the text, and can be carried out by enumerating all the permutations of the respective diagonal terms, as in Eq. [A9]. Subsequently, one must define the reduced matrix element in Eq. [A10].[52]

$$\langle \Omega | H^{\mathrm{eff}} | \Omega' \rangle = \left\langle \Psi_d \middle| \sum h(\mathrm{i}) \middle| \sum (-1)^{\mathrm{t}} P(\Psi'_d) \right\rangle \qquad [A9]$$

$$\langle \Omega | H^{\mathrm{eff}} | \Omega' \rangle_{\mathrm{reduced}} = \langle \Omega | H^{\mathrm{eff}} | \Omega' \rangle - 0.5 (E(\Omega) + E(\Omega')) \langle \Omega | \Omega' \rangle \qquad [A10]$$

Unfortunately, the retention of overlap leads to many energy and overlap terms that need to be collected and organized, making this procedure quite tedious. A practice that we found useful and productive is to focus on the leading term of the matrix element. In this respect, we show a few qualitative guidelines that were derived in detail in the original paper[52] and discussed elsewhere.[53,84,143] Initially, one has to arrange the two VB determinants with maximum correspondence of their spin–orbitals. Then, one must find the number of spin–orbitals that are different in the two determinants, and apply the following rules.

1. The first and foremost rule is that the entire matrix element between two VB determinants is signed as the corresponding determinant overlap and has the same power in AO overlap. For example, the overlap between the two determinants of an HL bond, $|\,\mathrm{a}\overline{\mathrm{b}}\,|$ and $|\,\overline{\mathrm{a}}\mathrm{b}\,|$ is $-S_{ab}^2$, and hence the matrix element is negatively signed, $-2\beta_{ab}S_{ab}$. Since β_{ab} is proportional to S_{ab}, both the matrix element and the determinant overlap involve AO overlap to the power 2. For the one-electron bond case (Eq. [51]), the overlap between the determinants is $+S_{ab}$ and the matrix element $+\beta_{ab}$, while for the three-electron bond situation (Eq. [52]) the overlap between the determinants $|\,\mathrm{a}\overline{\mathrm{a}}\,\mathrm{b}\,|$ and $|\,\mathrm{b}\overline{\mathrm{b}}\,\mathrm{a}\,|$ is $-S_{ab}$ and the matrix element is likewise $-\beta_{ab}$.
2. When the VB determinants differ by the occupancy of one spin-orbital, say orbital a in one determinant is replaced by b in the other (keeping the ordering of the other orbitals unchanged), the leading term of the matrix element will be proportional to β_{ab}. Both the one- and three-electron bonds are cases that differ by a single electron occupancy and the corresponding matrix elements are indeed $\pm\beta$, with a sign as the corresponding overlap between the determinants.

3. When the VB determinants differ by the occupancy of two spin–orbitals, the leading term of the matrix element will be the sum of the corresponding $\beta_{ij}S_{ij}$ terms with the appropriate sign. An example is the matrix element $-2\beta_{ab}S_{ab}$ between the $|\overline{a}b|$ and $|\overline{ab}|$ determinants, which differ by the occupancy of two spin–orbitals, *a* and *b*.
4. The above considerations are the same whether the spin–orbitals are AOs, CF orbitals, or FOs.

A.3 Computing Mono-Determinantal VB Wave Functions with Standard Ab Initio Programs

This technique utilizes a possibility that is offered by most ab initio standard programs to compute the energy of the guess function even if it is made of nonorthogonal orbitals. The technique orthogonalizes the orbitals without changing the Slater determinant, then computes the expectation energy by use of Slater's rules. In the course of the subsequent optimization of the Hartree–Fock orbitals, this expectation value of the energy appears as the energy at iteration zero. If the guess determinant is made of localized bonding orbitals that typify a given VB structure, then the expectation energy of this wave function at iteration zero defines the energy of this VB structure. Practically, the localized bonding orbitals that are used to construct the guess determinant can be determined by any convenient means. For example, a Kekulé structure of benzene will display a set of three two-centered π-bonding MOs that can arise from the Hartree–Fock calculation of an ethylene molecule.[196,281] In a VBSCD calculation, the energy of the crossing point will be the energy of a guess function made of the orbitals of the reactants, but in the geometry of the transition state, without further orbital optimization. The zero-iteration technique has also been used to estimate the energy of spin-alternated determinants (quasi-classical state).[175,198]

ACKNOWLEDGMENTS

The research at Hebrew University is supported in part by a grant (to SS) from the Israeli Science Foundation. The two authors are thankful to all their co-workers during their years of collaboration (1985–present). Joop van Lenthe and Wei Wu are especially thanked for making their programs (TURTLE and XIAMEN99) available to us. Sam de Visser is acknowledged for proofing the chapter.

REFERENCES

1. *Valence Bond Theory*, D. L. Cooper, Ed., Elsevier, Amsterdam, The Netherlands, 2002.
2. J. W. Servos, *Physical Chemistry from Ostwald to Pauling*, Princeton University Press, Princeton, New Jersey, 1990.

3. S. G. Brush, *Stud. Hist. Phil. Sci.*, **30**, 21 (1999). Dynamics of Theory Change in Chemistry: Part 1. The Benzene Problem 1865–1945.
4. S. G. Brush, *Stud. Hist. Phil. Sci.* **30**, 263 (1999). Dynamics of Theory Change in Chemistry: Part 2. Benzene and Molecular Orbitals, 1945–1980.
5. G. N. Lewis, *J. Am. Chem. Soc.*, **38**, 762 (1916). The Atom and the Molecule.
6. I. Langmuir, *J. Am. Chem. Soc.*, **41**, 868 (1919). The Arrangement of Electrons in Atoms and Molecules.
7. W. Heitler and F. London, *Z. Phys.*, **44**, 455 (1927). Wechselwirkung Neutraler Atome un Homöopolare Bindung nach der Quantenmechanik.
8. For an English translation, see H. Hettema, *Quantum Chemistry Classic Scientific Paper*, World Scientific, Singapore, 2000.
9. W. Heisenberg, *Z. Phys.*, **411**, 38, (1926). Mehrkorperproblem und Resonanz in der Quantenmechanik,
10. F. London *Z. Phys.*, **455**, 46, (1928). On The Quantum Theory of Homo-polar Valence Numbers.
11. L. Pauling, *Proc. Natl. Acad. Sci. U.S.A.*, **14**, 359 (1928). The Shared-Electron Chemical Bond.
12. J. C. Slater, *Phys. Rev.*, **34**, 1293 (1929). The Theory of Complex Spectra.
13. J. C. Slater, *Phys. Rev.*, **38**, 1109 (1931). Molecular Energy Levels and Valence Bonds.
14. G. Rumer, *Gottinger Nachr.*, **27**, 337 (1932). Zum Theorie der Spinvalenz.
15. G. A. Gallup, in *Valence Bond Theory*, D. L. Cooper, Ed., Elsevier, Amsterdam, The Netherlands, 2002, pp. 1–40. A Short History of VB Theory.
16. J. C. Slater, *Phys. Rev.*, **37**, 481 (1931). Directed Valence in Polyatomic Molecules.
17. J. C. Slater, *Phys. Rev.*, **41**, 255 (1931). Note on Molecular Structure.
18. L. Pauling, *J. Am. Chem. Soc.*, **53**, 1367 (1931). The Nature of the Chemical Bond. Application of Results Obtained from the Quantum Mechanics and from a Theory of Magnetic Susceptiblity to the Structure of Molecules.
19. L. Pauling, *J. Am. Chem. Soc.*, **53**, 3225 (1931). The Nature of the Chemical Bond. II. The One-Electron Bond and the Three-Electron Bond.
20. L. Pauling, *The Nature of the Chemical Bond*, Cornell University Press, Ithaca, New York, 1939 (3rd ed., 1960).
21. R. S. Mulliken, *Phys. Rev.*, **32**, 186 (1928). The Assignment of Quantum Numbers for Electrons in Molecules. I.
22. R. S. Mulliken, *Phys. Rev.*, **32**, 761 (1928). The Assignment of Quantum Numbers for Electrons in Molecules. II. Correlation of Atomic and Molecular Electron States.
23. R. S. Mulliken, *Phys. Rev.*, **33**, 730 (1929). The Assignment of Quantum Numbers for Electrons in Molecules. III. Diatomic Hydrides.
24. R. S. Mulliken, *Phys. Rev.*, **41**, 49 (1932). Electronic Structures of Polyatomic Molecules and Valence. II. General Considerations.
25. F. Hund, *Z. Phys.*, **73**, 1 (1931). Zur Frage der Chemischen Bindung.
26. F. Hund, *Z. Phys.*, **51**, 759 (1928). Zur Deutung der Molekelspektren. IV.
27. J. E. Lennard-Jones, *Trans. Faraday Soc.*, **25**, 668 (1929). The Electronic Structure of some Diatomic Molecules.
28. J. A. Berson, *Chemical Creativity. Ideas from the Work of Woodward, Hückel, Meerwein, and Others,* Wiley-VCH, NewYork, 1999.
29. E. Hückel, *Z. Phys.*, **60**, 423 (1930). Zur Quantentheorie der Doppelbindung.
30. E. Hückel, *Z. Phys.*, **70**, 204 (1931). Quantentheoretische Beitrag zum Benzolproblem. I. Dies Elektronenkonfiguration des Benzols und verwandter Verbindungen.

31. E. Hückel, *Z. Phys.*, **76**, 628 (1932). Quantentheoretische Beitrag zum Problem der Aromatischen Ungesättigten Verbindungen. III.
32. L. Pauling and G. W. Wheland, *J. Chem. Phys.*, **1**, 362 (1933). The Nature of the Chemical Bond. V. The Quantum-Mechanical Calculation of the Resonance Energy of Benzene and Naphthalene and the Hydrocarbon Free Radicals.
33. G. W. Wheland, *Resonance in Organic Chemistry*, Wiley, New York, 1955, pp. 4, 39, 148.
34. J. H. van Vleck and A. Sherman, *Rev. Mod. Phys.*, **7**, 167 (1935). The Quantum Theory of Valence.
35. P. Laszlo and R. Hoffmann, *Angew. Chem. Int. Ed.*, **39**, 123 (2000). Ferrocene: Ironclad History or Roshomon Tale?
36. G. W. Wheland, *Proc. R. Soc. London*, **A159**, 397 (1938). The Electronic Structure of Some Polyenes and Aromatic Molecules. V—A Comparison of Molecular Orbital and Valence Bond Methods.
37. G. W. Wheland, *J. Chem. Phys.*, **2**, 474 (1934). The Quantum Mechanics of Unsaturated and Aromatic Molecules: A Comparison of Two Methods of Treatment.
38. D. P. Craig, *J. Chem. Soc.*, 3175 (1951). Cyclobutadiene and Some Other Pseudoaromatic Compounds.
39. D. P. Craig, *Proc. R. Soc. London*, **A200**, 498 (1950). Electronic Levels in Simple Conjugated Systems. I. Configuration Interaction in Cyclobutadiene.
40. C. A. Coulson, *Proc. R. Soc. London*, **A207**, 63 (1951). Critical Survey of the Method of Ionic-Homopolar Resonance.
41. M. J. S. Dewar, *Electronic Theory of Organic Chemistry*, Clarendon Press, Oxford, 1949, pp. 15–17.
42. C. A. Coulson, *Valence*, Oxford University Press, London, 1952.
43. J. R. Platt, *Science*, **154**, 745 (1966). Nobel Laureate in Chemistry: Robert S. Mulliken.
44. K. Fukui, T. Yonezawa, and H. Shingu, *J. Chem. Phys.*, **20**, 722 (1952). A Molecular Orbital Theory of Reactivity in Aromatic Hydrocarbons.
45. R. B. Woodward and R. Hoffmann, *The Conservation of Orbital Symmetry*, Verlag Chemie, Weinheim, 1971.
46. M. G. Evans, *Trans. Faraday Soc.*, **35**, 824 (1939). The Activation Energies in Reactions Involving Conjugated Systems.
47. E. Heilbronner and H. Bock, *The HMO Model and its Applications*, Wiley, New York, 1976.
48. E. Honegger and E. Heilbronner, in *Theoretical Models of Chemical Bonding*, Z. B. Maksic, Ed., Springer-Verlag, Berlin- Heidelberg, 1991, Vol. 3, pp. 100–151. The Equivalent Orbital Model and the Interpretation of PE Spectra.
49. S. Wolfe and Z. Shi, *Isr. J. Chem.*, **40**, 343 (2000). The S–C–O (O–C–S) Edward-Lemieux Effect is Controlled by *p*-Orbital on Oxygen. Evidence from Electron Momentum Spectroscopy, Photoelectron Spectroscopy, X-Ray Crystallography, and Density Functional Theory.
50. P. Atkins and L. Jones, *Chemical Principles. The Quest for Insight,* W. H. Freeman and Co., New York, 1999, pp. xxiii and 121–122.
51. L. Jones and P. Atkins, *Chemistry Molecules, Matter and Change*, W. H. Freeman and Co., New York, 2000, pp. 400–401.
52. S. Shaik, in *New Theoretical Concepts for Understanding Organic Reactions*, J. Bertran and I. G. Csizmadia, Eds., NATO ASI Series, **C267**, Kluwer Academic Publ., 1989, pp. 165–217. A Qualitative Valence Bond Model for Organic Reactions.
53. S. Shaik and P. C. Hiberty, *Adv. Quant. Chem.*, **26**, 100 (1995). Valence Bond Mixing and Curve Crossing Diagrams in Chemical Reactivity and Bonding.
54. P. C. Hiberty, *J. Mol. Struct. (THEOCHEM)*, **398**, 35 (1997). Thinking and Computing Valence Bond in Organic Chemistry.

55. A. Shurki, F. Dijkstra, P. C. Hiberty, and S. Shaik, *J. Phys. Org. Chem.*, **16**, 731 (2003). Aromaticity and Antiaromaticity: What Role Do Ionic Configurations Play in Delocalization and Induction of Magnetic Properties?
56. W. Heitler and G. Pöschl, *Nature (London)*, **133**, 833 (1934). Ground State of C_2 and O_2 and the Theory of Valency.
57. S. Shaik, A. Shurki, D. Danovich, and P. C. Hiberty, *Chem. Rev.*, **101**, 1501 (2001). A Different Story of π-Delocalization—The Distortivity of the π-Electrons and Its Chemical Manifestations.
58. A. F. Voter and W. A. Goddard, III, *J. Am. Chem. Soc.*, **108**, 2830 (1986). The Generalized Resonating Valence Bond Description of Cyclobutadiene.
59. J. H. van Vleck, *J. Chem. Phys.*, **3**, 803 (1935). The Group Relation Between the Mulliken and Slater–Pauling Theories.
60. H. Zuilhof, J. P. Dinnocenzo, A. C. Reddy, and S. Shaik, *J. Phys. Chem.*, **100**, 15774 (1996). A Comparative Study of Ethane and Propane Cation Radicals by B3LYP Density Functional and High-Level Ab Initio Methods.
61. S. Shaik and P. C. Hiberty, *Helv. Chem. Acta,* **86**, 1063 (2003). Myth and Reality in the Attitude Toward Valence-Bond (VB) Theory: Are Its 'Failures' Real?"
62. D. J. Klein, in *Valence Bond Theory*, D. L. Cooper, Ed., Elsevier, Amsterdam, The Netherlands, 2002, pp. 447–502. Resonating Valence Bond Theories for Carbon π-Networks and Classical/Quantum Connections.
63. T. G. Schmalz, in *Valence Bond Theory*, D. L. Cooper, Ed., Elsevier, Amsterdam, The Netherlands, 2002, pp. 535–564. A Valence Bond View of Fullerenes.
64. J. P. Malrieu, in *Theoretical Models of Chemical Bonding*, Z. B. Maksic, Ed., Springer-Verlag, Berlin-Heidelberg, 1990, Vol. 1, pp. 108–136. The Magnetic Description of Conjugated Hydrocarbons.
65. J. P. Malrieu and D. Maynau, *J. Am. Chem. Soc.*, **104**, 3021 (1984). A Valence Bond Effective Hamiltonian for Neutral States of π-Systems. 1. Methods.
66. Y. Jiang and S. Li, in *Valence Bond Theory*, D. L. Cooper, Ed., Elsevier, The Netherlands, Amsterdam, 2002, 565–602. Valence Bond Calculations and Theoretical Applications to Medium-Sized Conjugated Hydrocarbons.
67. F. A. Matsen, *Acc. Chem. Res.*, **11**, 387 (1978). Correlation of Molecular Orbital and Valence Bond States in π Systems.
68. M. A. Fox and F. A. Matsen, *J. Chem. Educ.*, **62**, 477 (1985). Electronic Structure in π-Systems. Part II. The Unification of Hückel and Valence Bond Theories.
69. M. A. Fox and F. A. Matsen, *J. Chem. Educ.*, **62**, 551 (1985). Electronic Structure in π-Systems. Part III. Application in Spectroscopy and Chemical Reactivity.
70. S. Ramasesha and Z. G. Soos, in *Valence Bond Theory*, D. L. Cooper, Ed., Elsevier, Amsterdam, The Netherlands, 2002, pp. 635–697. Valence Bond Theory of Quantum Cell Models.
71. W. Wu, S. J. Zhong, and S. Shaik, *Chem. Phys. Lett.,* **292**, 7 (1998). VBDFT(s): A Hückel-Type Semi-empirical Valence Bond Method Scaled to Density Functional Energies. Applications to Linear Polyene.
72. W. Wu, D. Danovich, A. Shurki, and S. Shaik, *J. Phys. Chem., A* **104**, 8744 (2000). Using Valence Bond Theory to Understand Electronic Excited States. Applications to the Hidden Excited State (2^1A_g) of Polyenes.
73. W. Wu, Y. Luo, L. Song, and S. Shaik, *Phys. Chem. Chem. Phys.*, **3**, 5459 (2001). VBDFT(s): A Semiempirical Valence Bond Method: Application to Linear Polyenes Containing Oxygen and Nitrogen Heteroatoms.
74. P. C. Hiberty and C. Leforestier, *J. Am. Chem. Soc.*, **100**, 2012 (1978). Expansion of Molecular Orbital Wave Functions into Valence Bond Wave Functions. A Simplified Procedure.
75. T. Thorsteinsson, D. L. Cooper, J. Gerratt, and M. Raimondi, *Molecular Engineering*, **7**, 67 (1997). A New Approach to Valence Bond Calculations CASVB.

76. Thorsteinsson, D. L. Cooper, J. Gerratt, P. Kardakov, and M. Raimondi, *Theor. Chim. Acta (Berl.)*, **93**, 343 (1996). Modern Valence Bond Representation of CASSCF Wave Functions.

77. H. Nakano, K. Sorakubo, K. Nakayama, and H. Hirao, in *Valence Bond Theory*, D. L. Cooper, Ed. Elsevier, The Netherlands, Amsterdam, 2002, pp. 55–77. Complete Active Space Valence Bond (CASVB) Method and its Application in Chemical Reactions.

78. K. Hirao, H. Nakano, and K. Nakayama, *J. Chem. Phys.*, **107**, 9966 (1997). A Complete Active Space Valence Bond Method with Nonorthogonal Orbitals.

79. N. D. Epiotis, J. R. Larson, and H. L. Eaton, *Lecture Notes Chem.*, **29**, 1 (1982). Unified Valence Bond Theory of Electronic Structure.

80. N. D. Epiotis, *Deciphering the Chemical Bond. Bonding Across the Periodic Table*, VCH, New York, 1996, pp. 1-933.

81. S. S. Shaik, *J. Am. Chem. Soc.*, **103**, 3692 (1981). What Happens to Molecules As They React? A Valence Bond Approach to Reactivity.

82. A. Pross and S. S. Shaik, *Acc. Chem. Res.*, **16**, 363 (1983). A Qualitative Valence Bond Approach to Chemical Reactivity.

83. A. Pross, *Theoretical and Physical Principles of Organic Reactivity*, J. Wiley, New York, 1995, pp. 83–124; 235–290.

84. S. Shaik and P. C. Hiberty, in *Theoretical Models of Chemical Bonding*, Z.B. Maksic, Ed., Springer-Verlag, Berlin-Heidelberg, 1991, Vol. 4, pp. 269–322. Curve Crossing Diagrams as General Models for Chemical Structure and Reactivity.

85. S. Shaik and A. Shurki, *Angew. Chem. Int. Ed. Engl.*, **38**, 586 (1999). Valence Bond Diagrams and Chemical Reactivity.

86. J. W. Linnett, *The Electronic Structure of Molecules. A New Approach*, Methuen & Co Ltd, London, 1964, pp. 1–162.

87. R. D. Harcourt, *Lecture Notes Chem.*, **30**, 1 (1982). Qualitative Valence-Bond Descriptions of Electron-Rich Molecules: Pauling "3-Electron Bonds" and "Increased-Valence" Theory.

88. R. D. Harcourt, in *Valence Bond Theory*, D. L. Cooper, Ed., Elsevier, Amsterdam, The Netherlands, 2002, pp. 349–378. Valence Bond Structures for Some Molecules with Four Singly-Occupied Active-Space Orbitals: Electronic Structures, Reaction Mechanisms, Metallic Orbitals.

89. A. Th. Van der Lugt and L. J. Oosterhoff, *J. Am. Chem. Soc.*, **91**, 6042 (1969). Symmetry Control and Photoinduced Reactions.

90. J. J. C. Mulder and L. J. Oosterhoff, *Chem. Commun.*, 305 (1970). Permutation Symmetry Control in Concerted Reactions.

91. J. Michl, *Topics Curr. Chem.*, **46**, 1 (1974). Physical Basis of Qualitative MO Arguments in Organic Photochemistry.

92. W.Gerhartz, R. D. Poshusta, and J. Michl, *J. Am. Chem. Soc.*, **99**, 4263 (1977). Potential Energy Hypersurfaces for H_4. 2. "Triply Right" (C_{2v}) Tetrahedral Geometries. A Possible Relation to Photochemical "Cross Bonding" Processes.

93. F. Bernardi, M. Olivucci, and M. Robb, *Isr. J. Chem.*, **33**, 265 (1993). Modeling Photochemical Reactivity of Organic Systems. A New Challenge to Quantum Computational Chemistry.

94. M. Olivucci, I. N. Ragazos, F. Bernardi, and M. A. Robb, *J. Am. Chem. Soc.*, **115**, 3710 (1993). A Conical Intersection Mechanism for the Photochemistry of Butadiene. A MC-SCF Study.

95. M. Olivucci, F. Bernardi, P. Celani, I. Ragazos, and M. A. Robb, *J. Am. Chem. Soc.*, **116**, 1077 (1994). Excited-State Cis-Trans Isomerization of *cis*-Hexatriene. A CAS–SCF Computational Study.

96. M. A. Robb, M. Garavelli, M. Olivucci, and F. Bernardi, in *Reviews in Computational Chemistry*, K. B. Lipkowitz and D. B. Boyd, Eds., Vol. 15, pp. 87–146, (2000). A Computational Strategy for Organic Photochemistry.

97. S. Shaik and A. C. Reddy, *J. Chem. Soc. Faraday Trans.*, **90**, 1631 (1994). Transition States, Avoided Crossing States and Valence Bond Mixing: Fundamental Reactivity Paradigms.

98. S. Zilberg and Y. Haas, *Chem. Eur. J.*, **5**, 1755 (1999). Molecular Photochemistry: A General Method for Localizing Conical Intersections Using the Phase-Change Rule.

99. A. Warshel and R. M. Weiss, *J. Am. Chem. Soc.*, **102**, 6218 (1980). Empirical Valence Bond Approach for Comparing Reactions in Solutions and in Enzymes.

100. A. Warshel and S. T. Russell, *Quart. Rev. Biophys.*, **17**, 282 (1984). Calculations of Electrostatic Interactions in Biological Systems and in Solutions.

101. A. Warshel, *J. Phys. Chem.*, **83**, 1640 (1979). Calculations of Chemical Processes in Solutions.

102. H. J. Kim and J. T. Hynes, *J. Am. Chem. Soc.*, **114**, 10508 (1992). A Theoretical Model for S_N1 Ionic Dissociation in Solution. 1. Activation Free Energies and Transition-State Structure.

103. J. R. Mathias, R. Bianco, and J. T. Hynes, *J. Mol. Liq.*, **61**, 81 (1994). On the Activation Free Energy of the $Cl^- + CH_3Cl$ S_N2 Reaction in Solution.

104. J. I. Timoneda and J. T. Hynes, *J. Phys. Chem.*, **95**, 10431 (1991). Nonequilibrium Free Energy Surfaces for Hydrogen-bonded Proton Transfer Compexes in Solution.

105. S. Shaik, *J. Am. Chem. Soc.*, **106**, 1227 (1984). Solvent Effect on Reaction Barriers. The S_N2 Reactions. 1. Application to the Identity Exchange.

106. S. Shaik, *J. Org. Chem.*, **52**, 1563 (1987). Nucleophilic Reactivity and Vertical Ionization Potentials in Cation–Anion Recombinations.

107. W. A. Goddard, III, T. H. Dunning, Jr., W. J. Hunt, and P. J. Hay, *Acc. Chem. Res.*, **6**, 368 (1973). Generalized Valence Bond Description of Bonding in Low-Lying States of Molecules.

108. W. A. Goddard, III, *Phys. Rev.*, **157**, 81 (1967). Improved Quantum Theory of Many-Electron Systems. II. The Basic Method.

109. W. A. Goddard, III, and L. B. Harding, *Annu. Rev. Phys. Chem.*, **29**, 363 (1978). The Description of Chemical Bonding from Ab-Initio Calculations.

110. W. A. Goddard, III, *Int. J. Quant. Chem.*, **IIIS**, 593 (1970). The Symmetric Group and the Spin Generalized SCF Method.

111. C. A. Coulson and I. Fischer, *Philos. Mag.*, **40**, 386 (1949). Notes on the Molecular Orbital Treatment of the Hydrogen Molecule.

112. D. L. Cooper, J. Gerratt, and M. Raimondi, *Chem. Rev.*, **91**, 929 (1981). Application of Spin-Coupled Valence Bond Theory.

113. D. L. Cooper, J. P. Gerratt, and M. Raimondi, *Adv. Chem. Phys.*, **69**, 319 (1987). Modern Valence Bond Theory.

114. M. Sironi, M. Raimondi, R. Martinazzo, and F. A. Gianturco, in *Valence Bond Theory*, D. L. Cooper, Ed., Elsevier, Amsterdam, The Netherlands, 2002, pp. 261–277. Recent Developments of the SCVB Method.

115. G. G. Balint-Kurti and M. Karplus, *J. Chem. Phys.*, **50**, 478 (1969). Multistructure Valence-Bond and Atoms-in-Molecules Calculations for LiF, F_2, and F_2^-.

116. J. H. van Lenthe and G. G. Balint-Kurti, *Chem. Phys. Lett.*, **76**, 138 (1980). The Valence-Bond SCF (VB SCF) Method. Synopsis of Theory and Test Calculations of the OH Potential Energy Curve.

117. J. H. van Lenthe and G. G. Balint-Kurti, *J. Chem. Phys.*, **78**, 5699 (1983). The Valence-Bond Self-Consistent Field Method (VB–SCF): Theory and Test Calculations.

118. J. Verbeek and J. H. van Lenthe, *J. Mol. Struct. (THEOCHEM)*, **229**, 115 (1991). On the Evaluation of Nonorthogonal Matrix Elements.

119. J. Verbeek and J. H. van Lenthe, *Int. J. Quant. Chem.*, XL, 201(1991). The Generalized Slater–Condon Rules.

120. J. Verbeek, J. H. Langenberg, C. P. Byrman, F. Dijkstra, and J. H. van Lenthe, *TURTLE: An Ab Initio VB/VBSCF Program (1998–2000).*

121. J. H. van Lenthe, F. Dijkstra, and W. A. Havenith, in *Valence Bond Theory*, D. L. Cooper, Ed., Elsevier, Amsterdam, The Netherlands, 2002, pp. 79–116. TURTLE—A Gradient VBSCF Program Theory and Studies of Aromaticity.

122. F. A. Matsen, *Adv. Quant. Chem.*, **1**, 60 (1964). Spin-Free Quantum Chemistry.

123. F. A. Matsen, *J. Phys. Chem.*, **68**, 3282 (1964). Spin-Free Quantum Chemistry. II. Three-Electron Systems.

124. R. McWeeny, *Int. J. Quant. Chem.*, **XXXIV**, 23 (1988). A Spin Free Form of Valence Bond Theory.

125. Q. Zhang, and L. Xiangzhu, *J. Mol. Struct. (THEOCHEM),* **198**, 413 (1989). Bonded Tableau Method for Many Electron Systems.

126. X. Li and Q. Zhang, *Int. J. Quant. Chem.*, **XXXVI**, 599 (1989). Bonded Tableau Unitary Group Approach to the Many-Electron Correlation Problem.

127. W. Wu, Y. Mo, Z. Cao, and Q. Zhang, in *Valence Bond Theory*, D. L. Cooper, Ed., Elsevier, Amsterdam, The Netherlands, 2002, pp. 143–186. A Spin Free Approach for Valence Bond Theory and Its Application.

128. W. Wu, L. Song, Y. Mo, and Q. Zhang, *XIAMEN-99– An Ab Initio Spin-free Valence Bond Program*, Xiamen University, Xiamen, China, 1999.

129. J. Li and R. McWeeny, *VB2000: An Ab Initio Valence Bond Program Based on Product Function Method and the Algebrant Algorithm. 2000.*

130. G. A. Gallup, R. L. Vance, J. R. Collins, and J. M. Norbeck, *Adv. Quant. Chem.*, **16**, 229 (1982). Practical Valence Bond Calculations.

131. G. A. Gallup, The CRUNCH Suite of Atomic and Molecular Structure Programs, 2001. ggallup@phy-ggallup.unl.edu.

132. P. C. Hiberty, J. P. Flament, and E. Noizet, *Chem. Phys. Lett.,* **189**, 259 (1992). Compact and Accurate Valence Bond Functions with Different Orbitals for Different Configurations: Application to the Two-Configuration Description of F_2.

133. P. C. Hiberty, S. Humbel, C. P. Byrman, and J. H. van Lenthe, *J. Chem. Phys.*, **101**, 5969 (1994). Compact Valence Bond Functions with Breathing Orbitals: Application to the Bond Dissociation Energies of F_2 and FH.

134. P. C. Hiberty, S. Humbel, and P. Archirel, *J. Phys. Chem.*, **98**, 11697 (1994). Nature of the Differential Electron Correlation in Three-Electron Bond Dissociation. Efficiency of a Simple Two-Configuration Valence Bond Method with Breathing Orbitals.

135. P. C. Hiberty, in *Modern Electronic Structure Theory and Applications in Organic Chemistry*, E. R. Davidson, Ed., World Scientific, River Edge, NJ, 1997, pp. 289–367. The Breathing Orbital Valence Bond Method.

136. P. C. Hiberty and S. Shaik, in *Valence Bond Theory*, D. L. Cooper, Ed., Elsevier, Amsterdam, The Netherlands, 2002, pp. 187–226. Breathing-Orbital Valence Bond—A Valence Bond Method Incorporating Static and Dynamic Electron Correlation Effects.

137. P. C. Hiberty and S. Shaik, *Theor. Chem. Acc.*, **108**, 255 (2002). BOVB—A Modern Valence Bond Method That Includes Dynamic Correlation.

138. W. Wu, L. Song, Z. Cao, Q. Zhang, and S. Shaik, *J. Phys. Chem. A*, **106**, 2721 (2002). Valence Bond Configuration Interaction. A Practical Valence Bond Method Incorporating Dynamic Correlation.

139. J. J. W. McDouall, in *Valence Bond Theory*, D. L. Cooper, Ed., Elsevier, Amsterdam, The Netherlands, 2002, pp. 227–260. The Biorthogonal Valence Bond Method.

140. T. Albu, J. C. Corchado, and D. G. Truhlar, *J. Phys. Chem. A*, **105**, 8465 (2001). Molecular Mechanics for Chemical Reactions: A Standard Strategy for Using Multiconfiguration Molecular Mechanics for Variational Transition State Theory with Optimized Multidimensional Tunneling.

141. T. K. Firman and C. R. Landis, *J. Am. Chem. Soc.*, **123**, 1178 (2001). Valence Bond Concepts Applied to Molecular Mechanics Description of Molecular Shapes. 4. Transition Metals with π-bonds.

142. L. Song, W. Wu, P. C. Hiberty, and S. Shaik, *Chem. Eur. J.*, **9**, 4540 (2003). An Accurate Barrier for the Hydrogen Exchange Reaction. Is This Theory Coming of Age?

143. S. S. Shaik, E. Duzy, and A. Bartuv, *J. Phys. Chem.*, **94**, 6574 (1990). The Quantum Mechanical Resonance Energy of Transition States: An Indicator of Transition State Geometry and Electronic Structure.

144. R. McWeeny, *J. Mol. Struct. (THEOCHEM),* **229**, 29 (1991). On the Nature of the Oxygen Double Bond.

145. R. D. Harcourt, *J. Phys. Chem.*, **96**, 7616 (1992). Valence Bond Studies of Oxygen and Superoxides: A Note on One-electron and Two-electron Transfer Resonances.

146. H. Fischer and J. N. Murrell, *Theor. Chim. Acta (Berl.)*, **1**, 463 (1963). The Interpretation of the Stability of Aromatic Hydrocarbon Ions by Valence Bond Theory.

147. N. D. Epiotis, *Nouv. J. Chim.*, **8**, 421 (1984). How to "Think" at the Level of MO—CI Theory Using Hückel MO Information!

148. E. Heilbronner, *Tetrahedron Lett.*, 1923 (1964). Hückel Molecular Orbitals of Möbius-Type Conformation of Annulenes.

149. A. A. Frost and B. Musulin, *J. Chem. Phys.*, **21**, 572 (1953). A Mnemonic Device for Molecular Orbital Energies.

150. S. C. Wright, D. L. Cooper, J. Gerratt, and M. Raimondi, *J. Phys. Chem.*, **96**, 7943 (1992). Spin-coupled Description of Cyclobutadiene and 2,4-Dimethylenecyclobutane-1,3-diyls: Antipairs.

151. P. B. Karadakov, J. Gerratt, D. L. Cooper, and M. Raimondi, *J. Phys. Chem.*, **99**, 10186 (1995). The Electronic Structure of Cyclooctatetraene and the Modern Valence Bond Understanding of Antiaromaticity.

152. A. Shurki, *VB Theory as a Tool for Understanding Structure and Reactivity in Chemistry*, Ph.D. Dissertation, 1999, Hebrew University, Israel.

153. G. Sini, P. Maître, P. C. Hiberty, and S. S. Shaik. *J. Mol. Struct. (THEOCHEM)*, **229**, 163 (1991). Covalent, Ionic and Resonating Single Bonds.

154. S. Shaik, P. Maître, G. Sini, and P. C. Hiberty, *J. Am. Chem. Soc.*, **114**, 7861 (1992). The Charge-Shift Bonding Concept. Electron Pair Bonds with Very Large Resonance Energies.

155. A. Shurki, P. C. Hiberty, and S. Shaik, *J. Am. Chem. Soc.*, **121**, 822 (1999). Charge-Shift Bonding in Group IVB Halides: A Valence Bond Study of MH_3—Cl (M = C, Si, Ge, Sn, Pb) Molecules.

156. S. P. de Visser, D. Danovich, W. Wu, and S. Shaik, *J. Phys. Chem. A,* **106**, 4961 (2002). Ferromagnetic Bonds: Properties of "No-pair" Bonded High-Spin Lithium Clusters; $^{N+1}Li_N$ ($N = 2$–12).

157. D. Danovich and S. Shaik, *J. Am. Chem. Soc.*, **121**, 3165 (1999). No-Pair Bonding in the High-Spin $^3\Sigma_u^+$ State of Li_2. A Valence Bond Study of its Origins.

158. A. Pross, *Acc. Chem. Res.*, **18**, 212 (1985). The Single Electron Shift as a Fundamental Process in Organic Chemistry: The Relationship Between Polar and Electron-transfer Pathways.

159. G. Sini, S. S. Shaik, J.-M. Lefour, G. Ohanessian, and P. C. Hiberty, *J. Phys. Chem.*, **93**, 5661 (1989). Quantitative Valence Bond Computation of a Curve Crossing Diagram for a Model S_N2 Reaction, $H^- + CH_3H' \rightarrow HCH_3 + H'^-$.

160. G. Sini, S. Shaik, and P. C. Hiberty, *J. Chem. Soc. Perkin Trans., 2*, 1019 (1992). Quantitative Valence Bond Computations of Curve Crossing Diagrams for a Gas Phase Reaction, $F^- + CH_3F \rightarrow FCH_3 + F^-$.

161. J. Mestres and P. C. Hiberty, *New J. Chem.,* **20**, 1213 (1996). Quantitative Valence Bond Computations of Curve Crossing Diagrams for a Hydride Transfer Model Reaction: $CH_4 + CH_3^+ \rightarrow CH_3^+ + CH_4$.

162. G. Sini, G. Ohanessian, P. C. Hiberty, and S. S. Shaik, *J. Am. Chem. Soc.*, **112**, 1407 (1990). Why is SiH_5^- a Stable Intermediate While CH_5^- is a Transition State ? A Quantitative Curve Crossing Valence Bond Study.

163. G. Sini and P. C. Hiberty, *J. Chem. Soc. Chem. Commun.,* 772 (1989). The Origin of the Different Bonding Features in SiH_5^- and CH_5^-; A Valence Bond Curve Crossing Model.

164. P. Maître, F. Volatron, P. C. Hiberty, and S. S. Shaik, *Inorg. Chem.*, **29**, 3047 (1990). Hypercoordination in SiH_5^- and SiH_5. An Electron-count Dependence.

165. P. R. Benneyworth, G. G. Balint-Kurti, M. J. Davis, and I. H. Williams, *J. Phys. Chem.*, **96**, 4346 (1992). Ab initio Valence Bond Study of the Origin of Barriers to Hydrogen Exchange Reactions: Application of the Valence Bond Self-Consistent-Field Method to the $F + HF \rightarrow FH + F$ Reaction.

166. P. Maître, P. C. Hiberty, G. Ohanessian, and S. S. Shaik, *J. Phys. Chem.*, **94**, 4089 (1990). Quantitative Computations of Curve Crossing Diagrams for Model Atom Exchange Reaction.

167. S. Shaik, W. Wu, K. Dong, L. Song, and P. C. Hiberty, *J. Phys. Chem. A*, **105**, 8226 (2001). Identity Hydrogen Abstraction Reactions, $X + H{-}X' \rightarrow X{-}H + X'(X = X' = CH_3, SiH_3, GeH_3, SnH_3, PbH_3)$: A Valence Bond Modeling.

168. L. Song, W. Wu, K. Dong, P. C. Hiberty, and S. Shaik, *J. Phys. Chem. A*, **106**, 11361 (2002). Valence Bond Modeling of Barriers in the Nonidentity Hydrogen Abstraction Reactions, $X'\bullet + H{-}X \rightarrow X'{-}H + X\bullet\ (X' \neq X - CH_3, SiH_3, GeH_3, SnH_3, PbH_3)$.

169. S. S. Shaik, *Prog. Phys. Org. Chem.*, **15**, 197 (1985). The Collage of S_N2 Reactivity Patterns: A State Correlation Diagram Model.

170. S. S. Shaik, H. B. Schlegel, and S. Wolfe, *Theoretical Aspects of Physical Organic Chemistry,* Wiley-Interscience, New York, 1992.

171. Y. Mo and S. D. Peyerimhoff, *J. Chem. Phys.*, **109**, 1687 (1998). Theoretical Analysis of Electronic Delocalization.

172. F. Jensen and P.-O. Norrby, *Theor. Chim. Acc.* **109**, 1 (2003). Transition States from Empirical Force Fields.

173. Y. Kim, J. C. Corchado, J. Villa, J. Xing, and D. G. Truhlar, *J. Chem. Phys.*, **112**, 2718 (2000). Multiconfiguration Molecular Mechanics Algorithm for Potential Energy Surfaces of Chemical Reactions.

174. F. Jensen, *Introduction to Computational Chemistry,* Wiley, New York, 1999, pp. 48–49.

175. R. Mêreau, M. T. Rayez, J. C. Rayez, and P. C. Hiberty, *Phys. Chem. Chem. Phys.*, **3**, 3650 (2001). Alkoxy Radical Decomposition Explained by a Valence Bond Model.

176. H. Yamataka and S. Nagase, *J. Org. Chem.*, **53**, 3232 (1988). Ab Initio Calculations of Hydrogen Transfers. A Computational Test of Variations in the Transition State Structure and the Coefficient of Rate-Equilibrium Correlation.

177. A. Pross, H. Yamataka, and S. Nagase, *J. Phys. Org. Chem.*, **4**, *135* (1991). Reactivity in Radical Abstraction Reactions: Application of the Curve Crossing Model.

178. S. Shaik, *Acta Chem. Scand.*, **44**, 205 (1990). S_N2 Reactivity and its Relation to Electron Transfer Concepts.

179. I. M. Kovach, J. P. Elrod, and R. L. Schowen, *J. Am. Chem. Soc.*, **102**, 7530 (1980). Reaction Progress at the Transition State for Nucleophilic Attack on Esters.

180. D. G. Oakenfull, T. Riley, and V. Gold, *J. Chem. Soc. Chem. Commun.*, 385, (1966). Nucleophilic and General Base Catalysis by Acetate Ion in the Hydrolysis of Aryl Acetates: Substituent Effects, Solvent Isotope Effects, and Entropies of Activation.

181. E. Buncel, S. S. Shaik, I.-H. Um, and S. Wolfe, *J. Am. Chem. Soc.*, **110**, 1275 (1988). A Theoretical Treatment of Nucleophilic Reactivity in Additions to Carbonyl Compounds. Role of the Vertical Ionization Energy.

182. S. S. Shaik and E. Canadell, *J. Am. Chem. Soc.*, **112**, 1446 (1990). Regioselectivity of Radical Attacks on Substituted Olefins. Application of the State-Correlation-Diagram (SCD) Model.

183. J. H. Ren and J. I. Brauman, *Science*, **295**, 5563 (2002). Steric Effects and Solvent Effects in Ionic Reactions.

184. S. Shaik, A. C. Reddy, A. Ioffe, J. P. Dinnocenzo, D. Danovich, and J. K. Cho, *J. Am. Chem. Soc.*, **117**, 3205 (1995). Reactivity Paradigms. Transition State Structures, Mechanisms of Barrier Formation, and Stereospecificity of Nucleophilic Substitutions on σ-Cation Radicals.

185. J. H. Incremona and C. J. Upton, *J. Am. Chem. Soc.*, **94**, 301 (1972). Bimolecular Homolytic Substitution with Inversion. Stereochemical Investigation of an SH_2 Reaction.

186. C. J. Upton and J. H. Incremona, *J. Org. Chem.*, **41**, 523 (1976). Bimolecular Homolytic Substitution at Carbon. Stereochemical Investigation.

187. B. B. Jarvis, *J. Org. Chem.*, **35**, 924 (1970). Free Radical Additions to Dibenzotricyclo[3.3.0.02,8]-3,6-octadiene.

188. G. G. Maynes and D. E. Appliquist, *J. Am. Chem. Soc.*, **95**, 856 (1973). Stereochemistry of Free Radical Ring Cleavage of *cis*-1,2,3-Trimethylcyclopropane by Bromine.

189. K. J. Shea and P. S. Skell, *J. Am. Chem. Soc.*, **95**, 6728 (1973). Photobromination of Alkylcyclopropanes. Stereochemistry of Homolytic Substitution at a Saturated Carbon Atom.

190. M. L. Poutsma, *J. Am. Chem. Soc.*, **87**, 4293 (1965). Chlorination Studies of Unsaturated Materials in Nonpolar Media. V. Norbornene and Nortricyclene.

191. S. S. Shaik and J. P. Dinnocenzo, *J. Org. Chem.*, **55**, 3434 (1990). Nucleophilic Cleavages of One-electron σ Bonds are Predicted to Proceed with Stereoinversion.

192. J. P. Dinnocenzo, W. P. Todd, T. R. Simpson, and I. R. Gould, *J. Am. Chem. Soc.*, **112**, 2462 (1990). Nucleophilic Cleavage of One-electron σ Bonds. Stereochemistry and Cleavage Rates.

193. L. Eberson, R. Gonzalez-Luque, M. Merchan, F. Radner, B. O. Roos, and S. Shaik, *J. Chem. Soc. Perkin Trans. 2*, 463 (1997). Radical Cations of Non-Alternant Systems as Probes of the Shaik-Pross VB Configuration Mixing Model.

194. S. Shaik and R. Bar, *Nouv. J. Chim.*, **8**, 411 (1984). How Important is Resonance in Organic Species?

195. P. C. Hiberty, S. S. Shaik, J. M. Lefour, and G. Ohanessian, *J. Org. Chem.*, **50**, 4657 (1985). The Delocalized π-system of Benzene is not a Stable Electronic System.

196. S. S. Shaik, P. C. Hiberty, J.-M. Lefour, and G. Ohanessian, *J. Am. Chem. Soc.*, **109**, 363 (1987). Is Delocalization a Driving Force in Chemistry? Benzene, Allyl Radical, Cyclobutadiene and Their Isoelectronic Species.

197. S. S. Shaik, P. C. Hiberty, G. Ohanessian, and J.-M. Lefour, *J. Phys. Chem.*, **92**, 5086 (1988). When Does Electronic Delocalization Become a Driving Force of Chemical Bonding?

198. P. C. Hiberty, D. Danovich, A. Shurki, and S. Shaik, *J. Am. Chem. Soc.*, **117**, 7760 (1995). Why Does Benzene Possess a D_{6h} Symmetry? A Theoretical Approach Based on the π-Quasiclassical State for Probing π-Bonding Energies.

199. K. Jug and A. M. Koster, *J. Am. Chem. Soc.*, **112**, 6772 (1990). Influence of σ and π Electrons on Aromaticity.

200. A. Gobbi, Y. Yamaguchi, Y. Frenking, and H. F. Schaefer III, *Chem. Phys. Lett.*, **244**, 27 (1995). The Role of σ and π Stabilization in Benzene, Allyl Cation and Allyl Anion. A Canonical Orbital Energy Derivative Study.

201. R. Janoschek, *J. Mol. Struct. (THEOCHEM)*, **229**, 197 (1991). Has the Benzene Molecule an Extra Stability?

202. M.-C. Ou and S.-Y. Chu, *J. Phys. Chem.*, **98**, 1087 (1994). The π-Electron Stabilization in Benzocyclobutenes.

203. Y. Haas and S. Zilberg, *J. Am. Chem. Soc.*, **1995**, *117*, 5387. The ν_{14} (b_{2u}) Mode of Benzene in S_0 and S_1 and the Distortive Nature of the π Electron System: Theory and Experiment.

204. L. Wunsch, H. J. Neusser, and E. W. Schlag, *Chem. Phys. Lett.*, **31**, 433 (1975). Two Photon Excitation Spectrum of Benzene and Benzene-d_6 in the Gas Phase: Assignment of Inducing Modes by Hot Band Analysis.

205. L. Wunsch, F. Metz, H. J. Neusser, and E. W. Schlag, *J. Chem. Phys.*, **66**, 386 (1977). Two-Photon Spectroscopy in the Gas Phase: Assignments of Molecular Transitions in Benzene.

206. D. M. Friedrich and W. M. McClain, *Chem. Phys. Lett.*, **32**, 541 (1975). Polarization and Assignment of the Two-Photon Excitation Spectrum of Benzene Vapor.

207. E. C. da Silva, J. Gerratt, D. L. Cooper, and M. Raimondi, *J. Chem. Phys.*, **101**, 3866 (1994). Study of the Electronic States of the Benzene Molecule Using Spin-Coupled Valence Bond Theory.

208. U. Manthe and H. Köppel, *J. Chem. Phys.*, **93**, 1658 (1990). Dynamics on Potential Energy Surfaces with a Conical Intersection: Adiabatic, Intermediate, and Diabatic Behavior.

209. H. Köppel, W. Domcke, and L. S. Cederbaum, *Adv. Chem. Phys.*, **57**, 59 (1984). Multimode Molecular Dynamics Beyond the Born–Oppenheimer Approximation.

210. D. M. Cyr, G. A. Bishea, M. G. Scranton, and M. A. Johnson, *J. Chem. Phys.*, **97**, 5911 (1992). Observation of Charge-transfer Excited States in the $I^- \cdot CH_3I$, $I^- \cdot CH_3Br$, and $I^- \cdot CH_2Br_2$ S_N2 Reaction Intermediates Using Photofragmentation and Photoelectron Spectroscopies.

211. I. B. Bersuker, *Nouv. J. Chim.*, **4**, 139 (1980). Are Activated Complexes of Chemical Reactions Experimentally Observable Ones?

212. S. Zilberg, Y. Haas, D. Danovich, and S. Shaik, *Angew. Chem. Int. Ed. Engl.*, **37**, 1394 (1998). The Twin-Excited State as a Probe for the Transition State in Concerted Unimolecular Reactions. The Semibullvalene Rearrangement.

213. H. Quast, K. Knoll, E.-M. Peters, K. Peters, and H. G. von Schnering, *Chem. Ber.*, **126**, 1047 (1993). 2,4,6,8-Tetraphenylbarbaralan—Ein Orangeroter, Thermochromer Kohlenwasserstoff ohne Chromophor.

214. H. Quast and M. Seefelder, *Angew. Chem. Int. Ed. Engl.*, **38**, 1064 (1999). The Equilibrium Between Localized and Delocalized States of Thermochromic Semibullvalenes and Barbaralanes—Direct Observation of Transition States of Degenerate Cope Rearrangements.

215. M. Shapiro and P. Brumer, *Adv. At. Mol. Opt. Phys.*, **42**, 287 (2000). Coherent Control of Atomic, Molecular and Electronic Processes.

216. M. Said, D. Maynau, J. P. Malrieu, and M. A. Garcia-Bach, *J. Am. Chem. Soc.*, **106**, 571 (1984). A Nonempirical Heisenberg Hamiltonian for the Study of Conjugated Hydrocarbons. Ground-state Conformational Studies.

217. A. O. Ovchinnikov, *Theor. Chim. Acta (Berl.)*, **47**, 297 (1978). Multiplicity of the Ground State of Large Alternant Organic Molecules with Conjugated Bonds.

218. W. T. Borden, H. Iwamura, and J. A. Berson, *Acc. Chem. Res.*, **27**, 109 (1994). Violations of Hund's Rule in Non-Kekulé Hydrocarbons: Theoretical Predictions and Experimental Verifications.

219. W. T. Borden, in *Encyclopedia of Computational Chemistry*, P. v. R. Schleyer, N. L. Allinger, T. Clark, J. Gasteiger, P. A. Kollman, H. F. Schaefer, III, and P. R. Schreiner, Eds., Wiley, Chichester, 1998, Vol. 1, p. 708.

220. A. C. Hurley, J. Lennard-Jones, and J. A. Pople, *Proc. R. Soc. London*, **A220**, 446 (1953). The Molecular Orbital Theory of Chemical Valency. XVI. A Theory of Paired-Electrons in Polyatomic Molecules.

221. W. J. Hunt, P. J. Hay, and W. A. Goddard, III, *J. Chem. Phys.*, **57**, 738 (1972). Self-Consistent Procedures for Generalized Valence Bond Wave Functions.

222. F. B. Bobrowicz and W. A. Goddard, III, in *Methods of Electronic Structure Theory*, H. F. Schaefer, III, Ed., Plenum Press, New York, 1977, pp. 79–127.

223. D. L. Cooper, J. Gerratt, and M. Raimondi, *Int. Rev. Phys. Chem.*, **7**, 59 (1988). Spin-Coupled Valence Bond Theory.

224. D. L. Cooper, J. Gerratt, and M. Raimondi, in *Valence Bond Theory and Chemical Structure*, D. J. Klein and N. Trinajstic, Eds., Elsevier, 1990, p. 287.

225. D. L. Cooper, J. Gerratt, and M. Raimondi, in *Advances in the Theory of Benzenoid Hydrocarbons*, *Top. Current Chem.* I. Gutman and S. J. Cyvin (Eds.), **153**, 41 (1990).

226. P. C. Hiberty and D. L. Cooper, *J. Mol. Struct. (THEOCHEM),* **169**, 437 (1988). Valence Bond Calculations of the Degree of Covalency in a C–X Bond. Application to CH_4 and CH_3Li.

227. D. L. Cooper, J. Gerratt, and M. Raimondi, *Nature London*, **323**, 699 (1986). The Electronic Structure of the Benzene Molecule.

228. E. A. Carter and W. A. Goddard, III, *J. Chem. Phys.*, **88**, 3132 (1988). Correlation-consistent Configuration Interaction: Accurate Bond Dissociation Energies from Simple Wave Functions. Application to H_3, BH, H_2O, C_2H_6 and O_2.

229. F. Penotti, J. Gerratt, D. L. Cooper, and M. Raimondi, *J. Mol. Struct. (THEOCHEM),* **169**, 421 (1988). The Ab Initio Spin-Coupled Description of Methane: Hybridization Without Preconceptions.

230. E. Tornaghi, D. L. Cooper, J. Gerratt, M. Raimondi, and M. Sironi, *J. Mol. Struct. (THEOCHEM)*, **259**, 383 (1992). The Spin-Coupled Description of Lithium Clusters: Part I. Optimal Geometrical Arrangements and Body-Centred Cubic Fragments.

231. M. H. McAadon and W. A. Goddard, III, *Phys. Rev. Lett.*, **55**, 2563 (1985). New Concepts of Metallic Bonding Based on Valence-Bond Ideas.

232. M. H. McAadon and W. A. Goddard, III, *J. Phys. Chem.*, **91**, 2607 (1987). Generalized Valence Bond Studies of Metallic Bonding: Naked Clusters and Applications to Bulk Metals.

233. J. Verbeek, Ph. D. Dissertation, University of Utrecht, 1990.

234. J. Verbeek, J. H. van Lenthe, and P. Pulay, *Mol. Phys.*, **73**, 1159 (1991). Convergence and Efficiency of the Valence Bond Self-Consistent Field Method.

235. M. R. F. Siggel and T. D. Thomas, *J. Am. Chem. Soc.*, **108**, 4360 (1986). Why are Organic Acids Stronger Than Organic Alcohols?

236. T. D. Thomas, T. X. Carroll, and M. R. F. Siggel, *J. Org. Chem.*, **53**, 1812 (1988). Isodesmic Reaction Energies and the Relative Acidities of Carboxylic Acids and Alcohols.

237. T. D. Thomas, M. R. F. Siggel, and A. Streitwieser, Jr., *J. Mol. Struct. (THEOCHEM),* **165**, 309 (1988). Resonance Delocalization in the Anion Is Not the Major Factor Responsible for the Higher Acidity of Carboxylic Acids Relative to Alcohols.

238. M. R. F. Siggel, A. Streitwieser, Jr., and T. D. Thomas, *J. Am. Chem. Soc.,* **110**, 8022 (1988). The Role of Resonance and Inductive Effects in the Acidity of Carboxylic Acids.

239. P. C. Hiberty and C. P. Byrman, *J. Am. Chem. Soc.*, **117**, 9875 (1995). The Role of Delocalization in the Enhanced Acidity of Carboxylic Acids and Enols Relative to Alcohols.

240. K. B. Wiberg and K. E. Laidig, *J. Am. Chem. Soc.*, **109**, 5935 (1987). Barrier to Rotation Adjacent to Double Bonds. 3. The Carbon–Oxygen Barrier in Formic Acid, Methyl Formate, Acetic Acid, and Methyl Acetate. The Origin of Ester and Amide Resonance.

241. K. B. Wiberg and C. L. Breneman, *J. Am. Chem. Soc.,* **114**, 831 (1992). Resonance Interactions in Acyclic Systems. 3. Formamide Internal Rotation Revisited. Charge and Energy Redistribution Along the C–N Bond Rotational Pathway.

242. K. E. Laidig and L. M. Cameron, *J. Am. Chem. Soc.,* **118**, 1737 (1996). Barrier to Rotation in Thioformamide. Implications for Amide Resonance.

243. R. F. W. Bader, *Atoms in Molecules*: *A Quantum Theory*, Oxford University Press, Oxford, **1990**.

244. C. L. Perrin, *J. Am. Chem. Soc.,* **113**, 2865 (1991). Atomic Size Dependence of Bader Electron Populations: Significance for Questions of Resonance Stabilization.

245. S. Yamada, *Angew. Chem. Int. Ed. Engl.,* **34**, 1113 (1995). Relationship Between C(O)–N Twist Angles and ^{17}O NMR Chemical Shifts in a Series of Twisted Amides.

246. S. Yamada, *J. Org. Chem.*, **61**, 941 (1996). Effects of C(O)–N Bond Rotation on the ^{13}C, ^{15}N and ^{17}O NMR Chemical Shifts and Infrared Carbonyl Absorption in a Series of Twisted Amides.

247. A. J. Bennet, V. Somayaji, R. S. Brown, and B. D. Santarsiero, *J. Am. Chem. Soc.,* **113**, 7563 (1991). The Influence of Altered Amidic Resonance on the Infrared and Carbon-13 and

Nitrogen-15 NMR Spectroscopic Characteristics and Barriers to Rotation about the N–C(O) Bond in Some Anilides and Toluamides.

248. K. B. Wiberg and P. R. Rablen, *J. Am. Chem. Soc.*, **117**, 2201 (1995). Why Does Thioformamide Have a Larger Rotational Barrier Than Formamide?
249. D. Lauvergnat and P. C. Hiberty, *J. Am. Chem. Soc.*, **119**, 9478 (1997). Role of Conjugation in the Stabilities and Rotational Barriers of Formamide and Thioformamide. An ab initio Valence Bond Study.
250. J. Paldus and A. Veillard, *Mol. Phys.*, **35**, 445 (1978) and references therein. Doublet Stability of Ab Initio SCF Solutions for the Allyl Radical.
251. D. Feller, E. Huyser, W. T. Borden, and E. R. Davidson, *J. Am. Chem. Soc.*, **105**, 1459 (1983). MCSCF/CI Investigation of the Low-lying Potential Energy Surfaces of the Formyloxyl Radical, HCO_2.
252. C. F. Jackels and E. R. Davidson, *J. Chem. Phys.*, **64**, 2908 (1976). The Two Lowest Energy $^2A'$ States of NO_2.
253. D. Feller, W. T. Borden, and E. R. Davidson, *J. Am. Chem. Soc.*, **106**, 2513 (1984). Allylic Resonance—When is it Unimportant?
254. D. Feller, E. R. Davidson, and W. T. Borden, *J. Am. Chem. Soc.*, **105**, 334 (1983). When is Allylic Resonance Unimportant?
255. A. D. McLean, B. H. Lengsfield III, J. Pacansky, and Y. Ellinger, *J. Chem. Phys.*, **83**, 3567 (1985). Symmetry Breaking in Molecular Calculations and the Reliable Prediction of Equilibrium Geometries. The Formyloxyl Radical as an Example.
256. A. Rauk, D. Yu, and D. A. Armstrong, *J. Am. Chem. Soc.*, **116**, 8222 (1994). Carbonyl Free Radicals. Formyloxyl (HCOO) and Acetoxyl (CH_3OO) Revisited.
257. A. F. Voter and W. A. Goddard, III, *Chem. Phys.*, **57**, 253 (1981). A Method for Describing Resonance Between Generalized Valence Bond Wave Functions.
258. A. F. Voter and W. A. Goddard, III, *J. Chem. Phys.*, **75**, 3638 (1981). The Generalized Resonating Valence Bond Method: Barrier Heights in the HF + D and HCl + D Exchange Reactions.
259. W. R. Wadt and W. A. Goddard, III, *J. Am. Chem. Soc.*, **97**, 2034 (1975). Electronic Structure of Pyrazine. Valence Bond Model for Lone Pair Interactions.
260. M. Amarouche, G. Durand, and J. P. Malrieu, *J. Chem. Phys.*, **88**, 1010 (1988). Structure and Stability of Xe_n^+ Clusters.
261. M. Rosi and C. W. Bauschlicher, Jr., *Chem. Phys. Lett.*, **159**, 349 (1989). Ultrafast Shock Induced Uniaxial Strain in a Liquid.
262. F. Tarentelli, L. S. Cederbaum, and P. Campos, *J. Chem. Phys.*, **91**, 7039 (1989). Symmetry Breaking and Symmetry Restoring in Ions of Loosely Bound Systems.
263. O. K. Kabbaj, M. B. Lepetit, and J. P. Malrieu, *Chem. Phys. Lett.*, **172**, 483 (1990). Inclusion of Dynamical Polarization Effects is Sufficient to Obtain Reliable Energies and Structures of He_n^+ Clusters.
264. E. Hollauer and M. A. C. Nascimento, *Chem. Phys. Lett.*, **184**, 470 (1991). A Generalized Multi-Structural Wave Function. The He_2^+ Molecule as an Example.
265. E. Hollauer and M. A. C. Nascimento, *J. Chem. Phys.*, **99**, 1207 (1993). A Generalized Multi-Structural Wave Function.
266. D. Lauvergnat, P. C. Hiberty, D. Danovich, and S. Shaik, *J. Phys. Chem.*, **100**, 5715 (1996). A Comparison of C–Cl and Si–Cl Bonds. A Valence Bond Study.
267. J. H. Langenberg and P. J. A. Rutink, *Theor. Chim. Acta (Berl.)*, **85**, 285 (1993). Optimization of Both Resonance Structures of the Glyoxal Radical Cation by Means of the Valence Bond Self-Consistent Field Method.
268. H. Basch, J. L. Wolk, and S. Hoz, *J. Phys. Chem. A*, **101**, 4996 (1997). Valence Bond Study of the SiH_3–F Bond.

269. D. Lauvergnat and P. C. Hiberty, *J. Mol. Struct. (THEOCHEM),* **338**, 283 (1995). The Nonlinear Tendencies in Homonuclear X–X Bonds (X = Li to F) and the Lone-Pair Bond Weakening Effect. An Ab Initio Theoretical Analysis.

270. S. Humbel, I. Demachy, and P. C. Hiberty, *Chem. Phys. Lett.,* **247**, 126 (1995). $HO^{\cdot}\cdot OH^{-}$: A Model for Stable Three-Electron-Bonded Peroxide Radical Anions.

271. D. Lauvergnat, P. Maître, P. C. Hiberty, and F. Volatron, *J. Phys. Chem.,* **100**, 6463 (1996). A Valence Bond Analysis of the Lone Pair Bond Weakening Effect for the X–H Bonds in the Series $XH_n = CH_4$, NH_3, OH_2, FH.

272. J. M. Galbraith, E. Blank, S. Shaik, and P. C. Hiberty, *Chem. Eur. J.,* **6**, 2425 (2000). π-Bonding in Second and Third Row Molecules: Testing the Strength of Linus's Blanket.

273. J. M. Galbraith, A. Shurki, and S. Shaik, *J. Phys. Chem. A,* **104**, 1262 (2000). A Valence Bond Study of the Bonding in First Row Transition Metal Hydride Cations: What Energetic Role Does Covalency Play?

274. B. Braïda, L. Thogersen, W. Wu, and P. C. Hiberty, *J. Am. Chem. Soc.,* **124**, 11781 (2002). Stability, Metastability and Unstability of Three-Electron-Bonded Radical Anions. A Model ab initio Study.

275. F. London, *Z. Elekrochem.*, **35**, 552 (1929). Quantenmechanic Deutung des Vorgangs der Aktiverierung.

276. H. Eyring and M. Polanyi, *Z. Phys. Chem.*, **B12**, 279 (1931). On Simple Gas Phase Reactions.

277. J. N. Murrell, S. Carter, S. C. Farantos, P. Huxley, and A. J. C. Varandas, *Molecular Potential Energy Functions,* Wiley, New York, 1984.

278. D. G. Truhlar and R. E. Wyatt, *Adv. Chem. Phys.*, **36**, 141 (1977). $H + H_2$: Potential-Energy Surfaces and Elastic and Inelastic Scattering.

279. A. Shurki, M. Strajbl, J. Villa, and A. Warshel, *J. Am. Chem. Soc.*, **124**, 4097 (2002). How Much Do Enzymes Really Gain by Restraining Their Reacting Fragments?

280. S. P. de Visser and S. Shaik, *Angew. Chem. Int. Ed. Engl.*, **41**, 1947 (2002). Hydrogen Bonding Modulates the Selectivity of Enzymatic Oxidation by P450: A Chameleon Oxidant Behavior by Compound I.

281. H. Kollmar, *J. Am. Chem. Soc.,* **101**, 4832 (1979). Direct Calculation of Resonance Energies of Conjugated Hydrocarbons with ab initio MO Methods.